CHEMICAL MECHANISMS UNDERLYING THE MEDICINAL ACTIVITY OF METABOLICALLY-ACTIVATED *N*-OXIDE ANTITUMOR AGENTS

A Dissertation

Presented to

the Faculty of the Graduate School

University of Missouri-Columbia

In Partial Fulfillment

Of the Requirement of the Degree

Doctor of Philosophy

By

VENKATRAMAN JUNNOTULA

Prof. Kent S. Gates, Dissertation Supervisor

MAY 2008

The undersigned, appointed by the Dean of the Graduate School, have examined the dissertation entitled

CHEMICAL MECHANISMS UNDERLYING THE MEDICINAL ACTIVITY OF METABOLICALLY-ACTIVATED *N*-OXIDE ANTITUMOR AGENTS

Presented by **Venkatraman Junnotula**

A candidate for the degree of Doctor of Philosophy

and hereby certify that in their opinion it is worthy of acceptance

Professor Kent S. Gates

Professor Susan Z. Lever

Professor Thomas P. Quinn

Professor John J. Tanner

Professor Rainer E. Glaser

ACKNOWLEDGEMENTS

First of all I would like to extend my gratitude to my advisor Prof. Kent S. Gates for his guidance, encouragement and help during my graduate studies. His commitment in teaching and supportive nature always helped me to face both scientific and personal challenges successfully. I want to thank my committee members Prof. Susan Lever, Prof. Thomas Quinn, Prof. John Tanner and Prof. Rainer Glaser for their helpful comments in my career growth.

I also want to thank my past and current Gates group members. I would like to thank my past group members Dr. Scott Daniels, Dr. Tara Fuchs, Dr. Delshanee Kotandeniya and Dr. Goutam Chowdury for their valuable suggestions and help during my graduate career. I would like to thank all of current group members for making my stay in Gates group very memorable. I can't forget the memories of morning tea time with Jason, Derrick, Mostafa and Morjorie and hallway conversations with Dr. Santhosh and Dr. Sanjay. I also want to thank Ujjal, Sarmista and Anu for the scientific conversations on research projects. I want to thank all of my friends, who have made my stay at University of Missouri-Columbia more enjoyable

I would like to thank my parents for their love and sacrifice for my career growth. I want to thank my brother and sisters for their love and affection since my childhood. I also want to thank my mother-in-law for her help during challenging time in both career and personal life.

I want to thank my wife Sulochana Junnotula for her patience, moral support and being there for me during difficult times. Finally, I want to thank my daughter Kranthi Junnotula for her inspirational smile.

ABSTRACT

Tirapazamine (TPZ) is a clinically promising hypoxia-selective anti-tumor drug and currently undergoing in various clinical trials including phase I, II and III in treating human cancers in combination with radiation therapy and cisplatin based chemotherapy. Anti-cancer activity of TPZ derives from its ability to cause the DNA strand cleavage in oxygen poor environment found in solid tumors. TPZ achieves selectivity in causing DNA strand cleavage via producing oxygen sensitive radical anion intermediate upon one-electron reductive activation. In the presence of normal oxygenated cells, radical anion produced will be oxidized back to TPZ with generating superoxide radical, which toxicity is reduced by cellular protecting enzymes, superoxide dismutase, catalase and peroxy redoxins. On the other hand, in poorly oxygenated tumor cells the protonated form of radical anion generates DNA damaging agents. However, the exact nature of DNA damaging agent produced from activated TPZ is still a matter of debate. Our group studies suggested that protonated form of TPZ radical anion undergoes homolytic fragmentation to generate the well known DNA damaging agent hydroxyl radical. Alternative mechanism proposed by Denny's and co-workers, they suggest that protonated form of radical anion dehydrates to generate benzotriazinyl radical, which damages the DNA.

In this thesis, we reported various mechanistic studies that set out to examine the exact DNA damaging agent produced from TPZ and its structurally related heterocyclic dioxides. We used TPZ analog, Me-TPZ to examine the possible formation of benzotriazinyl radical upon reductive activation. We proposed that if Me-TPZ generates benzotriazinyl radical that can be trapped by deuterated solvents to yield metabolite with

deuterium incorporation, which can be detected with LC/MS. Accordingly, we carried out isotopic labeling studies on Me-TPZ. Our isotopic labeling studies show that Me-TPZ does not dehydrate to generate benzotriazinyl radical. Indeed TPZ and Me-TPZ hydroxylate DMSO and salicylic acid. Further, our *in vitro* DNA cleavage assays on Me-TPZ reveal that this compound shows similar DNA cleavage properties to TPZ irrespective its inability to undergo dehydration. We also examined the DNA cleavage properties of another TPZ analog, 1,2,4-benzotriazine-di-oxide (Des-TPZ), a molecule absolute incapable of undergoing dehydration mechanism. Our data shows that Des-TPZ shows similar DNA cleavage properties to TPZ and Me-TPZ. This data suggest that formation of benzotrizinyl radical is not necessary for the DNA cleavage properties of TPZ and its analogs. On the other hand data shows that TPZ and its analogs release hydroxyl radical upon one-electron reductive activation.

We further explored to understand the DNA cleavage properties of quinoxaline di-*N*-oxides upon bio-reductive activation. Our data shows that quinoxaline di-oxides display similar DNA cleavage properties to TPZ irrespective of their inability to undergo dehydration mechanism. In addition, these quinoxaline di-*N*-oxide compounds upon bio-reductive activation hydroxylate DMSO.

Overall, the data reported in this thesis suggests that release of hydroxyl radical is the common mechanism that explains the DNA cleavage properties of heterocyclic di-*N*-oxides. Thus data suggest that TPZ and its structurally related di-*N*-oxide compounds deliver known radiotherapeutic DNA damaging agent hydroxyl radical in oxygen poor environment found in solid tumors.

TABLE OF CONTENTS

Chapter 5: Activation of the Anti-tumor Agent Tirapazamine by Thiols and Dithiols

LIST OF SCHEMES

Chapter 1 Page

Chapter 2

Chapter 3

Chapter 4

Chapter 5

LIST OF FIGURES

Chapter 1

Chapter 2

Chapter 3

Chapter 4

Chapter 5

LIST OF TABLES

Chapter 5

Chapter 1: Investigation Into the Chemical Nature of Reactive Species Responsible for Oxidative DNA Damage by Hypoxia Selective Anti-Cancer Agent Tirapazamine and its analog, 3-methyl-1,2,4-Benzotriazine-1,4-Dioxide

1.1 Introduction to Tirapazamine

The compound 3-amino-1,2,4-benzotriazine 1,4-dioxide (tirapazamine, TPZ, **1**) belongs to a new class of bio-reductively activated and hypoxia-selective anti-cancer agents and is currently undergoing a variety of phase I, II and III clinical trials for the treatment of human cancers.[1,2,3] Studies shows that the anti-cancer activity of TPZ is derived from its ability to cause the DNA strand cleavage under oxygen poor (hypoxic) conditions found in solid tumors.[4,5,6,7,8] TPZ achieves its hypoxia-selective DNA strand cleavage ability *via* producing oxygen sensitive radical anion intermediate **2a** upon one-electron reductive activation. In normally-oxygenated cells the radical anion **2a** is oxidized to the TPZ (**1**) with the release of superoxide radical, which toxicity is reduced by cellular enzymes superoxide dismutase, catalase, glutathione peroxidase and peroxiredoxins.[4,9,10,11,12] On the other hand, in oxygen poor conditions found in solid

tumors, the protonated form of radical anion **2b** releases the DNA damaging agent(s), which cause oxidative damage to DNA bases and generate DNA strand breaks by the abstraction of hydrogen atoms from the deoxyribose of duplex DNA.[2,4,8] However, the exact DNA damaging agent involved in oxidative DNA damage by TPZ is still a matter of debate.[6,13]

1.1.1 Chemical mechanisms proposed for DNA damage by TPZ

Our studies support that protonated form of activated TPZ **2b** undergoes homolytic fragmentation to release small and diffusible species like hydroxyl radical.[6,7,14,15] This type of chemistry finds direct precedents in the literature. For example, the radical-induced fragmentation of Barton's *N*-hydroxypyridinethione esters is similar to that we

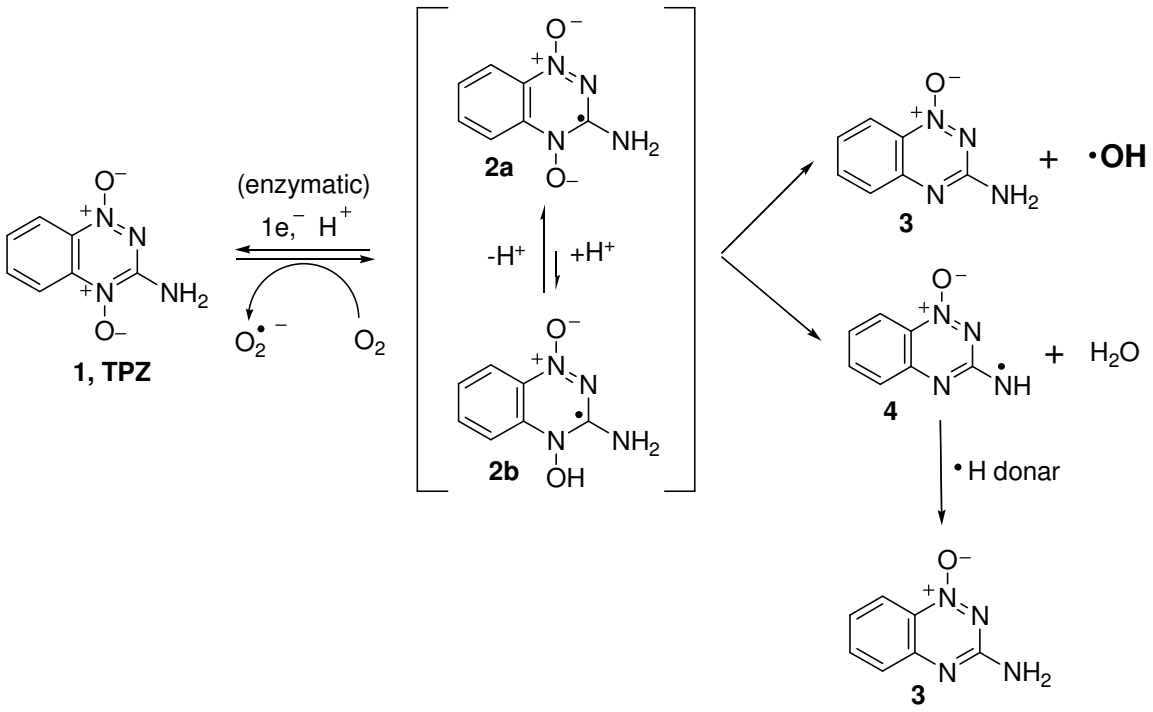

Scheme 1.1: Proposed mechanisms for DNA damage by activated TPZ

proposed for TPZ.[16,17,18,19] In addition, several other groups reported similar photoinduced fragmentations of *N*-(alkoxy)pyridinium salts.[20,21,22] Alternatively, Denny and co-workers suggested that protonated form of activated TPZ **2b** dehydrates to give benzotriazinyl radical **4**, which does the DNA strand cleavage (Scheme 1.1).[13] In addition, it is important to note that there is precedence for an alternative dehydration mechanism.

Christensen and co-workers reported that toluene (**5**), upon pulse radiolysis in aqueous solutions, generates benzyl radical (**7**) (Scheme 1.2).[23] The authors proposed that hydroxyl radical generated on pulse radiolysis reacts with toluene to give radical **6**, which dehydrates to form **7** (Scheme 1.2).**Error! Bookmark not defined.**

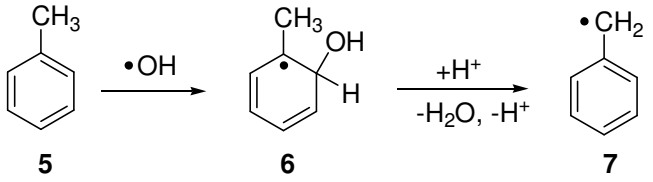

Scheme 1.2: Hydroxyl radical adduct of toluene dehydrates to give benzyl radical

Although, the above reaction requires an acidic environment, this chemistry is similar to the dehydration mechanism proposed for bio-reductively activated drug, tirapazamine (**1**).[13] Based on this observation, it is important to examine the possible role of dehydration chemistry in medicinal properties of TPZ and its analogs. Such studies not only will be helpful for better understanding of the molecular mechanisms underlying the medicinal properties of TPZ and its analogs but also facilitate drug development within this new chemical class of antitumor agents.

1.2 Goal: Examine the chemical mechanisms responsible for DNA damage by TPZ and its analog, Me-TPZ (8)

In this chapter, we aimed to examine the dehydration mechanism in benzotriazine class of compounds by using the TPZ analog, 3-methyl-1,2,4-benzotriazine 1,4-dioxide (Me-TPZ, **8**). There are three main reasons to choose **8** to examine the dehydration mechanism. First, **8** shows similar hypoxia-selective cytotoxicity to TPZ against cancer cell lines and considered as a clinical back up for TPZ.[23] Second, despite **8** promising preclinical properties, DNA strand cleavage by activated **8** has not been investigated. Third, **8** provides a mechanistic handle to examine dehydration mechanism.

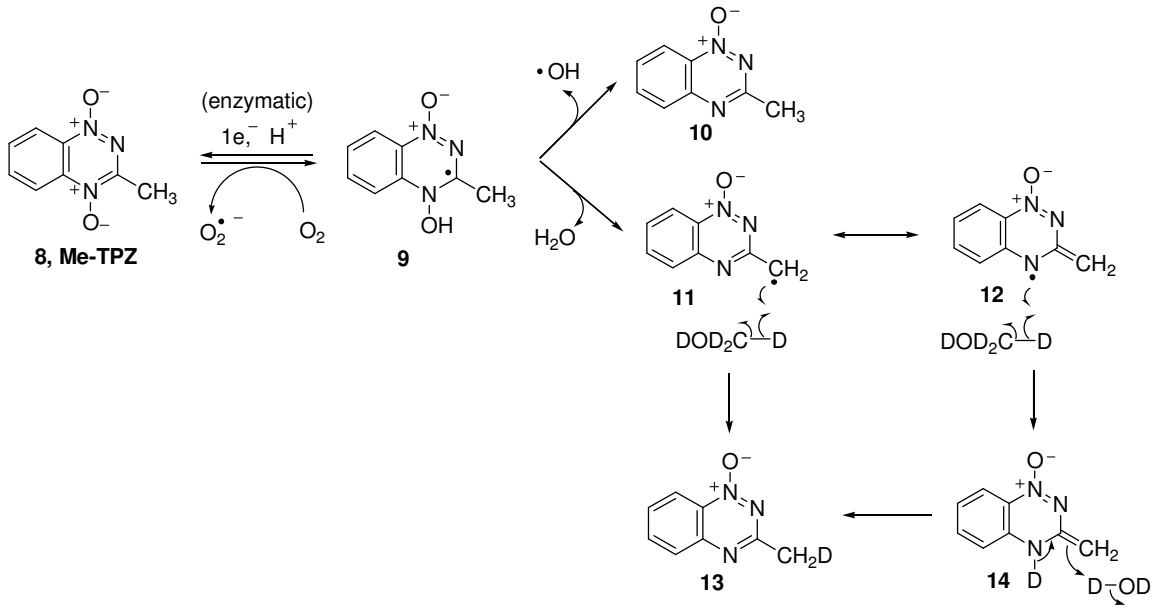

Scheme 1.3: Me-TPZ provides a mechanistic handle to examine the dehydration mechanism

For example, if dehydration occurs in activated **8**, the benzotriazinyl radical (in form **11** or **12**) generated in this process should be trapped by excess deuterium atom donor CD_3OD in D_2O to give deuterium labeled 1-*N*-oxide metabolite (**13**) (Scheme 1.3). On the other hand, if **8** releases hydroxyl radical no deuterium incorporation will occur

(Scheme 1.3). Incorporation of deuterium in 1-*N*-oxide metabolite (**10**) can be detected by LC/ESI-MS analysis in a positive ion mode.

As part of our mechanistic studies, we synthesized **8** and its metabolites by using literature protocols with minor modification.[24,25] Before conducting mechanistic studies on **8**, we examined whether **8** behaves analogous to TPZ upon bio-reductive activation *in vitro*.

1.3 Synthesis of 8

Compound **8** and its possible metabolites were synthesized using literature protocols.[24,] The compound 3-methyl-1,2,4-benzotriazine (**18**) was obtained using synthetic route devised by Khodja and coworkers with minor change (Scheme 1.4).[24] In our synthesis, we used dry ethanol and hydrated PtO_2 in the cyclization step. Briefly, the

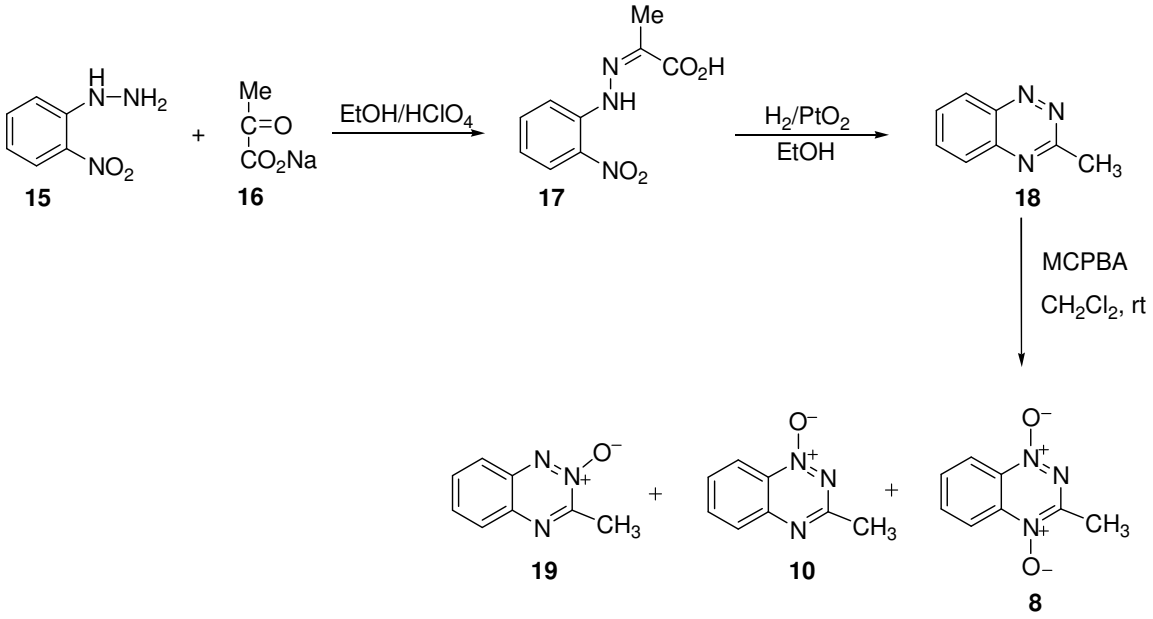

Scheme 1.4: Synthesis of Me-TPZ and its metabolites

compound **18** was obtained via reductive cyclization by a PtO_2-catalyzed hydrogenation of the 2-nitrophenylhydrazones of pyruvic acid (**17**).[24] Then **18** was oxidized with metachloroperbenzoic acid (MCPBA) to give mixture of **8, 10** and **19**.[25]

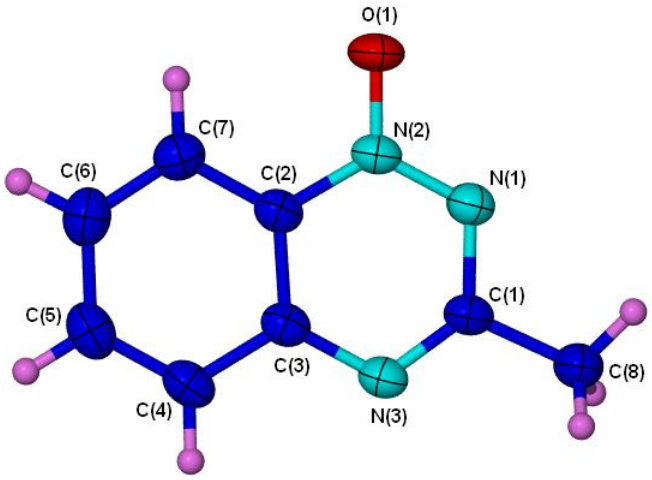

Figure 1.1: Crystal structure of 3-methyl-1,2,4-benzotriazine-1-oxide (**10**)

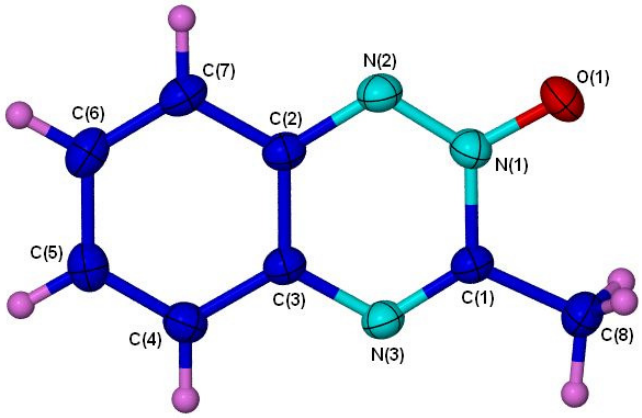

Figure 1.2: Crystal structure of 3-methyl-1,2,4-benzotriazine-2-oxide (**19**)

It is difficult to conclusively assign the site of oxygen attachment in mono-*N*-oxide compounds using NMR spectroscopy.[26] Accordingly, as part of our efforts to characterize **10** and **19** of Me-TPZ, we grew crystals of these compounds.[27] Upon slow

evaporation, dilute solutions of **10** and **19** of Me-TPZ in 1:1 ethyl acetate-hexane afforded crystals suitable to X-ray diffraction analysis.[27] Our crystallographic data provide unambiguous characterization of **10** and **19** of Me-TPZ.[27]

1.4 Me-TPZ (8) behaves similar to TPZ upon bio-reductive activation

As part of our efforts to understand the exact nature of reactive species responsible for medicinal properties of **8**, we set to examine whether **8** behaves analogous TPZ or not upon bio-reductive activation. Accordingly, we studied the DNA cleavage ability, the sequence specificity of DNA cleavage, the effect of radical scavengers on the DNA cleavage, the oxygen sensitivity of DNA cleavage and *in vitro* metabolism of **8** under anaerobic conditions and compared to TPZ. Such studies will be helpful to understand whether **8** and TPZ derives their medicinal properties by the same mechanism or not.

1.4.1 Me-TPZ cleaves DNA upon bio-reductive activation

In DNA cleavage assays, we examined the ability of **8** to generate strand cleavage in supercoiled plasmid DNA. We used NADPH:cytochrome P450 reductase as an activating system and reactions were carried out under anaerobic conditions. The ability of DNA cleavage by activated **8** is determined in terms of its ability to convert supercoiled DNA (form I) to the open-circular form (form II). These two forms of DNA are separated by using agarose gel electrophoresis and quantified by digital imaging analysis of the gel.[6]

Our data show that **8** cleaves DNA in the presence of NADPH:cytochrome P450 reductase under anaerobic conditions (Figure 1.3). In control reactions, with **8** (no NADPH:cytochrome P450 reductase) or with NADPH:cytochrome P450 reductase (no **8**) DNA cleavage was not observed. Under aerobic conditions, **8** didn't show any significant

DNA cleavage (Figures 1.6). This data shows that similar to TPZ, **8** generates an oxygen sensitive reactive intermediate upon enzymatic activation.[6]

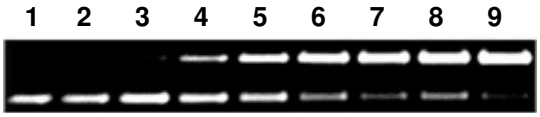

Figure 1.3: Concentration dependent anaerobic DNA-cleavage efficiency of **8** in the presence of NADPH:cytochrome P450 reductase as an activating system. Supercoiled plasmid DNA (33 µg/mL, pGL-2 Basic) was incubated with **8** (25-150 µM), NADPH (500 µM), cytochrome P450 reductase (33 mU/mL), catalase (100 µg/mL), superoxide dismutase (10 µg/mL), sodium phosphate buffer (50 mM, pH 7.0), and desferal (1 mM) under anaerobic conditions at room temperature for 4 h, followed by agarose gel electrophoretic analysis. Lane 1, DNA alone (S = 0.19 ± 0.02); lane 2, NADPH (500 µM) + reductase (33 mU/mL) (S = 0.2 ± 0.01); lane 3, **8** (150 µM) (S = 0.18 ± 0.03); lanes 4-9, NADPH (500 µM) + reductase (33 mU/mL) + **8** (25 µM, lane 4) (S = 0.46 ± 0.11); (50 µM, lane 5) (S = 0.71 ± 0.1); (75 µM, lane 6) (S = 0.81 ± 0.08); (100 µM, lane 7) (S = 1.13 ± 0.11); (125 µM, lane 8) (S = 1.22 ± 0.01); (150 µM, lane 9) (S = 1.46 ± 0.03). The value S represents the mean number of strand breaks per plasmid molecule and is calculated using the equation $S = -\ln f_I$, where f_I is the fraction of plasmid present as form I.[28]

1.4.2 DNA damaging ability of 8 is comparable to TPZ

We also compared the DNA cleavage ability of TPZ and **8** under identical conditions. Our results show that **8** shows comparable DNA cleavage to TPZ (Figures 1.3-1.5). In control reactions, with TPZ (no NADPH:cytochrome P450 reductase) or with NADPH:cytochrome P450 reductase (no TPZ) DNA cleavage was not observed as we reported in our earlier group studies.[6]

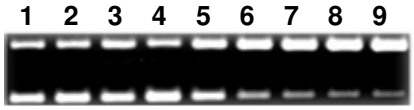

Figure 1.4: Concentration dependent anaerobic DNA-cleavage efficiency of TPZ in the presence of NADPH:cytochrome P450 reductase as an activating system. Supercoiled plasmid DNA (33 µg/mL, pGL-2 Basic) was incubated with TPZ (25-150 µM), NADPH (500 µM), cytochrome P450 reductase (33 mU/mL), catalase (100 µg/mL), superoxide dismutase (10 µg/mL), sodium phosphate buffer (50 mM, pH 7.0), and desferal (1 mM) under anaerobic conditions at room temperature for 4 h, followed by agarose gel electrophoretic analysis. Lane 1, DNA alone (S = 0.24 ± 0.01); lane 2, NADPH (500 µM) + reductase (33 mU/mL) (S = 0.26 ± 0.03); lane 3, TPZ (150 µM) (S = 0.24 ± 0.02); lanes 4-9, NADPH (500 µM) + reductase (33 mU/mL) + TPZ (25 µM, lane 4) (S = 0.38 ± 0.01); (50 µM, lane 5) (S = 0.51 ± 0.03); (75 µM, lane 6) (S = 0.61 ± 0.03); (100 µM, lane 7) (S = 0.72 ± 0.02); (125 µM, lane 8) (S = 0.82 ± 0.05); (150 µM, lane 9) (S = 1.04 ± 0.01). The value S represents the mean number of strand breaks per plasmid molecule and is calculated using the equation $S = -\ln f_I$, where f_I is the fraction of plasmid present as form I.[28]

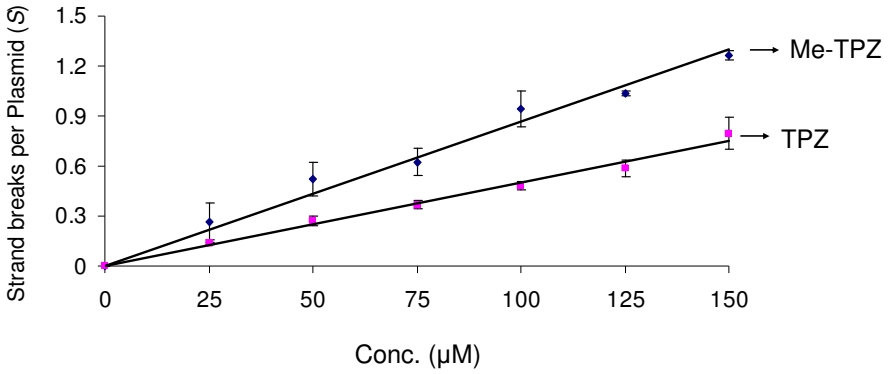

Figure 1.5: Comparision of anaerobic DNA-cleavage efficiency by various concentrations of TPZ or **8** in the presence of NADPH:cytochrome P450 reductase as an activating system. Supercoiled plasmid DNA (33 μg/mL, pGL-2 Basic) was incubated with TPZ or **8** (25-150 μM), NADPH (500 μM), cytochrome P450 reductase (33 mU/mL), catalase (100 μg/mL), superoxide dismutase (10 μg/mL), sodium phosphate buffer (50 mM, pH 7.0), and desferal (1 mM) under anaerobic conditions at room temperature for 4 h, followed by agarose gel electrophoretic analysis. The value *S* represents the mean number of strand breaks per plasmid molecule and is calculated using the equation $S = -\ln f_I$, where f_I is the fraction of plasmid present as form I.[28] Background cleavage in the untreated plasmid was subtracted to allow direct comparision of DNA strand cleavage yields between different experiments.

1.4.3 Radical scavengers inhibit the DNA cleavage by Me-TPZ (8)

In addition, DNA cleavage by activated **8** is inhibited in the presence of typical radical scavenger's methanol, ethanol, *t*-butanol, DMSO and mannitol (Lanes 3-8 in Figure 1.6). This data suggests that upon bio-reductive activation **8** releases radical species and causes DNA strand cleavage similar to TPZ (Figure 1.7).[2]

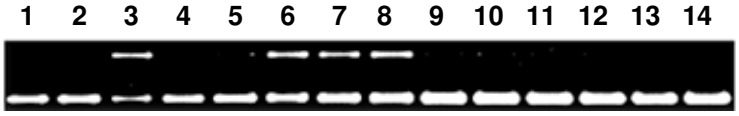

Figure 1.6: Cleavage of supercoiled plasmid DNA by **8** in the presence of NADPH:cytochrome P450 reductase as an activating system. All reactions contained DNA (33 μg/mL, pGL-2 Basic), sodium phosphate buffer (50 mM, pH 7.0), catalase (100 μg/ mL), superoxide dismutase (10 μg/mL), and desferal (1 mM) and were incubated under anaerobic conditions (except lane 9) at 24 °C for 3 h, followed by agarose gel electrophoretic analysis. Lane 1, DNA alone (S = 0.27 ± 0.01); lane 2, NADPH (500 μM) + reductase (33 mU/mL) (S = 0.28 ± 0.02); lane 3, **8** (250 μM) + NADPH (500 μM) + reductase (33 mU/mL) (S = 1.33 ± 0.06); lanes 4-8, **8** (250 μM) + NADPH (500 μM) + reductase (33 mU/mL) + methanol (500 mM, lane 4) (S = 0.41 ± 0.05); ethanol (500 mM, lane 5) (S = 0.41 ± 0.11); *tert*-butyl alcohol (500 mM, lane 6) (S = 0.66 ± 0.07); DMSO (500 mM, lane 7) (S = 0.5 ± 0.16); mannitol (500 mM, lane 8) (S = 0.57 ± 0.02); lane 9, **8** (250 μM) + NADPH (500 μM) + reductase (1 mU) + air (S = 0.26 ± 0.0); lane 10, **10** (250 μM) + NADPH (500 μM) + reductase (33 mU/mL) (S = 0.26 ± 0.01); lane 11, **18** (250 μM) + NADPH (500 μM) + reductase (33 mU/mL) (S = 0.27 ± 0.02); lanes 12-14, **8** alone (250 μM, lane 12) (S = 0.26 ± 0.01); **10** (250 μM, lane 13) (S = 0.27 ± 0.01); 18 alone (250 μM, lane 14) (S = 0.28 ± 0.0).

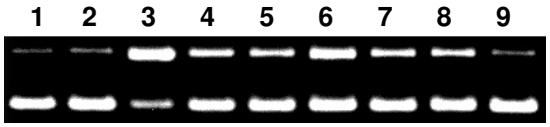

Figure 1.7: Cleavage of supercoiled plasmid DNA by TPZ in the presence of NADPH:cytochrome P450 reductase as an activating system. All reactions contained DNA (33 µg/mL, pGL-2 Basic), sodium phosphate buffer (50 mM, pH 7.0), catalase (100 μg/ mL), superoxide dismutase (10 μg/mL), and desferal (1 mM) and were incubated under anaerobic conditions at 24 °C for 4 h, followed by agarose gel electrophoretic analysis. Lane 1, DNA alone (S = 0.18 ± 0.01); lane 2, NADPH (500 μM) + reductase (33 mU/mL) (S = 0.18 ± 0.01); lane 3, TPZ (250 μM) + NADPH (500 μM) + reductase (33 mU/mL) (S = 1.07 ± 0.18); lanes 4-8, TPZ (250 μM) + NADPH (500 μM) + reductase (33 mU/mL) + methanol (500 mM, lane 4) (S = 0.38 ± 0.06); ethanol (500 mM, lane 5) (S = 0.36 ± 0.02); *tert*-butyl alcohol (500 mM, lane 6) (S = 0.57 ± 0.04); DMSO (500 mM, lane 7) (S = 0.36 ± 0.02); mannitol (500 mM, lane 8) (S = 0.36 ± 0.01); lane 9, TPZ alone (S = 0.17 ± 0.01). The value S represents the mean number of strand breaks per plasmid molecule and is calculated using the equation $S = -\ln f_I$, where f_I is the fraction of plasmid present as form I.[28]

1.4.4. Radical scavengers exhibit similar trends in their ability to inhibit the DNA cleavage by activated 8 (anaerobic), TPZ (anaerobic) and menadione (MD, 20) (aerobic).

It is interesting to note that radical scavengers show similar trends in their ability to inhibit the DNA cleavage by activated **8** and TPZ under anaerobic conditions. Importantly, these radical scavengers also show similar trends in inhibiting the DNA cleavage caused by activated **20** under aerobic conditions. The compound **20** is well known to derive its biological activity from its ability to produce reactive oxygen species via redox cycling.[29] On reductive activation, **20** redox cycles to produce superoxide radical, which produces the DNA damaging agent, hydroxyl radical via Fenton chemistry (Scheme 1.5).[29] The similar trends of radical scavengers in inhibiting the DNA cleavage by activated **8**, TPZ and **20** suggest that **8** and TPZ may release DNA damaging agent hydroxyl radical (Figure 1.8).

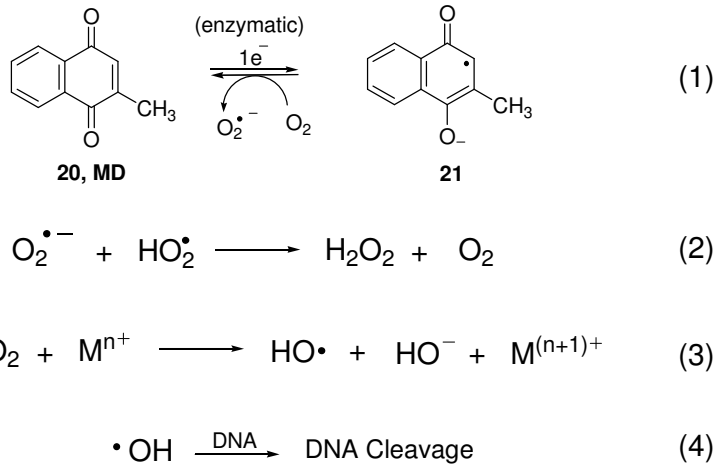

Scheme 1.5: Mechanism for DNA cleavage by menadione

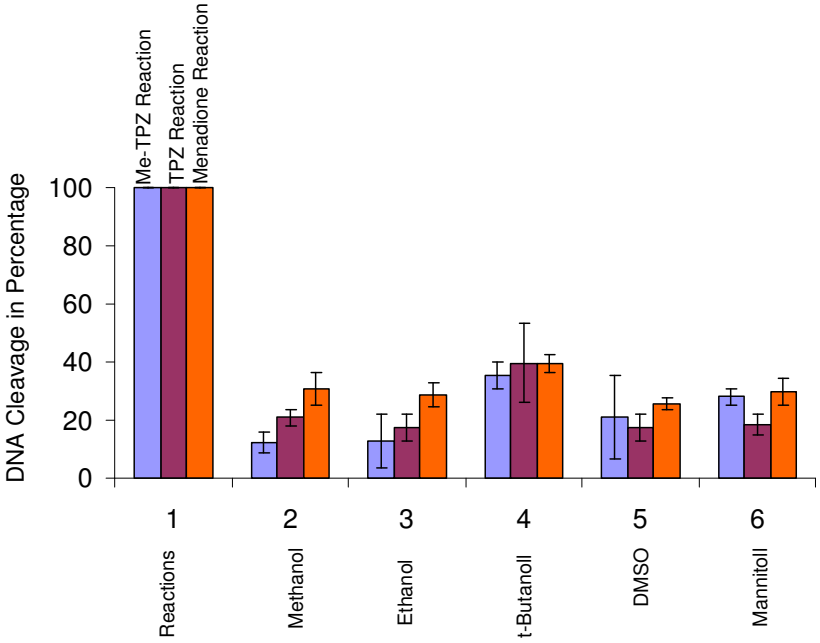

Figure 1.8: Inhibition of **1, 8** and **20** mediated DNA damage by radical scavengers, methanol, ethanol, t-butanol, DMSO and mannitol. All reactions w/wo radical scavengers (500 mM) were carried out as we described in an experimental section. DNA cleavage was detected and quantified in an identical manner to our earlier experiments.

1.4.5 Me-TPZ gives 1-*N*-oxide as a major metabolite

To determine *in vitro* metabolites arising from reductive-activation, **8** was incubated with NADPH:cytochrome P450 reductase under anaerobic conditions. Metabolites were analyzed by using HPLC and LC/MS. To confirm the identity of the metabolites, authentic metabolites were synthesized and co-injected onto HPLC with the metabolites generated in Me-TPZ reaction. Our results show that **8** gives the 1-*N*-oxide (**10**) as a major metabolite and no-*N*-oxide (**18**) as a minor metabolite in a manner analogous to TPZ (Figure 1.9 and Scheme 1.6).[26] Our DNA cleavage assays show that both minor and major metabolites of **8** are not DNA cleaving agents under anaerobic conditions (Figure 1.6).

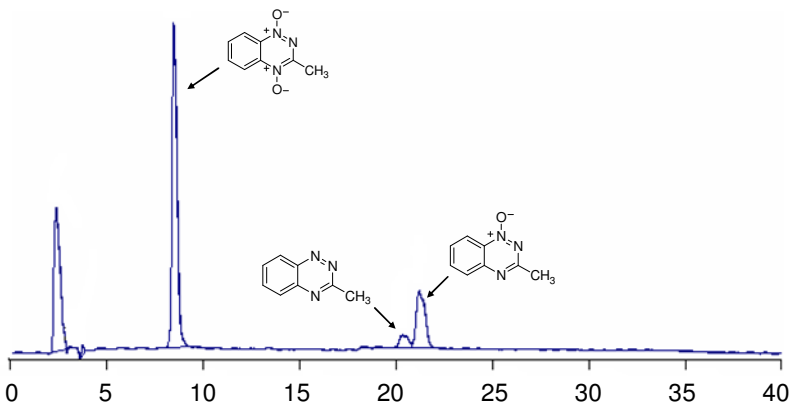

Figure 1.9: HPLC trace of products arising from *in vitro* anaerobic metabolism of **8**. A 300 µL solution of sodium phosphate buffer (pH 7.0, 50 mM), **8** (500 µM), desferal (1 mM) was incubated with cytochrome P450 reductase (10 mU) and NADPH (500, µM) under anaerobic conditions for 3 h.

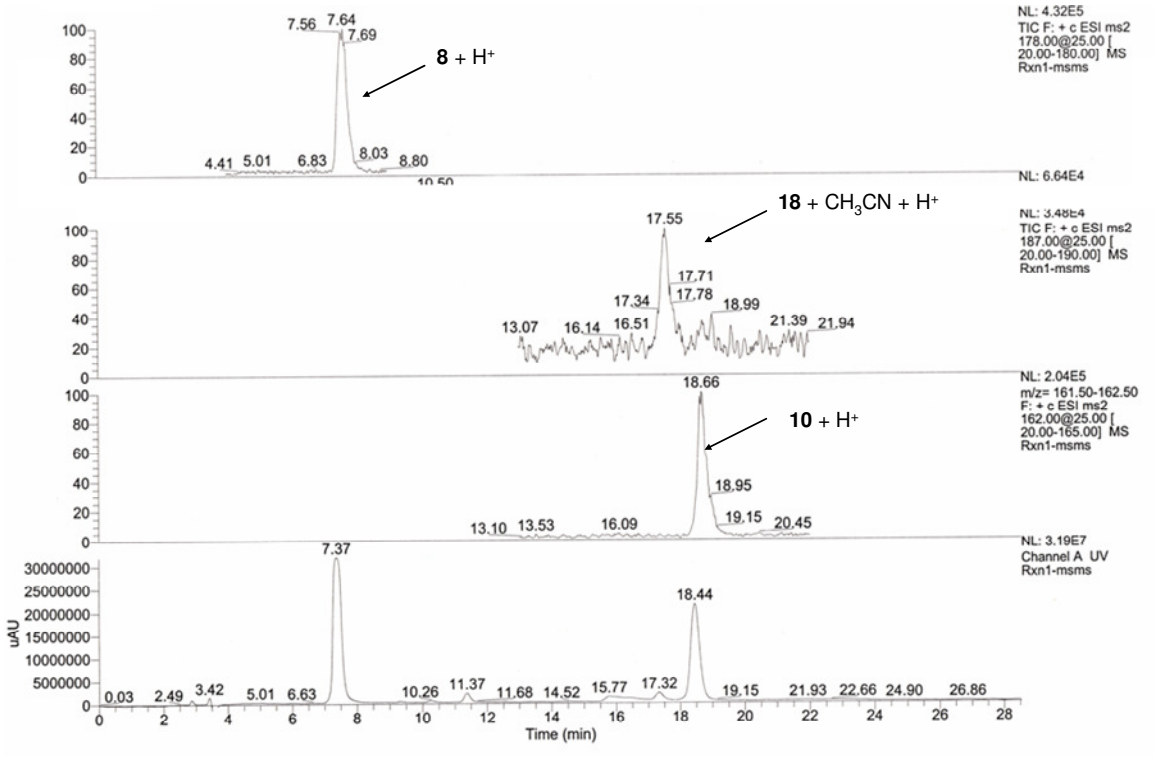

Figure 1.10: LC/ESI-MS traces of **10** and **18** metabolites arising from *in vitro* anaerobic metabolism of 3-methyl-1,2,4-benzotriazine *di*-oxide (**8**). A 300 µL solution of sodium phosphate buffer (pH 7.0, 50 mM), **8** (500 µM), desferal (1 mM) was incubated with cytochrome P450 reductase (10 mU) and NADPH (500, µM) under anaerobic conditions for 3 h. *In vitro* metabolites were extracted into ethyl acetate and the resulting samples were air dried redissolved in 1:1 methanol: water for LC/ESI-MS analysis with a positive ion mode.

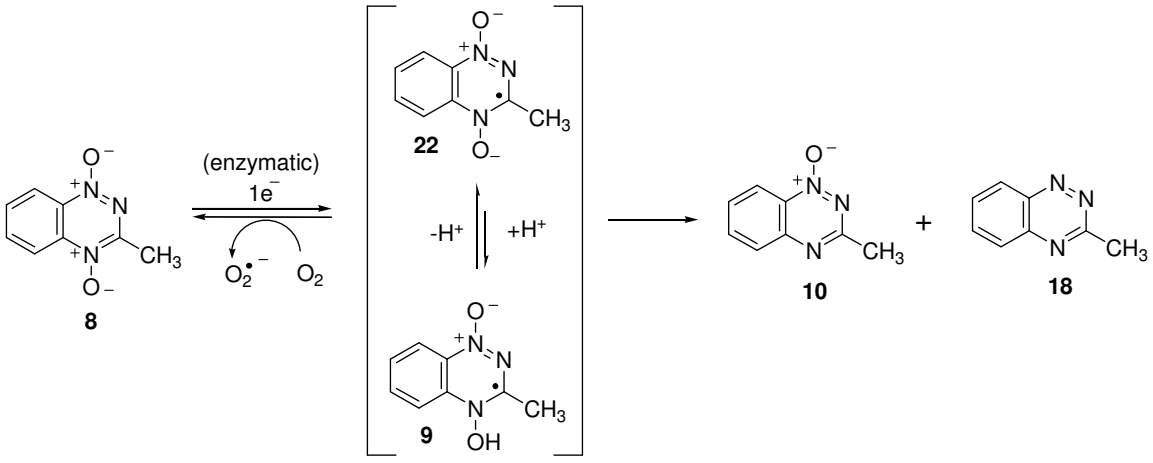

Scheme 1.6: *In vitro* metabolism of 3-methyl-1,2,4-benzotriazine di-*N*-oxide (**8**)

1.4.6 Compound 8 shows sequence independent DNA cleavage

Our group hypothesized that if **8** releases small and diffusible species like hydroxyl radical, the DNA cleavage by **8** should be sequence independent. To test this hypothesis, Ujjal Sarkar in our group examined the sequence specificity of DNA cleavage of a 30 base pair DNA fragment by **8** and compared to that by well known hydroxyl radical generating iron-EDTA system.[30] Our data show that **8** cleaves the DNA at all base pairs with some preference for cleavage at guanine similar to TPZ. The reason for moderate guanine sequence specificity in DNA cleavage by these 1,2,4-benzotriazine class of drugs is not clear. One possible reason is that a portion of damaged guanine sites may lead to strand breaks under our experimental conditions.[31]

1.5 Examining the dehydration mechanism in Me-TPZ

The above experimental results show that in the *in vitro* conditions employed here **8** behaves in an analogous to TPZ. In addition, **8** also shows similar biological activity in cancer cell lines to TPZ.[23] These data together suggest that **8** and TPZ may act by the same mechanism. This makes it especially interesting to ask whether activated **8** undergoes dehydration to yield benzotriazinyl radical. Here, we set to examine the possibility of **8** to undergo dehydration mechanism by using isotopic labeling studies.

1.5.1 Isotopic labeling studies of Me-TPZ (8)

In isotopic labeling experiments, we examined whether the dehydration mechanism is operative in the activated **8**. As part of our studies, compound **8** was activated in the presence of CD_3OD/D_2O and 1-*N*-oxide (**10** or **13**) metabolite generated from this reaction was analyzed by LCESI-/MS. Our LC/ESI-MS data show that there is only 3-5

% deuterium present in the 1-*N*-oxide (**10**) metabolite (Scheme 1.8). A control experiment with activated **8** in the absence of CD_3OD under the identical reaction conditions also yields 1-*N*-oxide (**10**) metabolite with 2-3% deuterium content (Scheme 1.7). This data show that there is no significant CD_3OD dependent deuterium incorporation occurs in the 1-*N*-oxide metabolite (**10**) produced in the reaction. This observation reveals that activated **8** doesn't dehydrate to generate the benzotriazinyl radical (**11** or **12**).

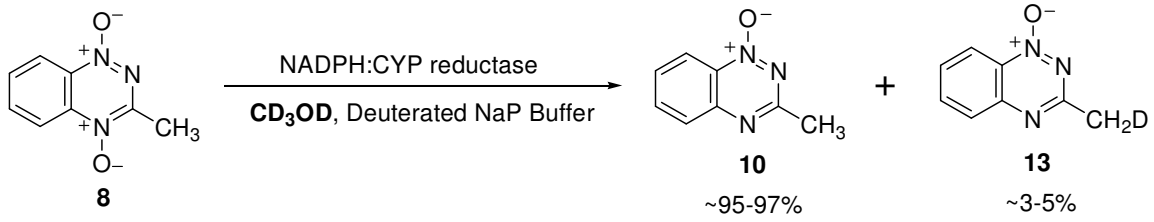

Scheme 1.7: Examination of deuterium incorporation in activated Me-TPZ in the absence of CD_3OD

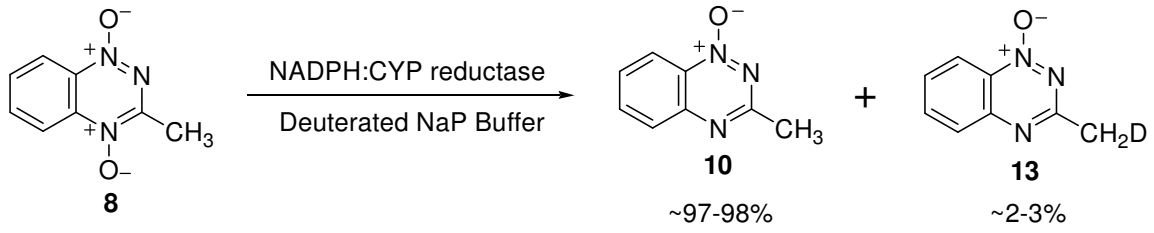

Scheme 1.8: Examination of deuterium incorporation in activated Me-TPZ in the presence of CD_3OD

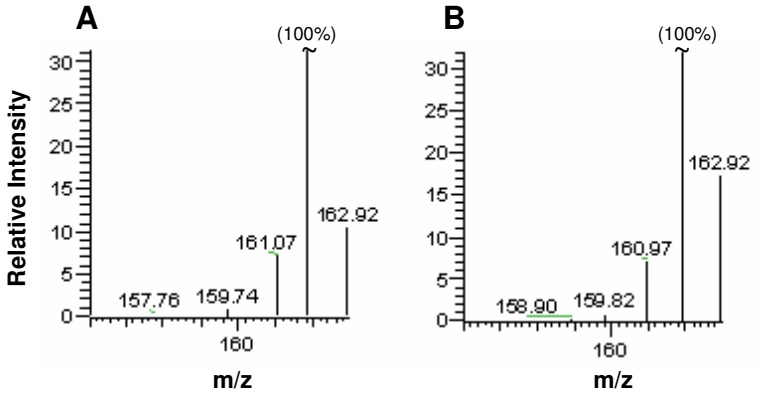

Figure 1.11: *In vitro* metabolism of **8** in deuterated sodium phosphate buffer and in the presence of deuterated atom donor (CD_3OD) yields predominantly undeuterated metabolite **10**. Panel **A** shows mass spectrometric data obtained by ESI-LC/MS analysis of authentic **8** in the positive ion mode. The base peak at m/z 162 is the $(M+H)^+$ ion of **10**. The peak at m/z 162.9 is due to natural abundance of ^{13}C, ^{15}N, and ^{2}D and is close to ~10% of base peak. Panel **B** shows mass spectrometric data obtained by LC/MS analysis of **10** generated by incubation of **8** (1 mM) with NADPH:cytochrome P450 reductase (0.6 units/mL) and NADPH (2 mM) in deuterated sodium phosphate buffer (50 mM, pD 6.6) containing desferal (1 mM) and deuterated methanol (CD_3OD, 2 M) under anaerobic conditions for 12 h. The small increase in the peak at m/z 163 indicates that approximately 5% of the deuterated metabolite of **13** was generated by the one-electron reduction of **8**.

1.5.2 Converse labeling experiments

In addition, we set out to examine the formation of benzotriazinyl radical from activated deuterium labeled Me-TPZ (CD_3-TPZ, **22**). For example, if activated labeled **22** undergoes dehydration to generate benzotriazinyl radical (**25** or **27**), deuterated methyl group in **22** should lose deuterium in the presence of excess CH_3OH in H_2O (Scheme 1.9). On the other hand, if it releases hydroxyl radical, deuterated methyl group in **22** should completely retain the deuterium label in the presence of excess CH_3OH (Scheme 1.9).

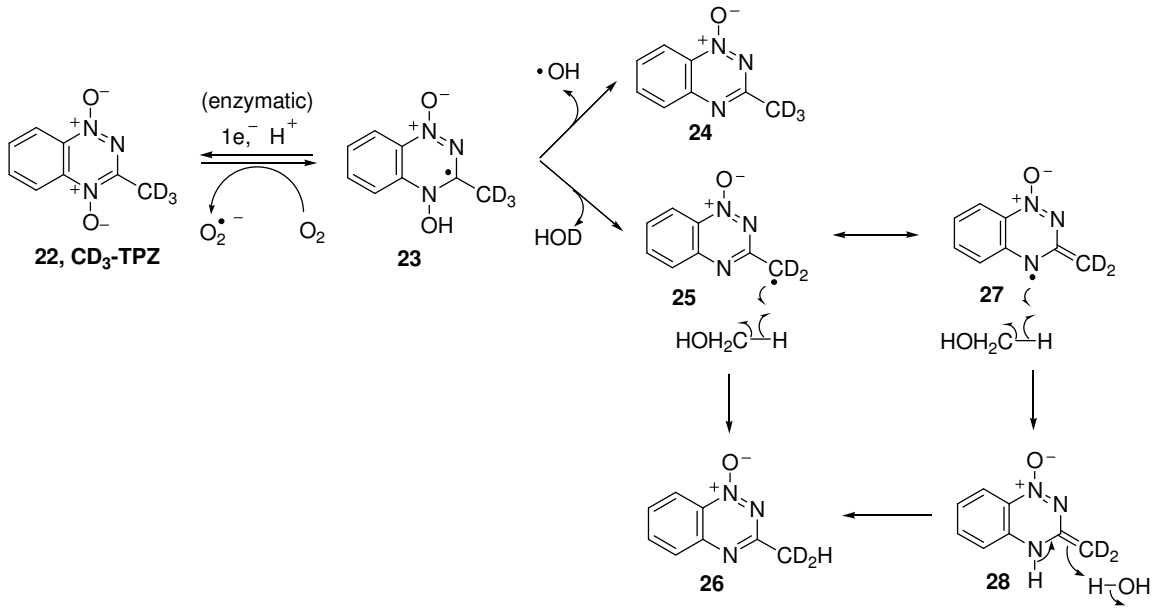

Scheme 1.9: Examine the formation of benzotriazenyl radical from activated **22**

As part of our goal to examine the dehydration mechanism in activated **22**, we aimed to label the methyl group of Me-TPZ with deuterium. We reasoned that low pKa of methyl protons compared to aromatic protons in **8** might facilitate the labeling of methyl group under basic conditions.

1.5.2.1 Labeling of methyl group in Me-TPZ (8) with deuterium under basic conditions

In labeling of methyl group in **8**, we set to exploit low pKa of methyl group. Accordingly, **8** was dissolved in deuterated sodium phosphate buffer (pH 8 or pD 7.6, 100 mM) and the deuterium incorporation into methyl group was monitored at 25 ^{o}C by using ^{1}H-NMR spectroscopy (Scheme 1.10). Under the reaction conditions employed here, we observed incorporation of deuterium into methyl group of **8**. Integration of Me-TPZ protons in ^{1}H-NMR shows that 50% deuterium incorporation occurs in methyl group

and benzo protons are intact after 25 days at 24 ^{o}C. Further, ESI-MS experiments on deuterated Me-TPZ mixture reveal that 1:2.8:2.5:0.9 ratio of *no*n-deuterated:*mono*-deuterated:*di*-deuterated:*tri*-deuterated Me-TPZ (**29**).

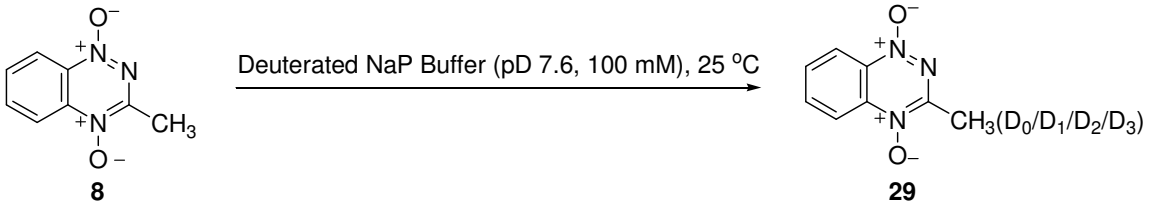

8 **29**

Scheme 1.10: Labeling of methyl group in Me-TPZ (**8**) under basic conditions

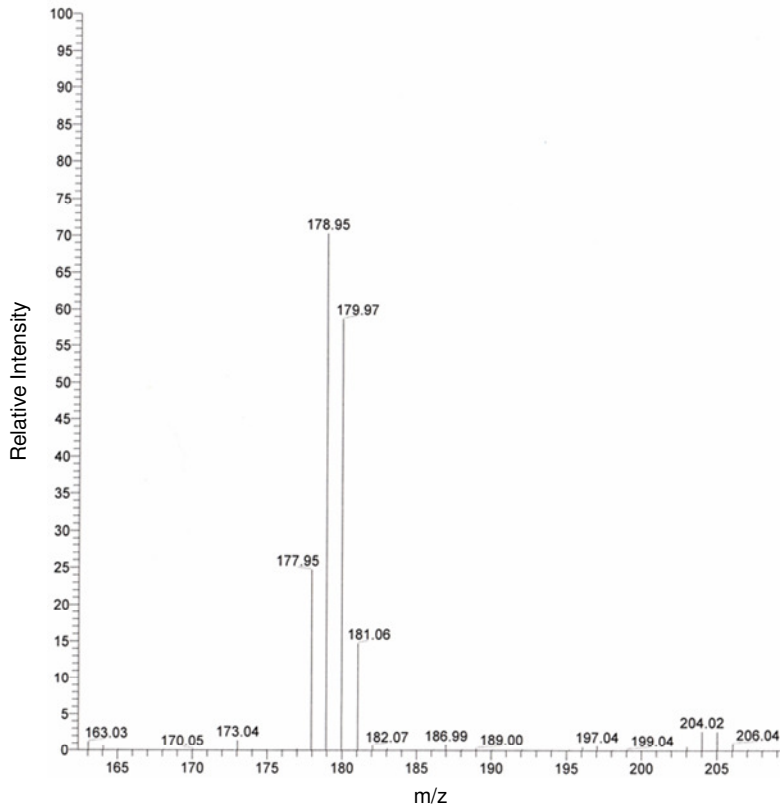

Figure 1.12: LC/ESI-MS trace of authentic deuterated mixture **29** obtained from base catalyzed deueterium incorporation into the compound **8**. Base catalyzed deuterium incorporation experiments carried out as we reported in experimental section.

To increase the rate of deuterium incorporation into methyl group of Me-TPZ, we increased the pH of sodium phosphate buffer to pH 9 or pD 8.6 (100 mM). But, our NMR and TLC experiments show that **8** decomposes at pH 9. The decomposition of **8** at pH 9 leads us to proceed our mechanistic studies with the deuterium labeled mixture of Me-TPZ (**29**).

1.5.2.2 Mechanistic studies with labeled Me-TPZ, 29

In our converse labeling experiments, we examined whether the dehydration mechanism occurs is in the activated labeled mixture **29**. If dehydration occurs in the activated labeled mixture **29**, the benzotriazinyl radicals generated in this process should be trapped by excess hydrogen atom donor CH_3OH in sodium phosphate buffer and thus leads to loss of deuterium in the mixture of 1-*N*-oxide metabolites (**30**) (Scheme 1.9). On the other hand, if activated labeled mixture **29** releases hydroxyl radical no deuterium loss is expected (Scheme 1.9). Loss of deuterium in the 1-*N*-oxide metabolites (**30**) can be detected and quantified by LC/ESI-MS analysis in positive ion mode.

Accordingly, labeled Me-TPZ mixture (**29**) was activated in the presence of excess CH_3OH in sodium phosphate buffer and 1-*N*-oxide metabolites (**30**) generated from these reactions were analyzed by LCESI-/MS in positive ion mode. Our LC/ESI-MS data show that there is no significant deuterium loss in 1-*N*-oxide metabolites (**30**) in the presence of excess CH_3OH (Scheme 1.12). A control experiment contains no CH_3OH also show no significant deuterium loss in 1-*N*-oxide metabolites (**30**) (Scheme 1.11). These observations are consistent with the idea that activated **8** doesn't dehydrate to release benzotriazinyl radical (**11** or **12**).

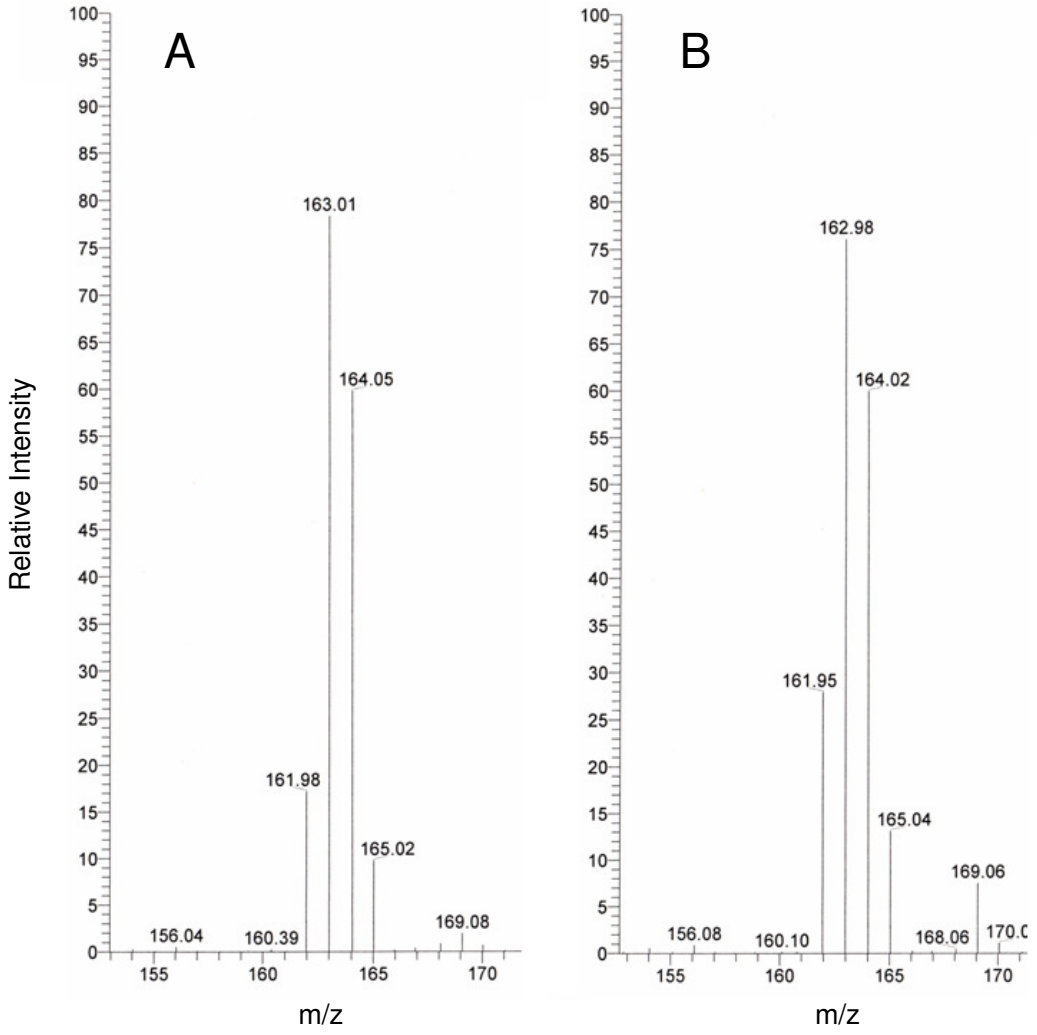

Figure 1.13: *In vitro* metabolism of deuterated mixture **29** in sodium phosphate buffer and w/wo hydrogen atom donor (CH_3OH). Deuterated mixture **29** yields predominantly deuterated mixture metabolite **30** with out significant loss of deuterium. Panel **A** shows mass spectrometric data obtained by LC-ESI/MS analysis of generated metabolite **30** in an experiment with no CH_3OH. Panel **B** shows mass spectrometric data obtained by LC-ESI/MS analysis of generated metabolite **30** in an experiment with CH_3OH.

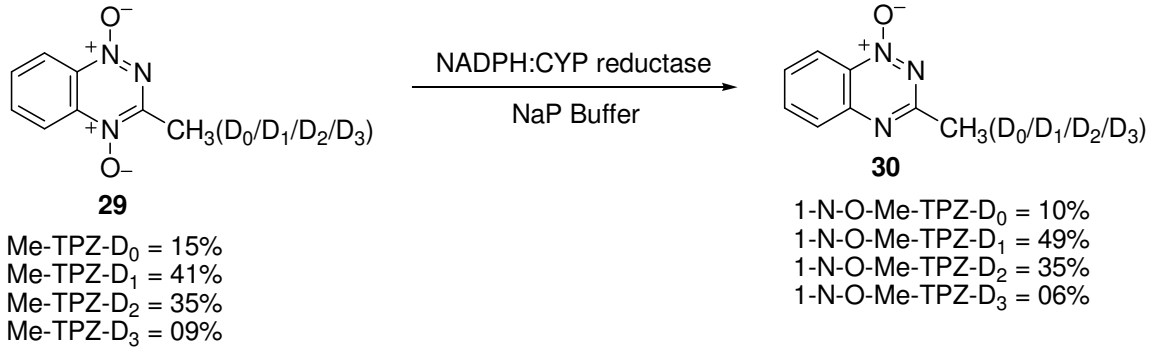

Scheme 1.11: Examination of proton incorporation in activated deuterium labeled Me-TPZ in the absence of CH_3OH

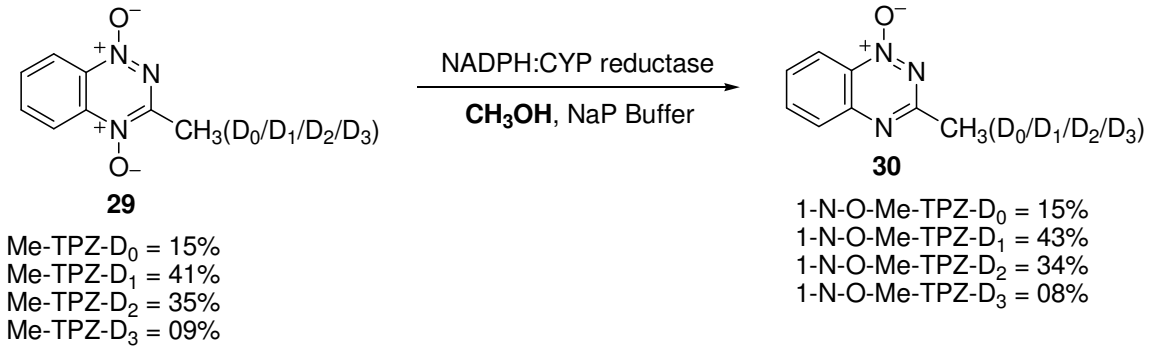

Scheme 1.12: Examination of proton incorporation in activated deuterium labeled Me-TPZ in the presence of CH_3OH

1.5.3 Isotopic labeling studies argue against dehydration mechanism

Our isotopic labeling studies with Me-TPZ (**8**) in excess CD_3OD, and with deuterium labeled mixture (**29**) in excess CH_3OH show that **8** does not dehydrate to release benzotrizinyl radical. The data directly argues against the dehydration mechanism and indirectly argues for hydroxyl radical mechanism in activated **8**. In our studies we asked whether **8** produces hydroxyl radical upon reductive activation (Scheme 1.13).

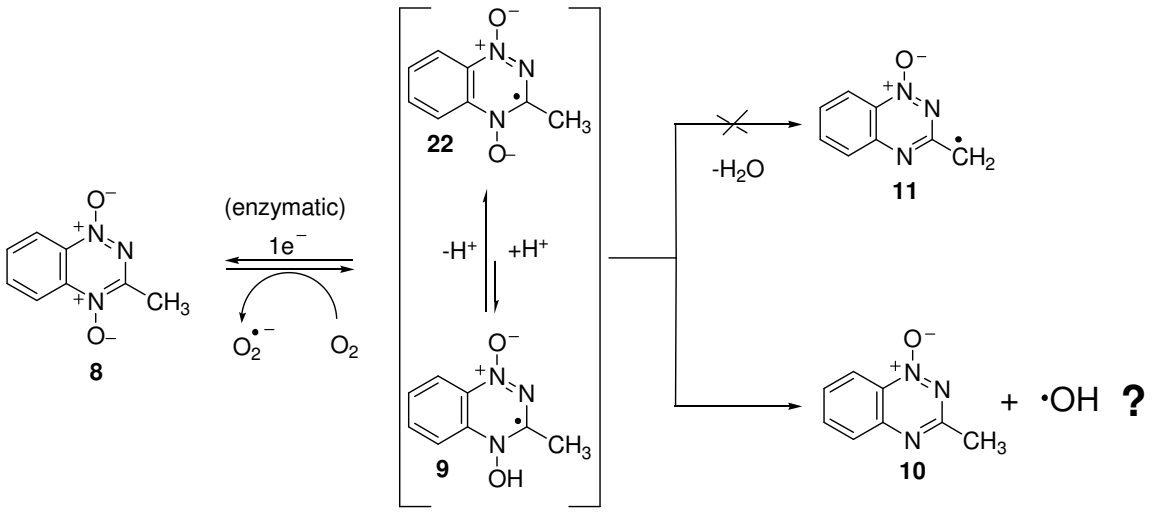

Scheme 1.13: Isotopic labeling studies argues against dehydration mechanism in **8**

1.6 Trapping of hydroxyl radical with DMSO

If activated **8** releases hydroxyl radical, we expect it might be possible to capture that radical with known trapping agents. For example, hydroxyl radical is known to oxidize DMSO to give methane sulfinic acid (**31**), which can be readily derivatized with diazonium salts (**32**) to generate methane diazosulfone (**33**) (Scheme 1.14).[32] The formation of diazosulfone (**33**) can be detected and quantified with HPLC.

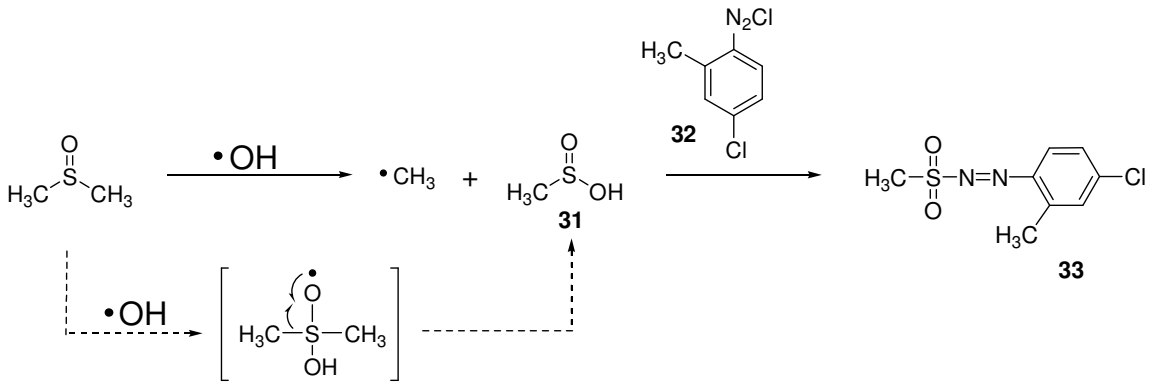

Scheme 1.14: Trapping of hydroxyl radical with DMSO

1.6.1 Activated TPZ and 8 hydroxylate DMSO and generates methane sulfinic acid (31)

Based on the isotopic labeling studies results, we assume that activated **8** releases hydroxyl radical. Here, we set to trap hydroxyl radical with DMSO. Accordingly, **8** was activated with NADPH:cytochrome p450 reductase under hypoxic conditions in the presence of excess DMSO. The methanesulfinic acid (**31**) generated in the presence of

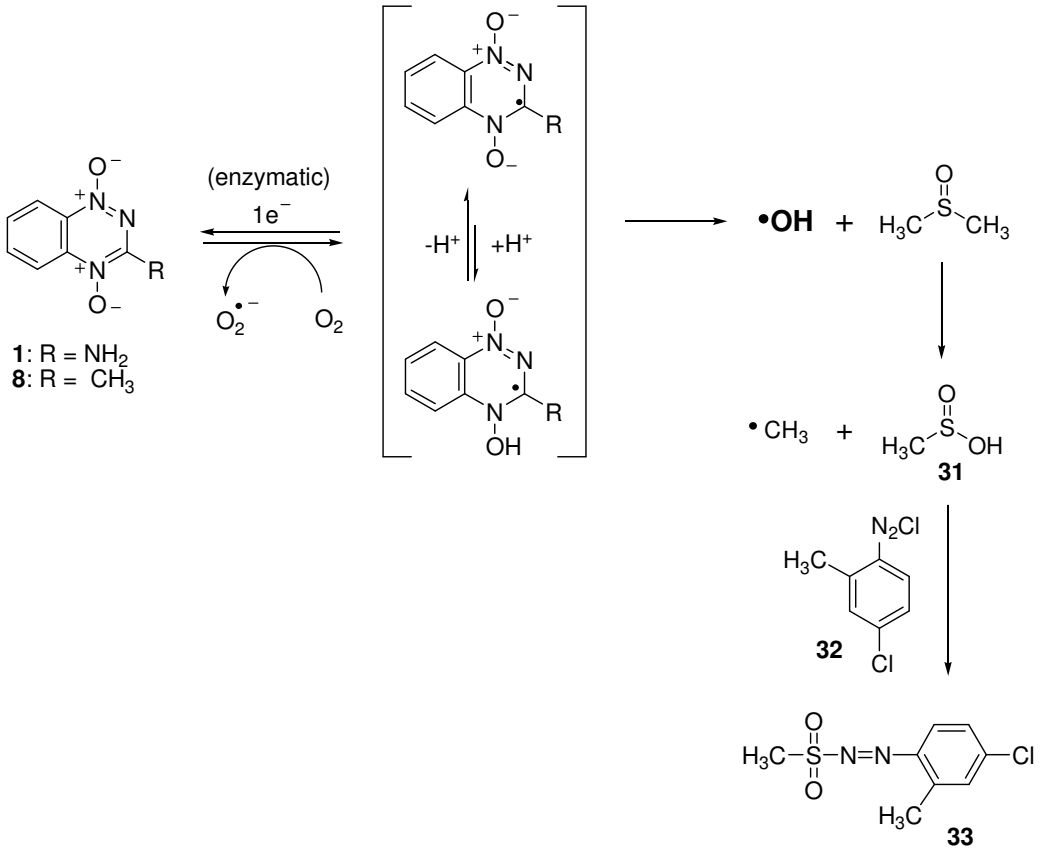

Scheme 1.15: Activated **8** and TPZ hydroxylate DMSO

activated **8** was derivatized with diazonium salt (**32**) to give the diazosulfone (**33**). The diazosulfone (**33**) was detected and quantified using HPLC. Our HPLC data show that activated **8** does indeed generate diazosulfone (**33**) under the reaction conditions

employed here (Figure 1.15). Further, formation of **33** from activated **8** was confirmed by co-injection of authentic diazosulfone (**33**) with the diazosulfone produced in Me-TPZ reaction. It is important to note that TPZ also hydroxylates DMSO upon reductive activation with NADPH:cytochrome p450 reductase under the same conditions employed here. This data is consistant with our earlier group data, where TPZ hydroxylated DMSO upon reductive activation with xanthine:xanthine oxidase under anaerobic conditions.[6]

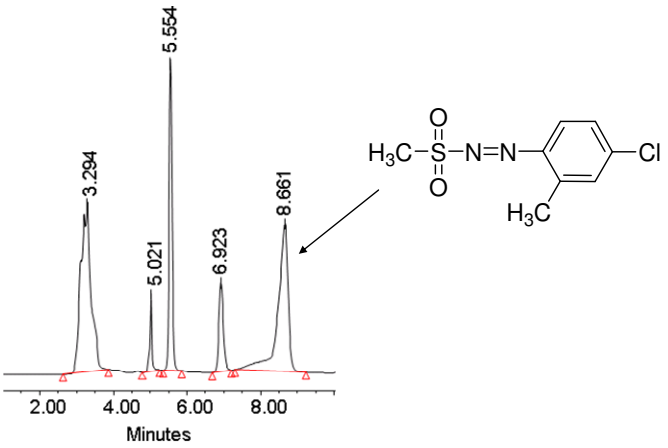

Figure 1.14: HPLC trace of diazosulfone produced in the reaction of reductively activated **8** with DMSO

Assay	**HPLC Peak Area for MSA-Diazosulfone**
NADPH+Cytochrome P450 Reductase	185791
NADPH+Me-TPZ	236871
NADPH+Cytochrome P450 Reductase+Me-TPZ	710105

Figure 1.15: HPLC peak areas of diazosulfone produced in control reactions and in the reaction of reductively activated **8**.

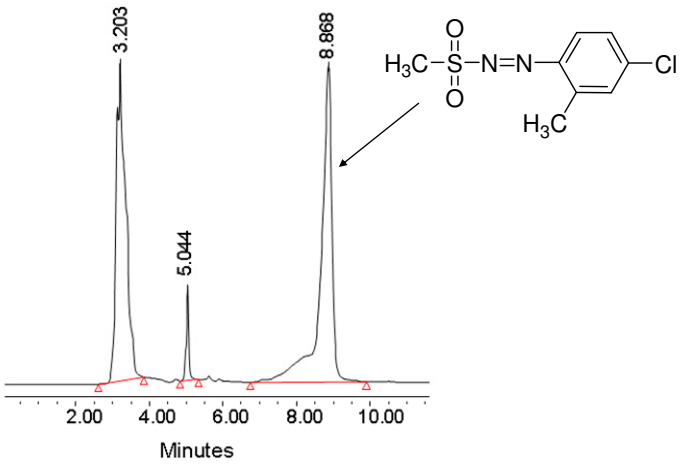

Figure 1.16: HPLC trace of diazosulfone produced in the reaction of reductively activated TPZ with DMSO.

Assay	**HPLC Peak Area for MSA-Diazosulfone**
NADPH+Cytochrome P450 Reductase	185791
NADPH+TPZ	248435
NADPH+Cytochrome P450 Reductase+TPZ	821425

Figure 1.17: HPLC peak areas of diazosulfone produced in control reactions and in the reaction of reductively activated TPZ.

1.6.2 Quantification of methane sulfinic acid (31) produced in the presence of activated 8 and TPZ

As part of our efforts to quantify the amount of methane sulfinic acid produced in the presence of activated TPZ and **8**, we constructed calibration curves by quantitative detection of known amounts of methanesulfinic acid (**31**). We also quantified the consumption of TPZ and **8** in their corresponding reactions by using the UV-Vis spectroscopy. We calculated yields of methane sulfinic acid generated based on the amount of TPZ or **8** consumed vs the amount of diazosulfone **33** produced in corresponding reactions. Our data show that activated TPZ produces 89% yield of

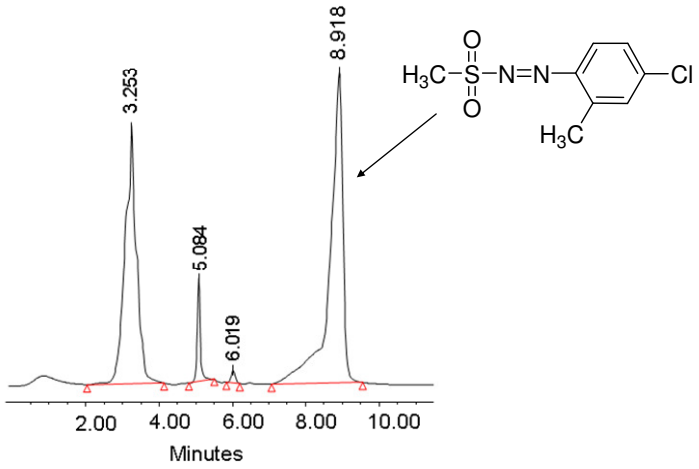

Figure 1.18: HPLC trace of diazosulfone (**33**) produced from derivatization of methanesulfinicacid (**31**)(500 µM)

Calibration Assay	**HPLC Peak Area for MSA-Diazosulfone**
0.1 µmol MSA (1 mL of 100 µM soln)	173242
0.2 µmol MSA (1 mL of 200 µM soln)	316948
0.3 µmol MSA (1 mL of 300 µM soln)	483191
0.4 µmol MSA (1 mL of 400 µM soln)	541646
0.5 µmol MSA (1 mL of 500 µM soln)	692508

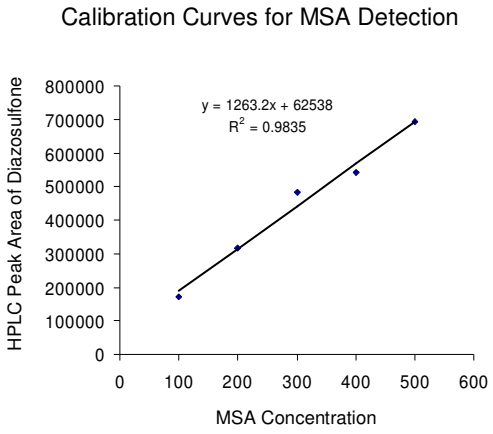

Figure 1.19: Calibration assays for detection of methanesulfinic acid (**31**)

methane diazosulfone **33**, whereas activated **8** produces 41% yield of methane diazosulfone **33**. Control reactions with incubation of DMSO with the NADPH:cytochrome P450 reductase (no **8** or TPZ) and with **8** or TPZ (no NADPH:cytochrome P450 reductase) produces only the small amounts of methane diazosulfone **33**.

The somewhat lower yield of methane sulfinic acid (**31**) produced in the presence of activated **8** compared to activated TPZ is interesting. For example, isotopic labeling studies on **8** argue against dehydration mechanism and indirectly argue for hydroxyl radical mechanism. However, the data presented here show that activated **8** produces lower yields of methane sulfinic acid irrespective of its inability to undergo dehydration. The low yield of methane sulfinic acid produced in activated **8** compared to in activated TPZ may be due to both one electron and two electron (one by one) reduction process occurs in **8** where as only one electron reduction occurs in TPZ in the presence of NADPH:cytochrome P450 reductase.

To understand the possibility of **8** to undergo two-electron reduction, we examined the metabolism of **8** or TPZ in the presence of oxygen by using UV-Vis spectroscopy. For example, if **8** or TPZ undergo one-electron reductive activation, we do not expect to observe the loss of **8** or TPZ in the presence of oxygen. On the other hand, if **8** and TPZ undergo two-electron reductive activation, we do observe the loss of **8** or TPZ. Accordingly, **8** and TPZ were activated with NADPH:cytochrome P450 reductase under aerobic conditions and the rate of metabolism of **8** and TPZ were monitored by UV-Vis spectroscopy at 400 nm and 474 nm respectively. Our data show that the rate of metabolism of **8** is less oxygen sensitive compared to rate of metabolism of TPZ (Figure

1.17). This data suggest that **8** may undergo both one-electron and two-electron reductive activation.

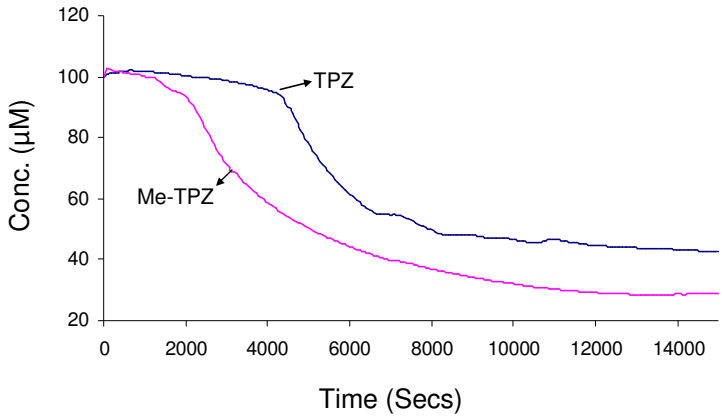

Figure 1.20: Rate of metabolism of **8** and TPZ in the presence of NADPH:cytochromeP450 reductase under aerobic conditions and at pH 7. In a typical assay, a solution containing **8** (100 µM) or TPZ (100 µM), desferal (1 mM) and sodium phosphate buffer of pH 7 (50 mM) was incubated with NADPH (500 µM) / CytP450 (50 mU) at room temperature. The loss of **8** and TPZ was monitored at 400 nm and 474 nm respectively.

1.7 Activated TPZ and Me-TPZ (8) hydroxylate salicylic acid (34)

Hydroxylation of salicylic acid is the well known detection method for hydroxyl radical.[33] Our group hypothesized that if **8** and TPZ release hydroxyl radical on reductive activation, these compounds should also hydroxylate salicylic acid on reductive activation. Accordingly, Sarmistha Sinha in our group set to trap hydroxyl radical released from activated **8** and TPZ with salicylic acid (**34**). Data show that activated TPZ and **8** in the presence of salicylic acid gave 2,3-dihydroxy-salicylic acid (**36**) and 2,5-dihydroxy-salicylic acid (**35**), which is a qualitative test for hydroxyl radical (Scheme 1.6). This data further confirm that activated **8** and TPZ release the well known DNA-damaging agent, hydroxyl radical, which is consistent with our earlier studies.

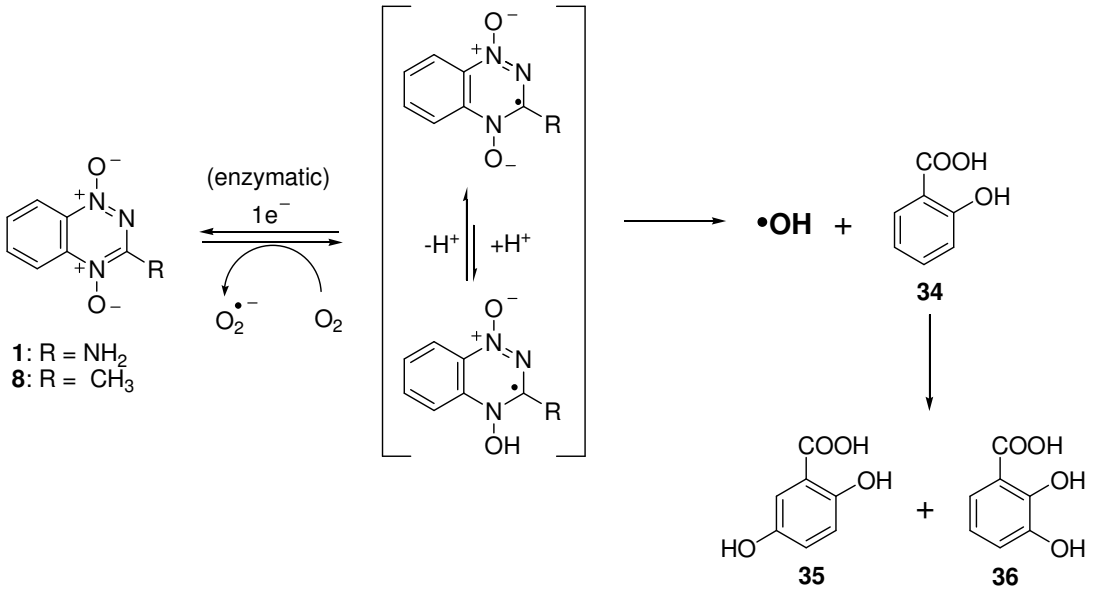

Scheme 1.16: Activated TPZ and **8** hydroxylate salicylic acid (**34**)

1.8 Conclusions

In this chapter, we used TPZ analog, **8** as a tool to examine dehydration mechanism in 1,2,4-benzotriazine di-oxides. As part of our studies, we probed the DNA cleavage properties of **8** under hypoxic conditions. Our data reported here show that **8** shows comparable hypoxia selective DNA strand cleavage to TPZ upon one-electron reductive activation, which is consistent with its potent hypoxia-selective cytotoxicity against cancer cell lines. Isotopic labeling studies with **8** provide evidence against the formation of benzotriazinyl radical (**11** or **12**). Studies with labeled mixture **29** further support the evidence against the dehydration mechanism and indirectly argues for hydroxyl radical mechanism.

Comparable DNA cleavage by **8** to TPZ irrespective of its ability to undergo dehydration mechanism suggests that this drug releases hydroxyl radical on reductive activation. Hydroxylation of DMSO and salicylic acid in the presence of activated **8** and

TPZ supports for hydroxyl radical mechanism. Sequence independent DNA cleavage by **8** and TPZ is also consistent with the involvement of hydroxyl radical. Our overall results suggest that **8** and TPZ on one-electron reductive-activation releases the well known DNA damaging agent, hydroxyl radical.

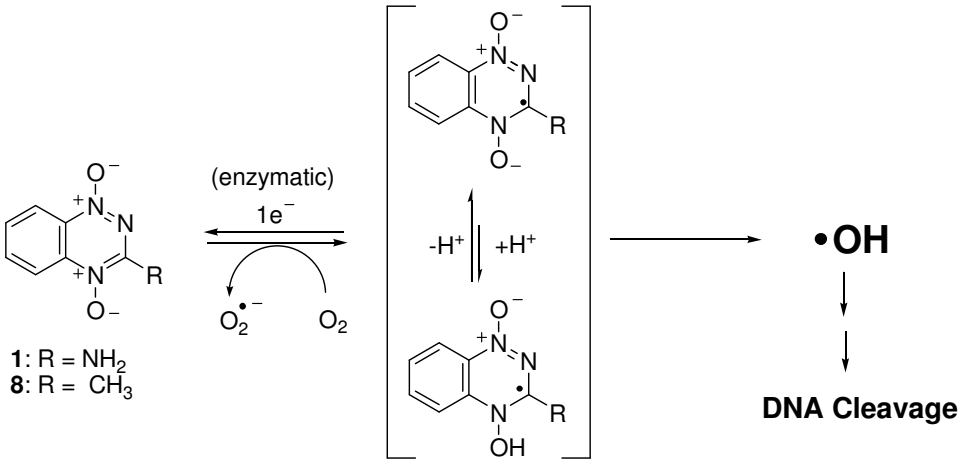

Scheme 1.17: General mechanism for DNA cleavage by **8** and TPZ

Overall, we have presented the results of various mechanistic studies, which support the hypothesis that on one-electron reductive-activation, 1,2,4-benzotriazine-1,4-dioxides releases well known DNA damaging agent, hydroxyl radical. Thus, our studies suggest that benzotriazine-dioxides deliver hydroxyl radical, the active agent of radiotherapy, selectively to the hypoxic cells found in tumors.

1.9 Experimental

Materials. Materials with highest purity available were obtained from following sources. Sodium phosphate, mannitol, DMSO and TLC plates from Aldrich Chemical Co. (Milwaukee, WI); NADPH, desferal, cytochrome P450 reductase, catalase, calf thymus DNA, and SOD from Sigma Chemical Co. (St. Louis, MO); agarose from Seakem; HPLC grade solvents (acetonitrile, methanol, ethanol, *tert*-butyl alcohol), ethyl acetate, hexane, and acetic acid from Fischer (Pittsburg, PA); ethidium bromide from Roche Molecular Biochemicals (Indianapolis, IN); Silica gel (0.04-0.063 mm pore size) for column chromatography from Merck; The plasmid pGL2BASIC was prepared using standard protocols.[34] TPZ, 1-*N*-oxide of TPZ (**10**) and no-*N*-oxide of TPZ (**18)** were synthesized according to literature methods.[26] High resolution mass spectroscopy was performed at the University of Illinois Urbana-Champaign Mass Spectroscopy facility and low resolution mass spectroscopy were performed at the University of Missouri-Columbia. NMR spectra were recorded using Bruker DRX 500 or ARX 250 MHz instruments at the University of Missouri-Columbia.

1.9.1 Synthesis of Me-TPZ (8)

Synthesis of 3-methyl-1,2,4-benzotriazine (18). The compound **18** was synthesized by the synthetic route designed by Khodja and coworkers with minor change.[24] In our procedure, dry ethanol and hydrated form of PtO_2 was used instead of anhydrous PtO_2 in the cyclization step.

1.9.1.1 Synthesis of 2-nitrophenyl hydrazone of pyruvic acid (17). Sodium pyruvate (**16**) (1.1 g, 10 mmol) and 2-nitrophenyl hydrazine (**15**) were dissolved in 10 mL of 35%

ethanolic solution of perchloric acid. Immediately, a yellow compound precipitated and was sequentially filtered, washed with water until neutral pH and dried. Finally the compound was purified with recrystalization by using toluene (400 mL) to obtain hydrazone **17** (1.9 g, 8.52 mmol) in 85 % yield: ^{1}H-NMR (300 MHz, DMSO-d6) δ 12.80 (s, 1H), 10.61 (s, 1H), 8.15 (dd, 1H), 8.02 (d, 1H), 7.74 (t, 1H), 7.07 (t, 1H); ^{13}H-NMR (300 MHz, DMSO-d6) δ 165.40, 140.21, 140.07, 136.61, 132.57, 125.70, 120.41, 116.37, 11.20.

1.9.1.2 Synthesis of 3-methyl-1,2,4-benzotriazine (18). Hydrazone **17** (669 mg, 3 mmol) dissolved in 50 mL of dry ethanol was hydrogenated in the presence of hydrated PtO_2 (50 mg, 0.2 mmol) at room temperature (25 ^{o}C) and atmospheric pressure for 24 h. Then solvent was evaporated and the product was extracted into hexane. Hexane was evaporated and the resultant residue was purified with flash column chromatography by using 1:4 EtOAc:hexane solvent system to obtain 3-methyl-1,2,4-benzotriazine (**18**) (180 mg, 1.24 mmol) in 42% yield. R_f = 0.68 (1:1 EtOAc/hexane): ^{1}H-NMR ($CDCl_3$, 500 MHz) δ 3.15 (s, 3H), 7.83 (m, 1H), 7.97 (m, 2H), 8.51 (d, *J* = 8.41 Hz, 1H); ^{13}C-NMR ($CDCl_3$, 125.8 MHz) 163.42, 146.02, 140.77, 135.46, 129.92, 129.57, 128.34, 24.27; HRMS ESI $[M+H]^+$ calcd for $C_8H_8N_3$ 146.0718, found 146.0718.

1.9.1.3 Oxidation of 3-methyl-1,2,4-benzotriazine (18). Compound **18** (50 mg, 0.3448 mmol) was dissolved in dichloromethane (10 mL) at 25 ºC and MCPBA (177.16 mg, 1.03 mmol) was added and the resultant reaction mixture stirred at room temperature until the disappearance of the starting material. After the evaporation of the solvent, the resulting residue was purified by gravity column chromatography (3:5 EtOAc/hexane) to

afford 2-*N*-oxide (**19**) (12 mg, 0.07 mmol, 22%), 1-*N*-oxide (**10**) (6 mg, 0.04 mmol, 11%) and Me-TPZ (**8)** (5 mg, 0.05 mmol, 8%).

R_f of 2-*N*-oxide (**19**) is 0.64 (1:1 EtOAc/hexane): ^{1}H-NMR of **19** ($CDCl_3$, 500 MHz) δ 2.87 (s, 3H), 7.71 (m, 1H), 7.75 (ddd, *J* = 6.85, 5.65, 1.51 Hz, 1H), 7.84 (dd, *J* = 7.21, 0.91 Hz, 1H), 7.89 (dd, *J* = 7.08, 0.95 Hz, 1H); ^{13}C-NMR ($CDCl_3$, 125.8 MHz) 154.98, 141.68, 132.61, 132.43, 131.64, 128.02, 125.47, 20.92; HRMS ESI $[M+H]^+$ calcd for $C_8H_8N_3O$ 162.0667, found 162.0670.

R_f of 1-*N*-oxide (**10**) is 0.51 (1:1 EtOAc/hexane): ^{1}H-NMR of **10** ($CDCl_3$, 500 MHz) δ 2.80 (s, 3H), 7.69 (ddd, *J* = 7.07, 5.56, 1.28 Hz, 1H), 7.94 (m, 2H), 8.45 (d, *J* = 8.72 Hz, 1H); ^{13}C-NMR ($CDCl_3$, 125.8 MHz) 163.82, 147.23, 135.36, 132.85, 129.65, 128.30, 119.85, 23.59; HRMS ESI $[M+H]^+$ calcd for $C_8H_8N_3O$ 162.0667, found 162.0671.

R_f of Me-TPZ (**8**) is 0.48 (EtOAc): ^{1}H-NMR of **8** (D_2O, 500 MHz) δ 2.72 (s, 3H), 7.95 (t, *J* = 7.91 Hz, 1H), 8.15 (t, *J* = 7.92 Hz, 1H), 8.35 (d, *J* = 8.72 Hz, 1H), 8.40 (d, *J* = 8.75 Hz, 1H); ^{13}C-NMR ($CDCl_3$, 125.8 MHz) 155.03, 139.93, 138.42, 135.65, 133.74, 121.77, 119.04, 17.74; HRMS ESI $[M+H]^+$ calcd for $C_8H_8N_3O$ 178.0617, found 178.0613.

1.9.2 Concentration dependent DNA cleavage assays. In concentration dependent DNA cleavage assays, individual components, except DNA, NADPH, and enzymes were deoxygenated by using three cycles of freeze-pump-thaw in pyrex tubes and then torch-sealed under high vacuum. Sealed tubes were scored, and opened in a glove bag filled with argon, and used to prepare individual reactions. Enzymes, NADPH, and DNA were diluted with degassed water in the glove bag to prepare stock solutions. In all DNA cleavage assays, solutions of 30 μL containing supercoiled plasmid DNA (33 μg/mL),

NADPH (500 μM), cytochrome P450 reductase (0.03 units/mL), catalase (100 μg/mL), superoxide dismutase (10 μg/mL), sodium phosphate buffer (50 mM, pH 7.0), and desferal (1 mM) were incubated with different concentrations of **8** or TPZ (25 μM-150 μM) under anaerobic conditions at 25 ºC for 4 h. Then the reactions were stopped by adding 5 μL of 50% glycerol loading buffer and were loaded onto a 0.9% agarose gel. The gel was electrophoresed for approximately 2.5 h at 82 V in 1 X TAE buffer then stained in a solution of aqueous ethidium bromide (0.3 μg/mL) for 3 h. DNA in gel was visualized by UV-transillumination, and the amount of DNA in each band was quantified using an Alpha Innotech IS-1000 digital imaging system. The values reported are not corrected for differential staining of form I and form II DNA by ethidium bromide.

1.9.3 Inhibition of activated TPZ or 8 mediated DNA cleavage by radical scavengers. DNA-cleavage assays containing radical scavengers were carried out in a similar manner to the above experiments with the exception that radical scavengers such as a methanol, ethanol, *tert*-butyl alcohol, DMSO, or mannitol (500 mM) were added to the reactions before addition of cytochrome P450 reductase. Radical scavengers were deoxygenated by bubbling argon through each solution for 2 min. To prevent the background DNA damage from superoxide radical, superoxide dismutase, catalase and desferal were added to reactions.

1.9.4 Inhibition of menadione mediated DNA cleavage by radical scavengers. In menadione mediated DNA cleavage assays, supercoiled plasmid DNA (33 μg/mL, pGL-2 Basic), menadione (25 μM), NADPH (500 μM) and NADPH/cytochrome P450 reductase (1 mU) were incubated in sodium phosphate buffer (50 mM, pH 7) containing 2.5%

acetonitrile were incubated under aerobic conditions at 24 ^{o}C for 2 h. DNA cleavage assays containing radical scavengers were carried out in a manner identical to the standard reaction, except adding radical scavengers prior to the addition of NADPH and NADPH/cytochrome P450 reductase.

1.9.5 *In vitro* metabolic studies. In a metabolic studies assay, a solution containing **8** (500 μM) and desferal (1 mM) in sodium phosphate (pH 7, 50 mM) was deoxygenated by three freeze-pump-thaw cycles and then torch-sealed under vacuum. The sealed tube was scored before being transferred to an argon filled glove bag. The tube was then opened and degassed solution was transferred to an eppendorf tube. Then NADPH (1 mM), and cytochrome P450 reductase (0.33 U/mL), were added and the resulting samples were incubated in an argon filled glove bag at 25 ºC for 3 h. The proteins were then removed by centrifugation through Amicon Microcon (YM3) filters. The filtrate was analyzed by HPLC employing a C18 reverse phase Rainin Microsorb-MV column (5 μm particle size, 100 A˚ pore size, 25 cm length, 4.6 mm i.d.) eluted with gradient solvent system starting with 80% A (0.5% acetic acid in water) and 20% B (2:1 methanol/acetonitrile) followed by linear increase to 30% B from 0 min to 20 min. Then, 30% B was held until 30 min and in next 10 min 20% B was achieved. The flow rate of 0.9 mL/min was used and the products were monitored by UV-absorbance at 240 nm. In *vitro* metabolism of **8** by NADPH:cytochrome P450 reductase yields two products whose relative yields were estimated on the basis of their relative peak areas in the HPLC chromatogram. The major product was identified as 1-*N*-oxide (**10**) and minor product was identified as no-*N*-oxide (**18**) by co-injection of reaction mixture with authentic compounds.

In LC/MS analysis, metabolites were extracted into ethyl acetate and air dried, and redissolved in 50:50 methanol:water. Resultant metabolites were analyzed by LC/ESI-MS in positive ion mode.

1.9.6 Isotopic labeling studies. A solution containing **8** (1 M) was prepared by using deuterated sodium phosphate buffer (pH 7 or pD 6.6, 50 mM). Deuterated buffer (pH 7 or pD 6.6, 50 mM) was prepared by dissolving Na_2HPO_4 (20.5 mg, 28.9 mmol) and NaH_2PO_4 (12.7 mg, 21.2 mmol) in D_2O (5 mL). Then solution of **8** was deoxygenated by using three cycles of freeze-pump-thaw in pyrex tubes, followed by torch sealing. Pyrex tubes were scored, opened and transferred into an eppendorf tube in a glove bag filled with argon. Then the control reaction without addition of further additives, and reactions containing NADPH (2 mM or 3 mM) and NADPH/cytochrome P450 reductase (0.6 U/mL) with and without excess CD_3OD (2 M) were prepared with deoxygenated solution of **8** and incubated under argon atmosphere at 24 ^oC for 16 h. Then metabolites generated from these reactions were extracted into ethyl acetate (2 mL) and the resultant solutions were dried and redissolved in 300 μL of 1: 1 methanol:water. Then the metabolites were analyzed by using LC/ESI-MS in a positive ion mode. For the separation of metabolites on LC, we employed the same HPLC conditions that we used in metabolic studies.

1.9.7 Deuterium labeling of methyl group of 8 under basic conditions. In deuterium labeling experiment, **8** (1 mg) was dissolved in deuterated NaP buffer (pH 8 or pD 7.6, 100 mM) and resultant solution was incubated at 25 ^oC. Deuterated buffer (pH 8 or pD 7.6, 100 mM) was prepared by dissolving Na_2HPO_4 (66.2 mg, 93.3 mmol) and NaH_2PO_4

(4.1 mg, 6.7 mmol) in D_2O (5 mL). Deuterium incorporation into methyl group of **8** was monitored by using ^{1}H-NMR and Mass analysis. Data show that under the conditions employed here deuterium incorporation occurs and gives a mixture of *no*n-deuterated, *mono*-deuterated, *di*-deuterated and *tri*-deuterated Me-TPZ (**29**).

1.9.8 Reduction of deuterium labeled mixture (29) to 1-*N*-oxide (30). A solution containing labeled mixture **29** was prepared by using sodium phosphate buffer (pH 7, 50 mM). Then this solution was deoxygenated by using three cycles of freeze-pump-thaw in pyrex tubes, followed by torch sealing. Pyrex tubes were scored, opened and transferred into an eppendorf tube in a glove bag filled with argon. Then the control reaction without addition of further additives, and reactions containing NADPH (3 mM) and NADPH/cytochrome P450 reductase (0.6 U/mL) with and without excess CH_3OH (2 M) were prepared with deoxygenated labeled **29** solution and incubated under argon atmosphere at 24 ^oC for 16 h. Then metabolites generated from these reactions were extracted into ethyl acetate (2 mL) and the resultant solutions were dried and redissolved in 100 µL of 1:1 methanol:water. Then the metabolites were analyzed by using LC/ESI-MS in a positive ion mode. For the separation of metabolites on LC, we employed the same HPLC conditions that we used in metabolic studies of **8**.

1.9.9 Hydroxylation of DMSO with activated 8. Methanesulfinic acid (**31**) produced by the oxidation of DMSO was detected and quantitated using a modified version of the protocol reported by Fukui et al. [Fukui, S.; Hanasaki, Y.; Ogawa, S. *J. Chromatogr.* 1993, *630*, 187-193]. In a typical assay, individual components of the reactions were deoxygenated similar to earlier experiments. To a degassed solution containing TPZ or **8**

(500 μM), desferal (1 mM), deoxygenated DMSO (0.5 M or 1 M), sodium phosphate (50 mM, pH 7.0), were added NADPH (2 mM) and cytochrome P450 reductase (0.29 U/mL). The reaction (1 mL final volume) was capped, mixed, and allowed to incubate under argon atmoshere at 24 °C for 4 h. Then sodium phosphate (0.5 mL, 500 mM, pH 4.0) was added to the reaction, followed by Fast Red TR diazonium salt (**32**) (0.5 mL of 10 mg/mL) and the mixture allowed to stand at room temperature for 10 min. During 10 min orange color was developed and the resulting orange color solution was extracted with ethyl acetate (2 X 1 mL) and exactly 1.2 mL of the upper ethyl acetate layer recovered by pipet. A portion of this ethyl acetate solution (20 μL) containing the methane diazosulfone was then analyzed by HPLC. The diazosulfone conjugate monitored at 310 nm has a retention time of approximately 9 min on a Rainin Microsorb-MV propylamine column eluted with hexane-2-propanol (100:3) and flow rate of 1 mL/min.

1.9.10 Synthesis of authentic diazosulfone 33. The compound diazosulfone **33** was synthesized using synthetic route designed by Ahern and coworkers.[35] Briefly, diazonium salt (**32**) (55 mg, 0.214 mmol) and sodium methane sulfinate (20 mg, 0.196 mmol) in a 10 mL of dichloromethane was added. The mixture was stirred for 16 h at 25 ^{o}C. After 16 h reaction was stopped and salts were removed by filtration. Then the solvent was removed to give pure diazosulfone (**33**) (20 mg, 0.086 mmol) in 44% yield: ^{1}H-NMR of diazosulfone ($CDCl_3$, 500 MHz) δ 2.66 (s, 3H), 3.20 (s, 3H), 7.30 (dd, *J* = 2.5, 8.5 Hz, 1H), 7.42 (d, *J* = 2 Hz, 1H), 7.68 (d, *J* = 9 Hz 1H); ^{13}C-NMR ($CDCl_3$, 125.8 MHz) 17.69, 35.20, 118.09, 127.76, 132.14, 142.07, 143.48, 145.72; HRMS ESI $[M+Na]^+$ calcd for $C_8H_9N_2O_2SCl$ 254.9971, found 254.9972.

1.9.10.1 Calibration assays for detection of methane sulfinic acid (31). In calibration assays, known amounts of methanesulfinic acid was dissolved in sodium phosphate buffer (50 mM, pH 7.0) to make 1 mL of different concentrations of methane sulfinic acid (**31**) (100-500 µM). Then sodium phosphate buffer (0.5 mL, 500 mM, pH 4.0) was added to methane sulfinic acid solutions, followed by Fast Red TR diazonium salt (**32**) (0.5 mL of 10 mg/mL) and the resulting reactions were allowed to stand at room temperature for 10 min. During 10 min orange color was developed and the resulting orange color compound from these reactions was extracted into ethyl acetate (2 X 1 mL) and exactly 1.2 mL of the upper ethyl acetate layer recovered by pipet. A portion of this ethyl acetate solution (20 µL) containing the methane diazosulfone (**33)** was then analyzed and quantified by HPLC. Calibration curves for the detection of methanesulfinic acid (**31**) were constructed based on the amount of diazosulfone (**33**) produced at different concentrations of methane sulfinic acid (**31)**.

Supporting Information:

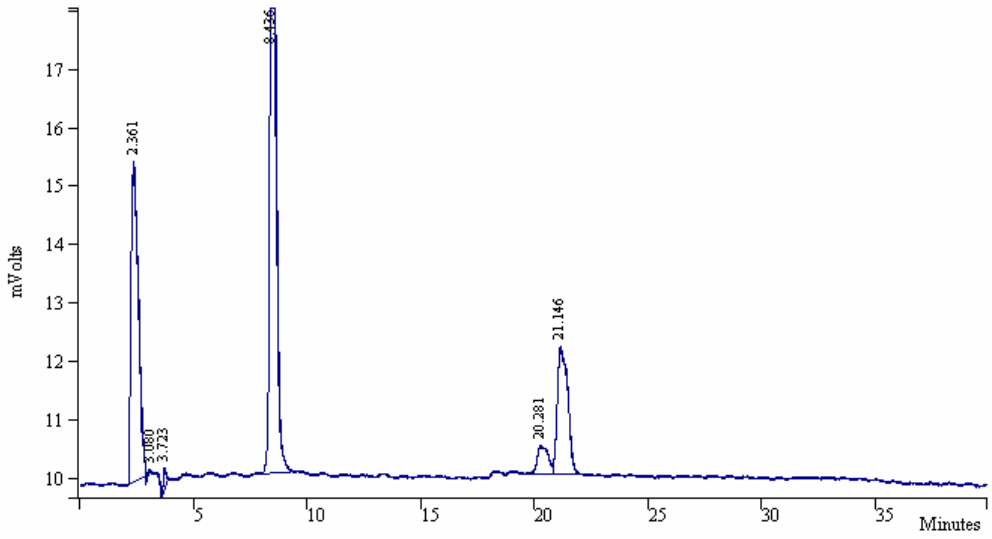

Figure S1.1: HPLC trace of products generated from *in vitro* metabolism of Me-TPZ

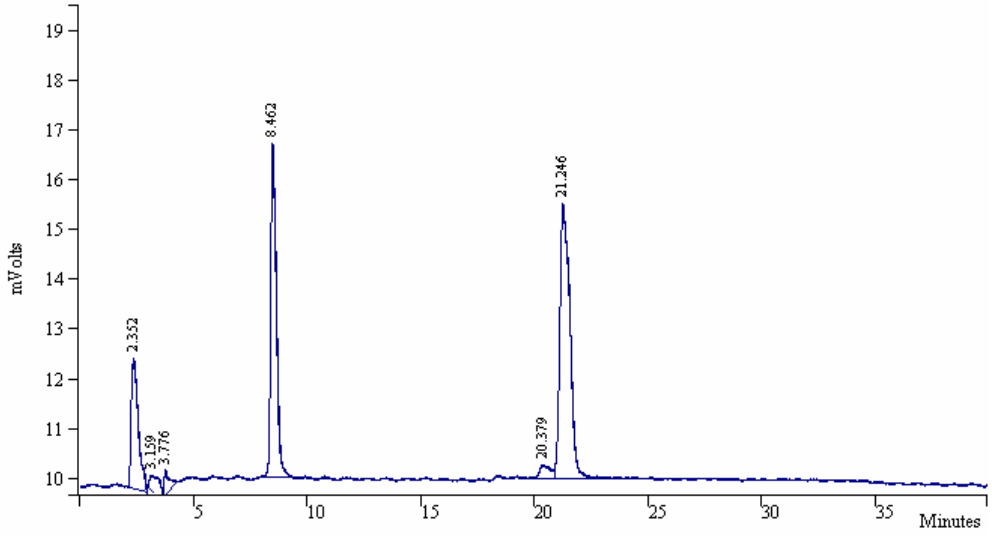

Figure S1.2: HPLC trace of reaction with co-injection of 1-*N*-oxide of Me-TPZ

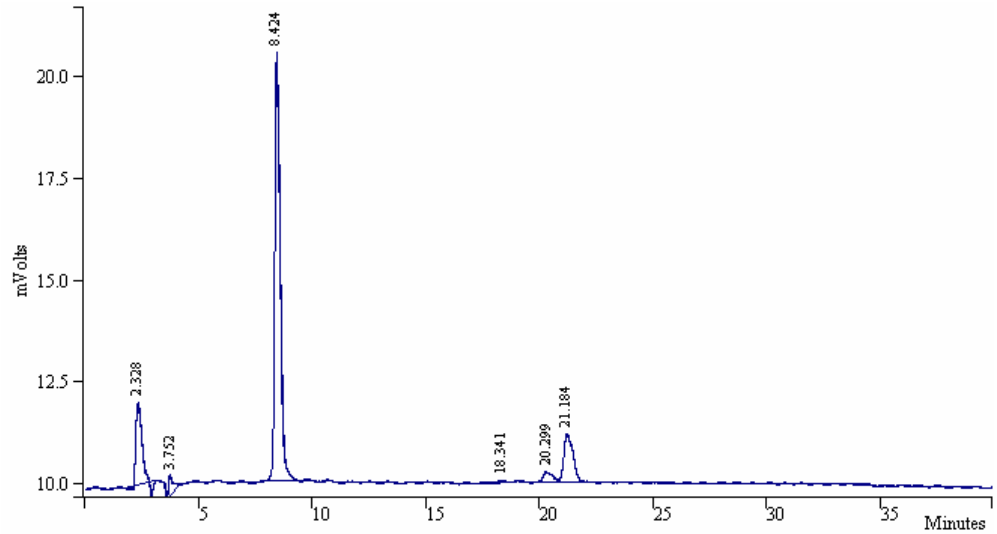

Figure S1.3: HPLC trace of reaction with co-injection of Me-TPZ

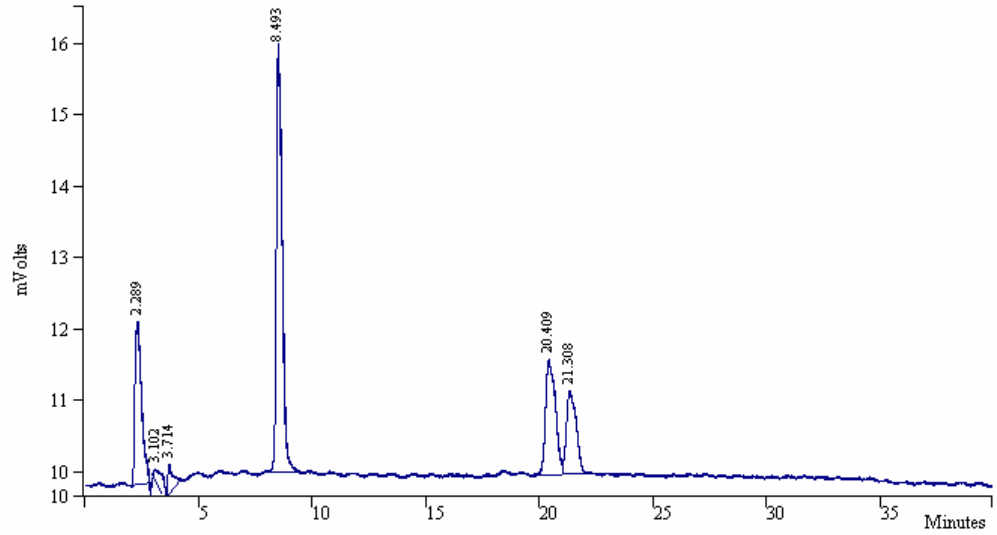

Figure S1.4: HPLC trace of reaction with co-injection of no-*N*-oxide of Me-TPZ

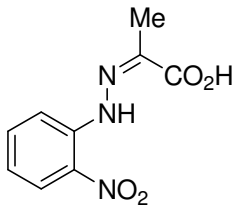

^{1}H-NMR of **17** in DMSO-d_6

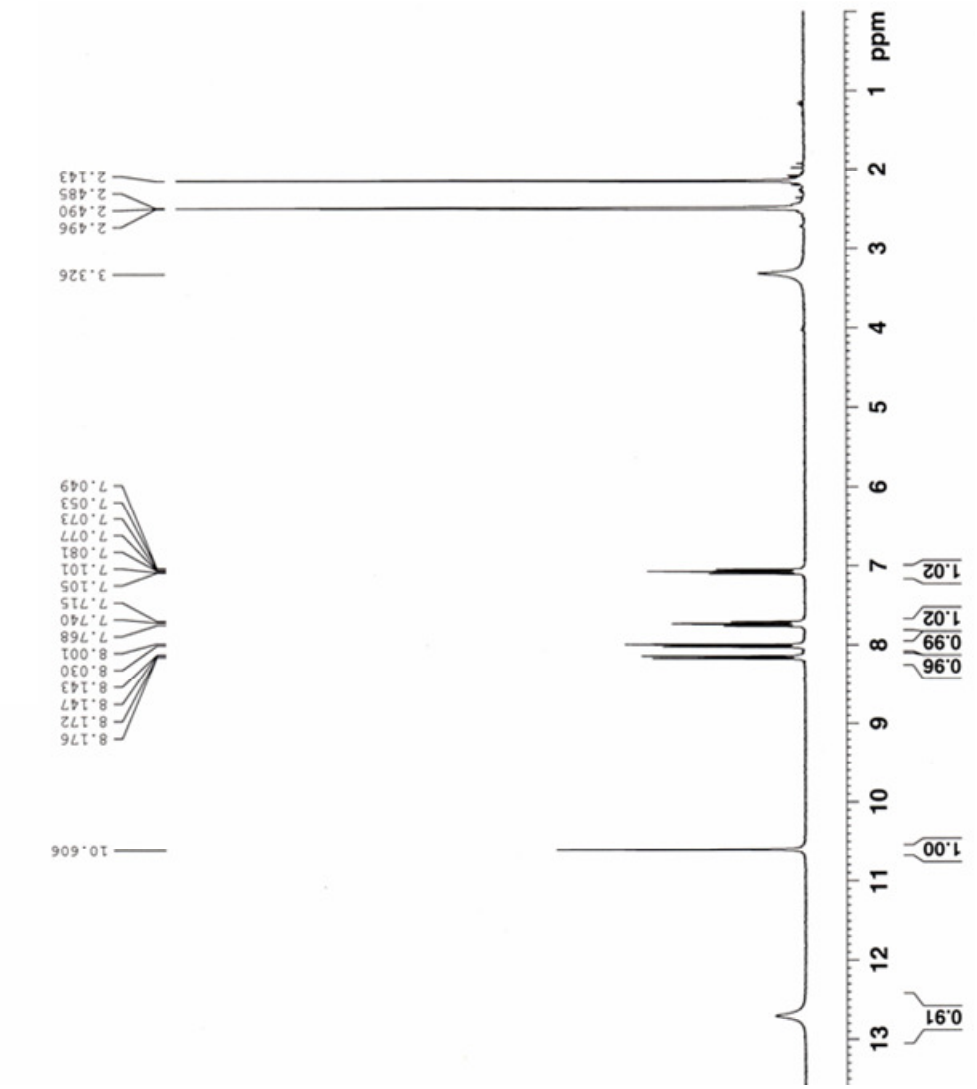

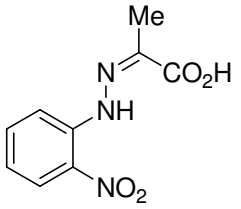

^{13}C-NMR of **17** in DMSO-d_6

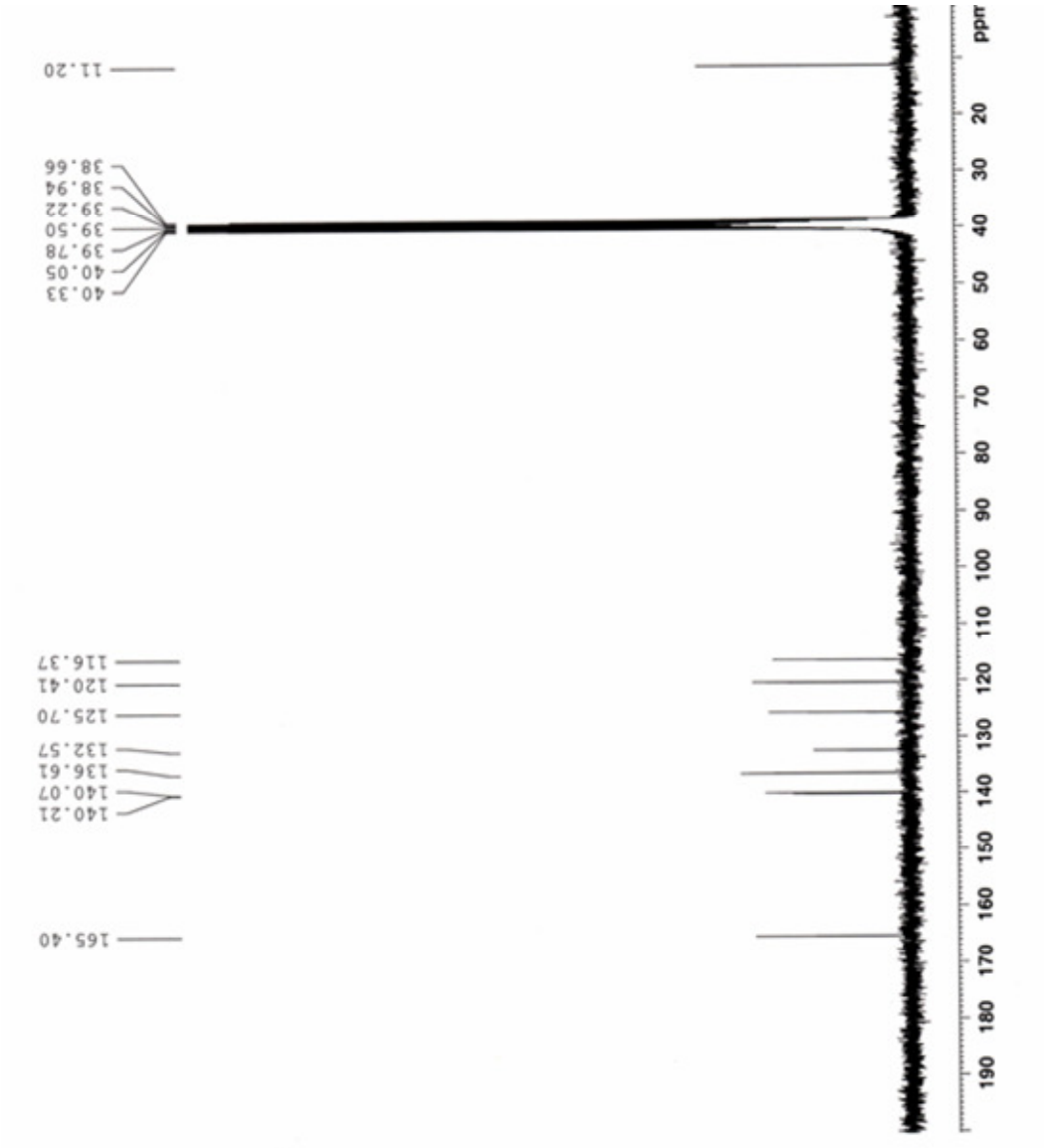

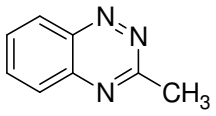

^{1}H-NMR of **18** in $CDCl_3$

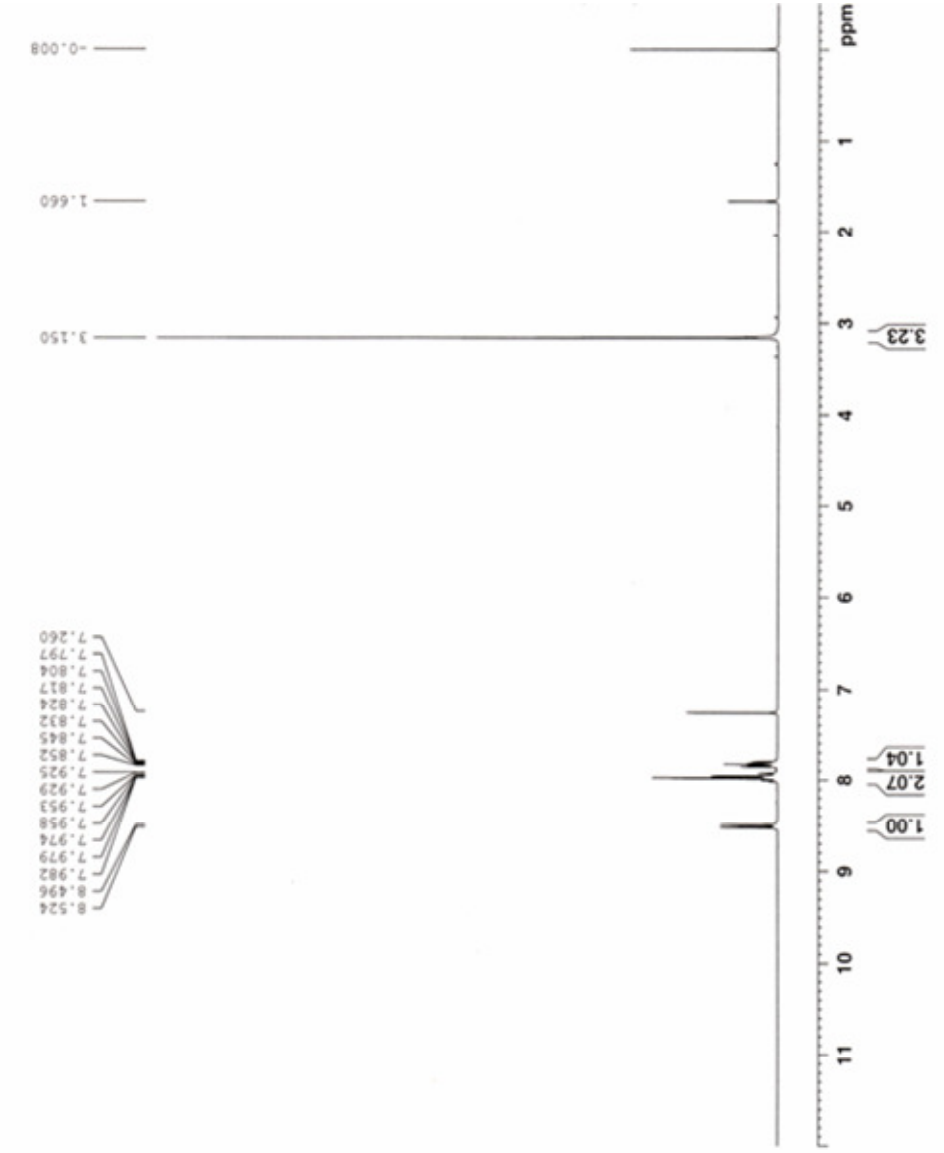

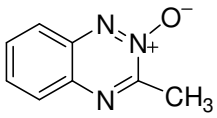

^{1}H-NMR of **19** in $CDCl_3$

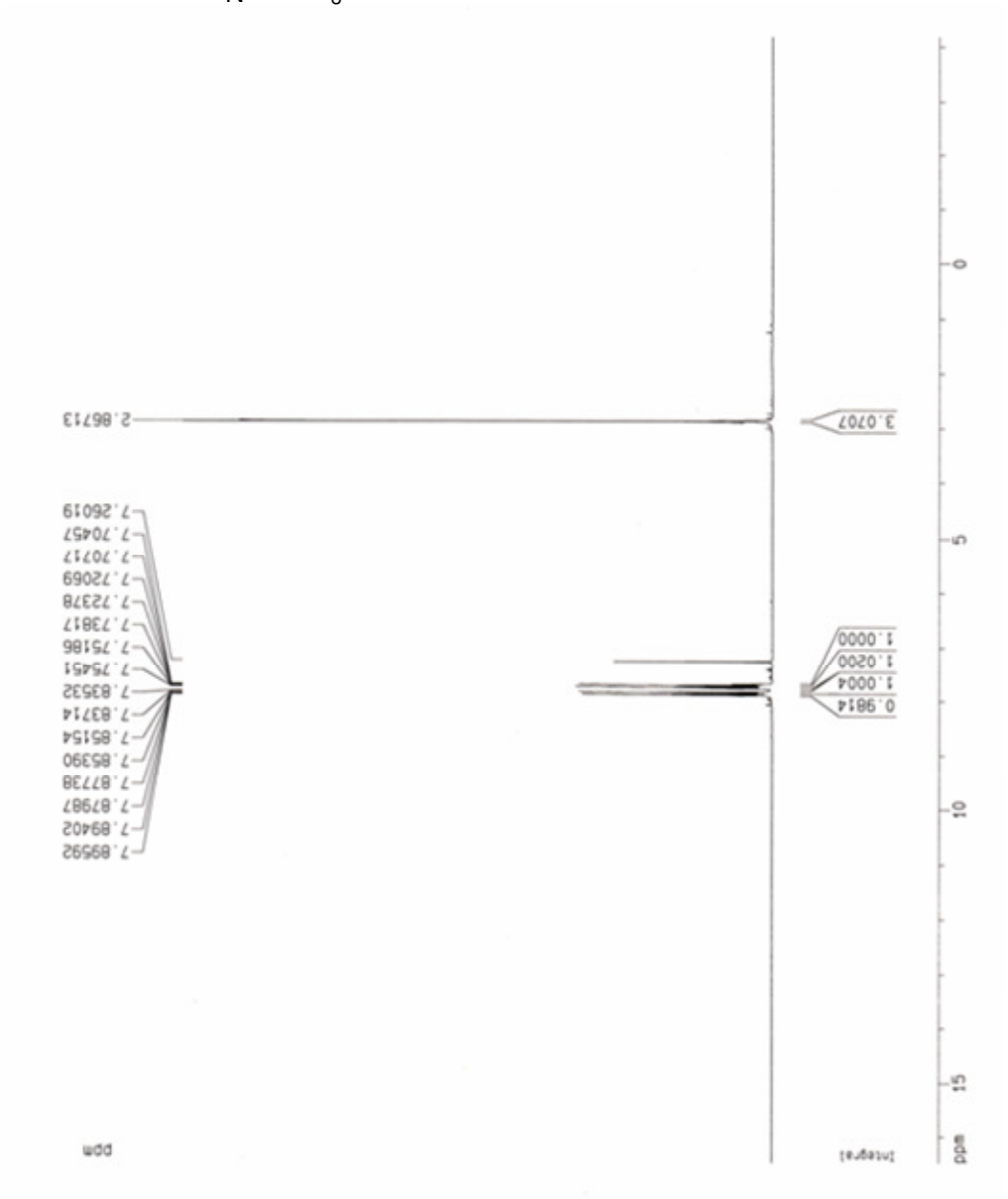

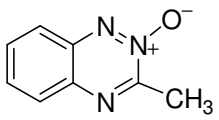

^{13}C-NMR of **19** in $CDCl_3$

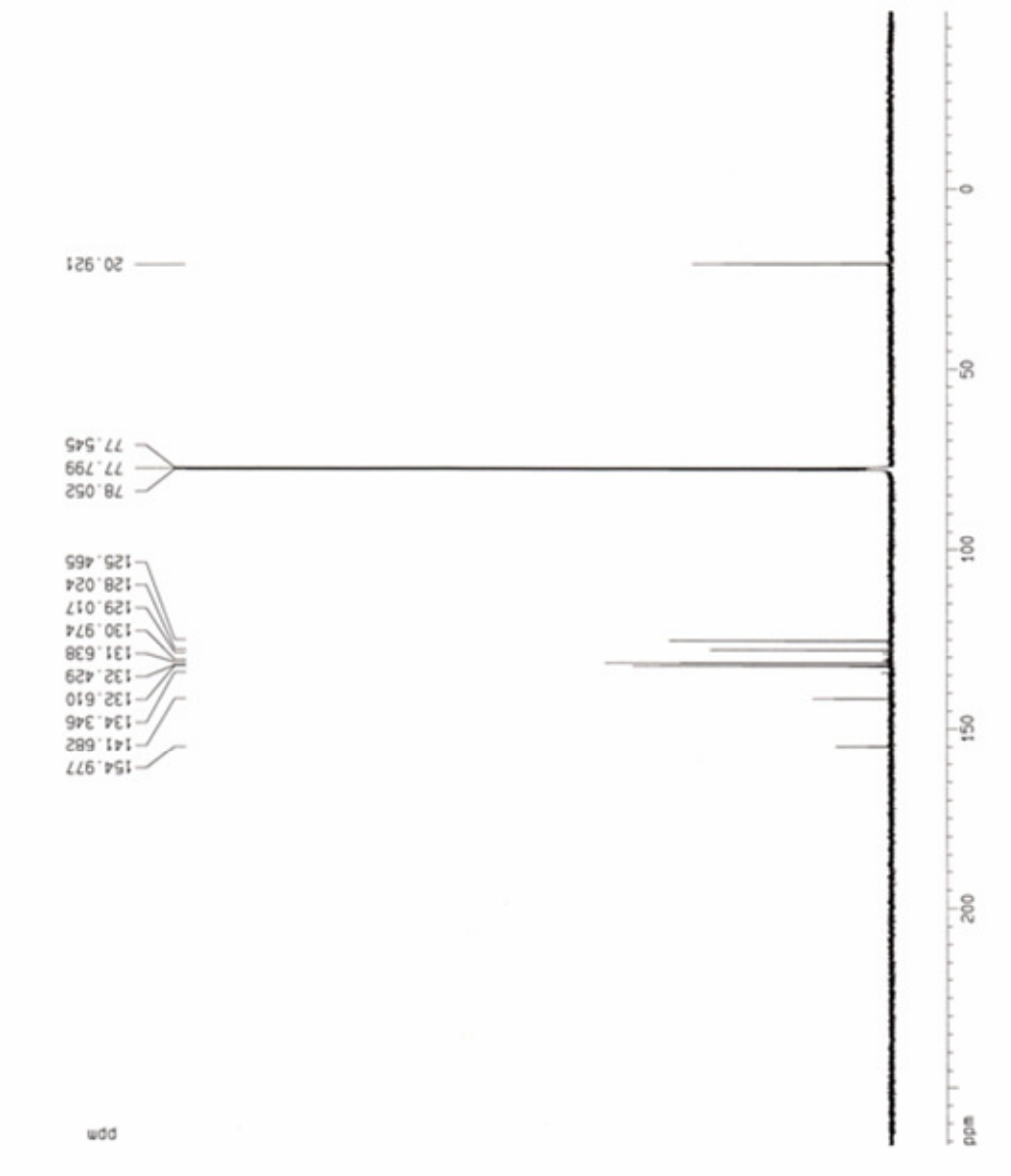

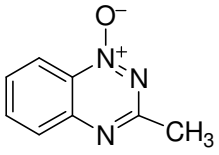

^{1}H-NMR of **10** in $CDCl_3$

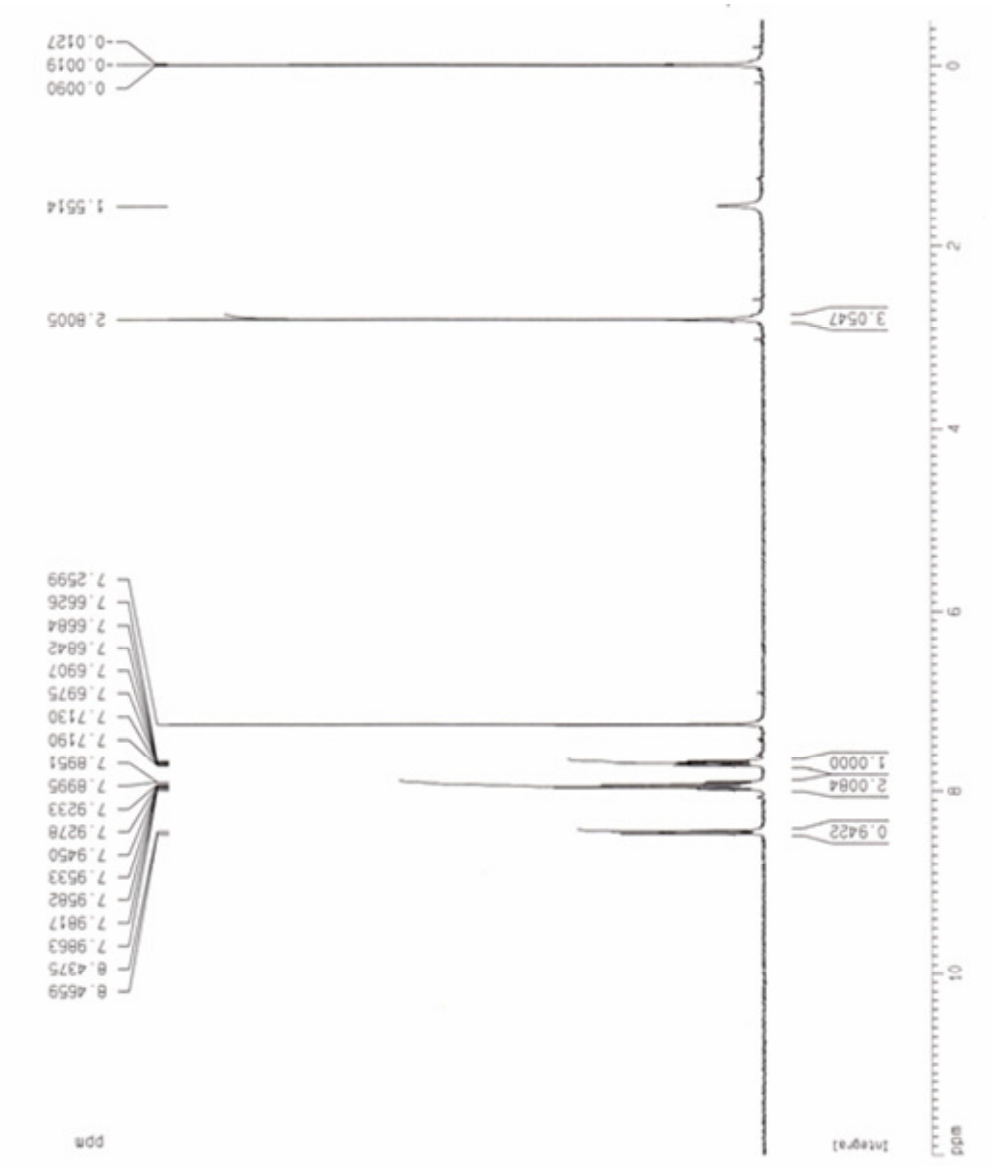

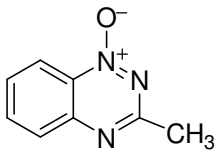

^{13}C-NMR of **10** in $CDCl_3$

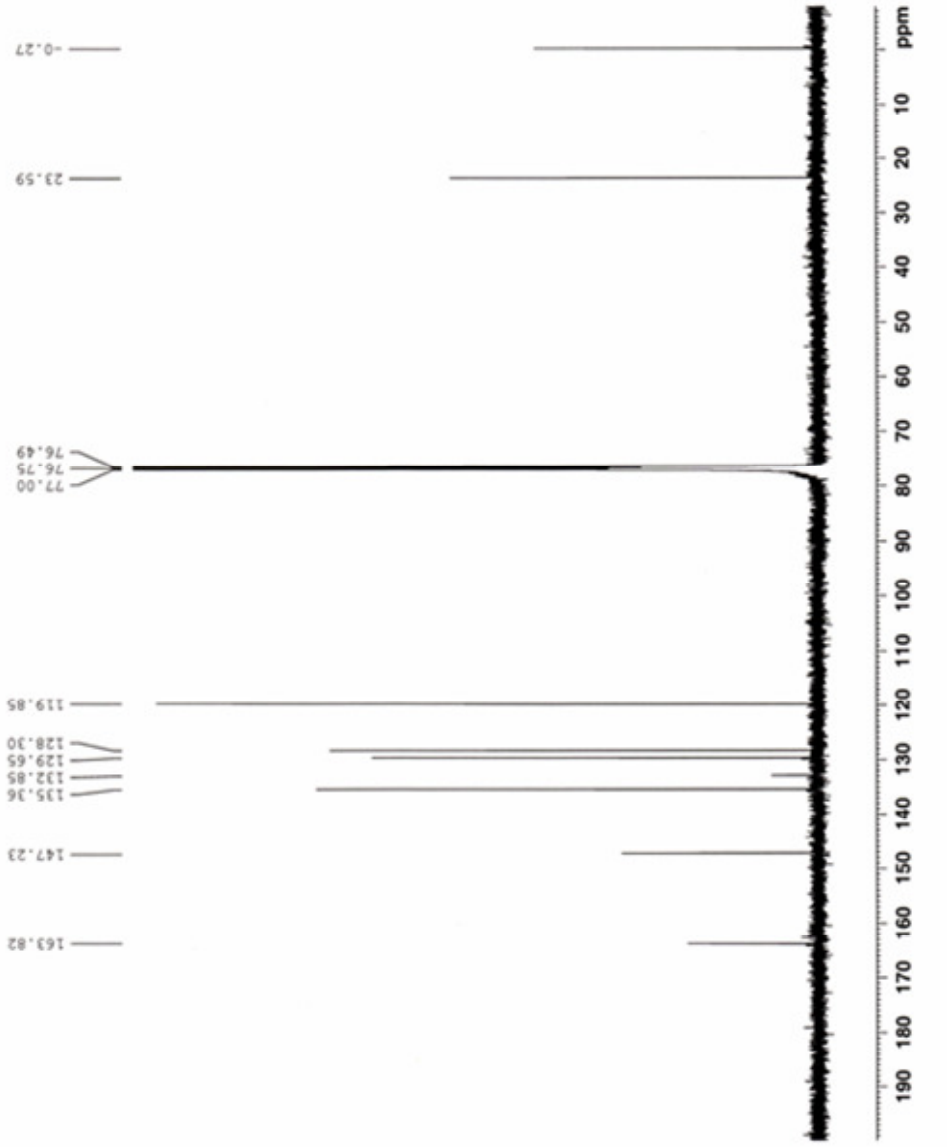

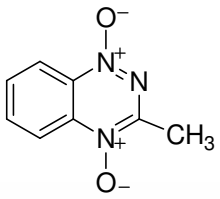

^{1}H-NMR of **8** in D_2O

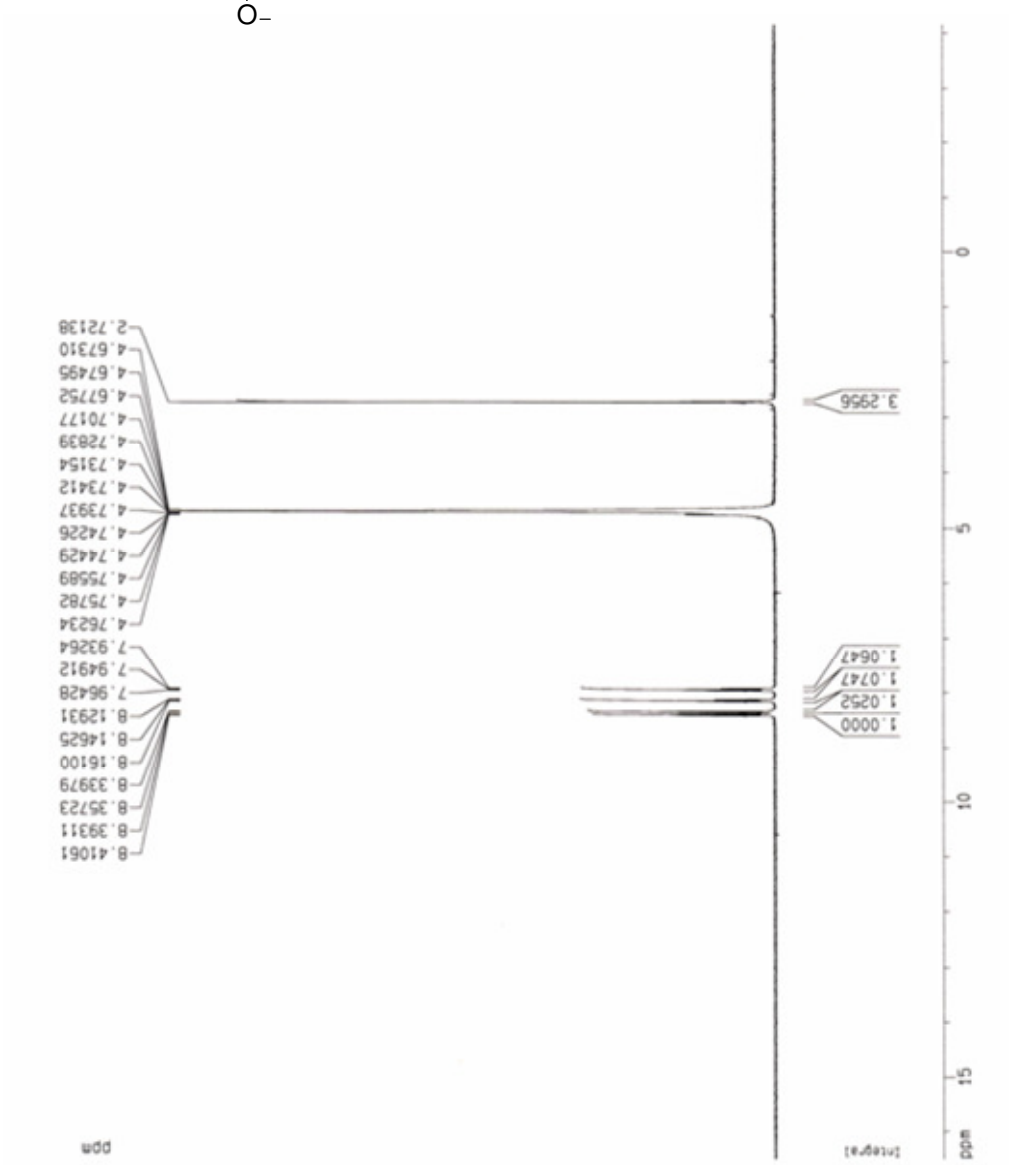

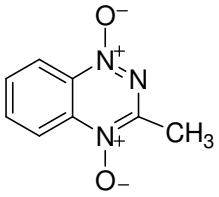

^{13}C-NMR of **8** in D_2O

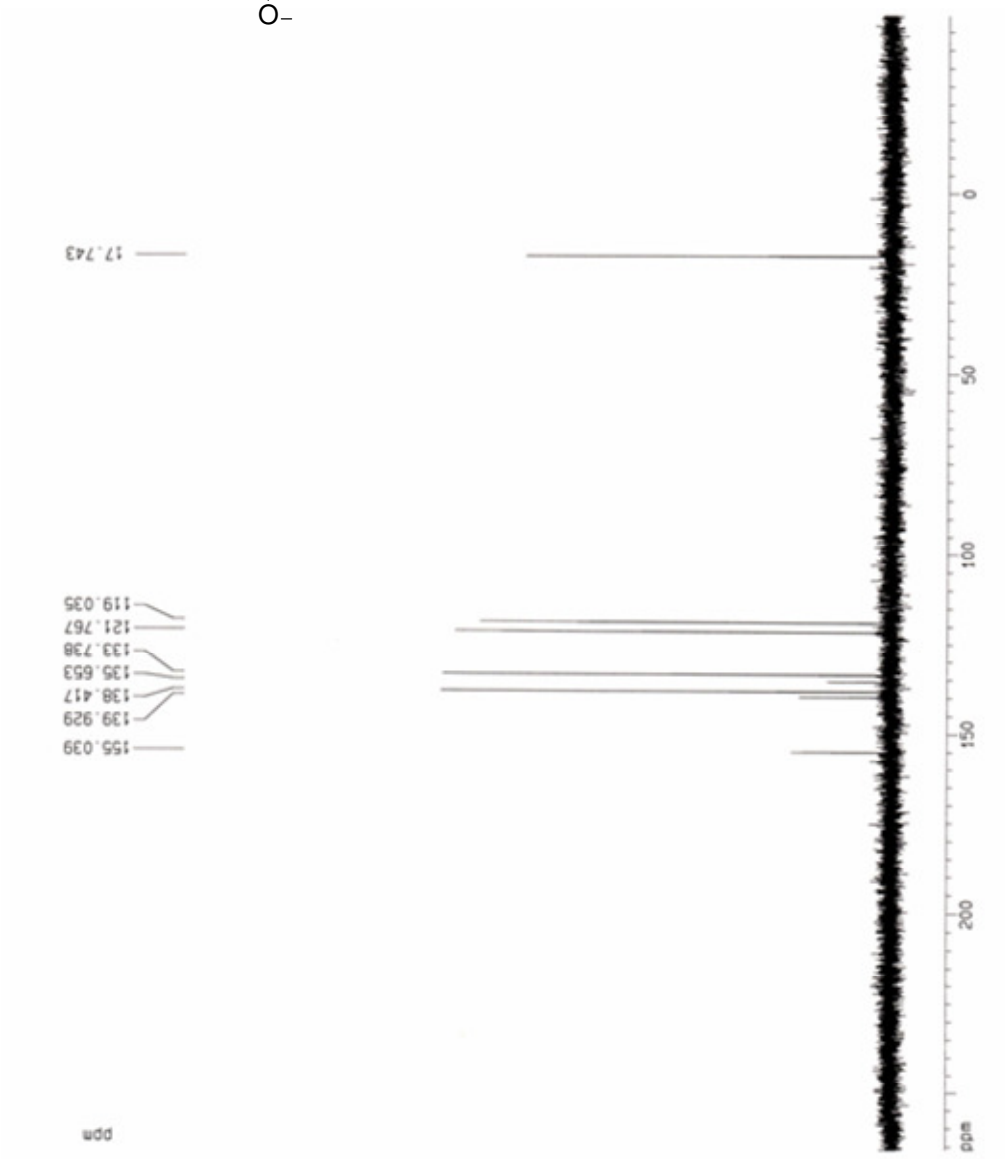

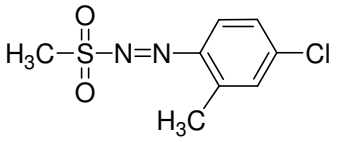

^{1}H-NMR of **33** in $CDCl_3$

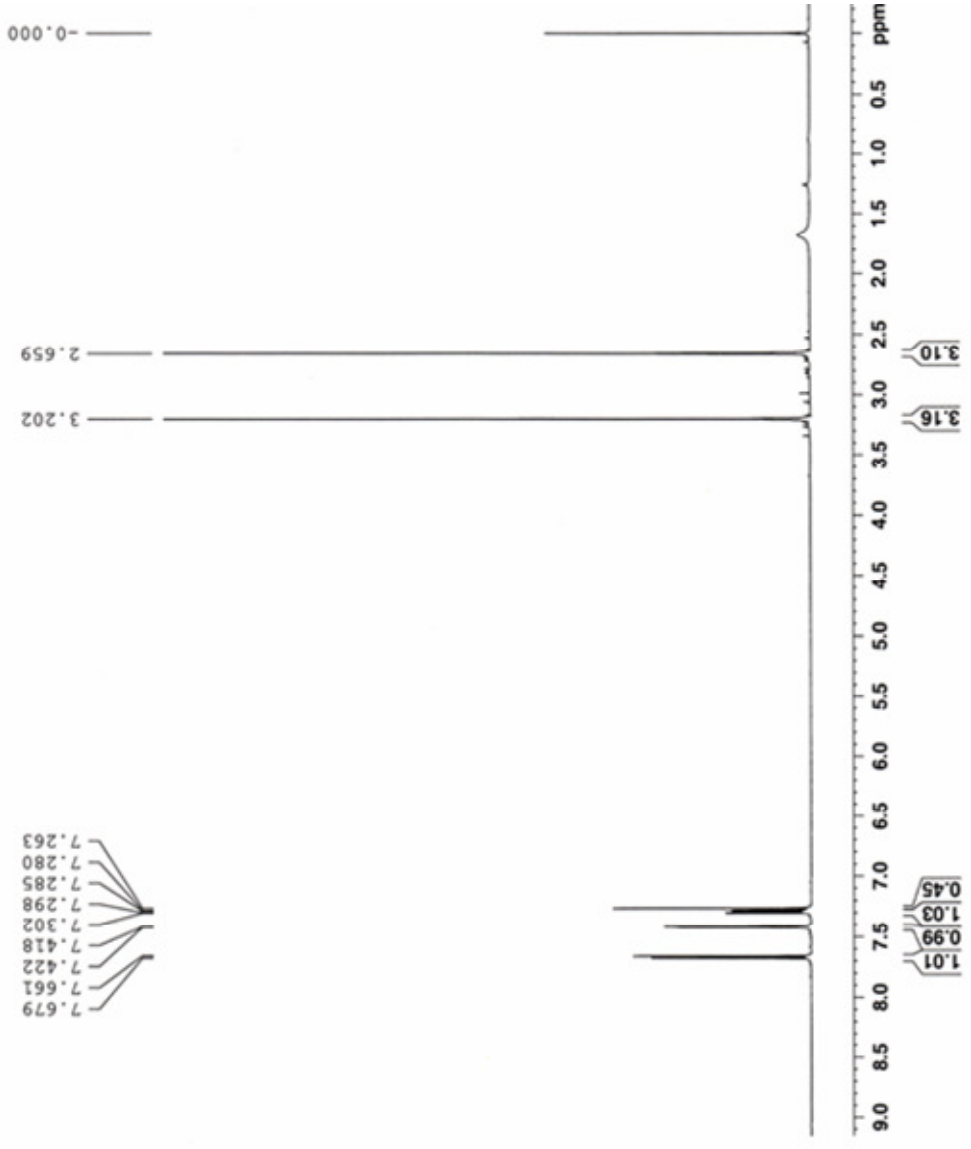

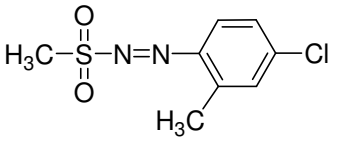

^{13}C-NMR of **33** in $CDCl_3$

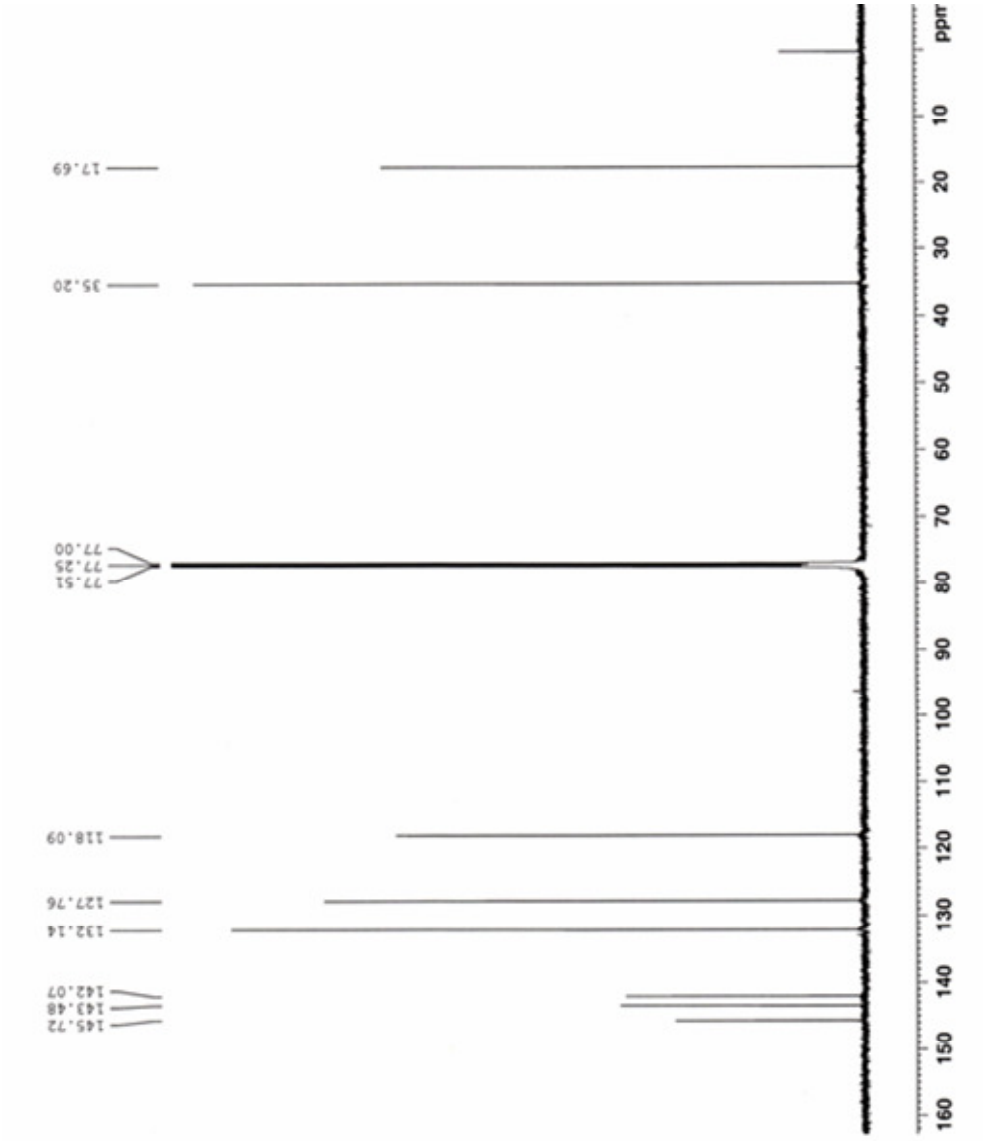

References:

[1] Brown, J. M.; Wilson, W. R. *Nature Re*V. *Cancer* **2004**, *4*, 437-447.

[2] Brown, J. M. *Cancer Res.* **1999**, *59*, 5863-5870.

[3] Zeman, E. M.; Brown, J. M.; Lemmon, M. J.; Hirst, V. K.; Lee, W. W. *Int. J. Radiat. Oncol. Biol. Phys.* **1986**, *12*, 1239-1242.

[4] Laderoute, K. L.; Wardman, P.; Rauth, M. *Biochem. Pharmacol.* **1988**, *37*, 1487-1495.

[5] Fitzsimmons, S. A.; Lewis, A. D.; Riley, R. J.; Workman, P. *Carcinogenesis.* **1994**, *15*, 1503-1510.

[6] Daniels, J. S.; Gates, K. S. *J. Am. Chem. Soc.* **1996**, *118*, 3380-3385.

[7] Birincioglu, M.; Jaruga, P.; Chowdhury, G.; Rodriguez, H.; Dizdaroglu, M.; Gates, K. S. *J. Am. Chem. Soc.* **2003**, *125*, 11607-11615.

[8] Biedermann, K. A.; Wang, J.; Graham, R. P. *Br. J. Cancer* **1991**, *63*, 358-362.

[9] Wardman, P.; Priyadarsini, K. I.; Dennis, M. F.; Everett, S. A.; Naylor, M. A.; Patel, K. B.; Stratford, I. J.; Stratford, M. R. L.; Tracy, M. *Br. J. Cancer* **1996**, *74*, S70-S74.

[10] Sies, H. *Angew. Chem., Int. Ed. Engl.* **1986**, *25*, 1058-1071.

[11] Finkel, T.; Holbrook, N. J. *Nature* **2000**, *408*, 239-247.

[12] Wood, Z. A.; Poole, L. B.; Karplus, P. A. *Science 300*, 650-653.

[13] Anderson, R. F.; Shinde, S. S.; Hay, M. P.; Gamage, S. A.; Denny, W. A. *J. Am. Chem. Soc.* **2003**, *125*, 748-756.

[14] Chowdhury, G.; Junnotula, V.; Daniels, J. S.; Greenberg, M. M.; Gates, K. S. *J. Am. Chem. Soc.* **2007**, 129, 12870-12879.

[15] Zagorevski, D.; Yuan, Y.; Fuchs, T.; Gates, K. S.; Song, M.; Breneman, C.; Greenlief, C. M. *J. Am. Soc. Mass Spectrosc.* **2003**, *14*, 881-892.

[16] Barton, D. H. R.; Crich, D.; Motherwell, W. B. *Tetrahedron* **1985**, *41*, 3901-3924.

[17] Boivin, J.; Crepon, E.; Zard, S. Z. *Tetrahedron Lett.* **1990**, *31*, 6869-6872.

[18] Adam, W.; Ballmaier, D.; Epe, B.; Grimm, G. N.; Saha-Moller, C. R. *Angew. Chem., Int. Ed. Engl*. **1995**, *34*, 2156-2158.

[19] Barton, D. H. R.; Jasberenyi, J. C.; Morrell, A. I. *Tetrahedron Lett.* **1991**, *32*, 311-314.

[20] Aveline, B. M.; Kochevar, I. E.; Redmond, R. W. *J. Am. Chem. Soc.* **1996**, *118*, 289-290.

[21] Wo¨lfle, I.; Lodays, J.; Sauerwein, B.; Schuster, G. B. *J. Am. Chem. Soc.* **1992**, *114*, 9304-9309.

[22] Lorance, E. D.; Kramer, W. H.; Gould, I. R. *J. Am. Chem. Soc.* **2002**, *124*, 15225-15238.

[23] Kelson, Andrew B.; McNamara, James P.; Pandey, Anjali; Ryan, Kenneth J.; Dorie, Mary Jo; McAfee, Patricia A.; Menke, Douglas R.; Brown, J. Martin; Tracy, Michael. Anti-Cancer Drug Design. **1998**, 13(6), 575-592.

[24] Khodja, M.; Moulay, S.; Boutoumi, H.; Wilde, H. Heterocycles. **2006**, 17, 166-172.

[25] Atallah, R. H.; Nazar, M. Z. Tetrahedron. **1982**, 38, 1793-1796.

[26] Fuchs, T.; Chowdhury, G.; Barnes, C. L.; Gates, K. S. *J. Org. Chem.* **2001**, 66, 107-114.

[27] Junnotula, V.; Sarkar, U.; Barnes, C. L.; Thallapally, P. K.; Gates, K. S. *J. Chem. Cryst.* **2006**, 36(9), 557-561.

[28] Povirk, L. F.; Wubker, W.; Kohnlein, W.; Hutchinson, F. *Nuceic Acid Res.* **1977,** 4, 3573-3580.

[29] Nutter, Louise M.; Ngo, Emily O.; Fisher, Geoffrey R.; Gutierrez, Peter L. *J. Biol. Chem.* **1992**, 267(4), 2474-2479.

[30] Pogozelski, W. K.; McNeese, T. J.; Tullius, T. D. *J. Am. Chem. Soc.* **1995**, 117, 6428-6433.

[31] Burrows, C. J.; Muller, J. G. *Chem. Rev.* **1998**, 98, 1109-1151.

[32] Atzrodt, J.; Derdau, V.; Fey, T.; Zimmermann, J. Angew. Chem. **2007**, 46(41), 7744-7765.

[33] Fukui, S.; Hanasaki, Y.; Ogawa, S. *J. Chromatogr.* 1993, *630*, 187-193.

[34] Sambrook, J.; Fritsch, E. F.; Maniatis, T. (1989) *Molecular Cloning: A Lab Manual,* Cold Spring Harbor Press, Cold Spring Harbor. NY

[35] Ahern, M.F.; Leopold, A.; Beadle, J. R.; Gokel, G. W. *J. Am. Chem. Soc*. 1982, 104, 548-554.

Chapter 2: DNA Damage by 1,2,4-Benzotriazine 1,4-Dioxide

2.1 Introduction

In the second chapter of this thesis, we used 3-methyl-1,2,4-benzotriazine 1,4-dioxide (Me-TPZ, **8**) as a tool to examine the dehydration mechanism in the benzotriazine dioxide class of compounds. Our data show that upon bioreductive activation, **8** causes similar DNA cleavage to clinically promising drug, TPZ. Importantly, our labeling studies revealed that activated **8** does not undergo dehydration to release benzotriazinyl radical **11**. On the other hand, **8** and TPZ hydroxylate DMSO and salicylic acid (**34**) upon reductive activation under anaerobic conditions. These studies together suggest that **8** and TPZ, upon reductive activation, release the known DNA-damaging agent, hydroxyl radical, which causes hypoxic cytotoxicity.

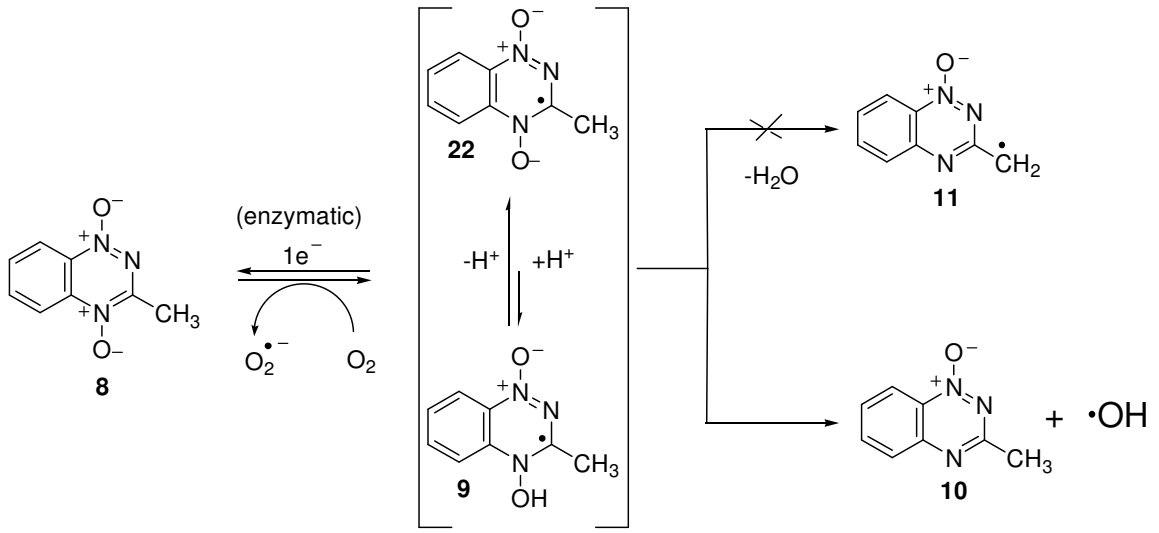

Scheme 2.1: Mechanism for DNA damage by Me-TPZ

2.2 Goal: Examine reactive species responsible for DNA strand cleavage by benzotriazine class of compounds

In our current studies, we used 1,2,4- benzotriazine 1,4-dioxide (Des-TPZ, **37**), a molecule absolutely incapable of undergoing a dehydration mechanism as another tool to investigate the reactive species responsible for DNA strand cleavage by the 1,2,4-benzotriazine dioxide class of compounds. TPZ analogue **37** is used as another tool because of the following reasons. First, data shows that **37** causes comparable hypoxic cytotoxicity to TPZ and **8** in cancer cell lines.[1,2,3] Second, the DNA-cleavage properties of **37** have not been well examined. Third, **37** provides a tool to know the common reactive species responsible for DNA strand cleavage by the benzotriazine class of compounds. For example, data show that **37** is one of the most potent analogs of the benzotriazine dioxide class of compounds in causing hypoxic cytotoxicity in cancer cell lines.[1,2,3] In addition, dehydration mechanism is not possible in **37**. Studies with **37**

might provide the additional evidence that all benzotriazines act via common mechanism involving hydroxyl radical.

As part of our goal to understand the common mechanism responsible for hypoxic cytotoxicity of benzotriazine dioxides, we synthesized **37** via known literature protocols with some minor modifications.[2,3] The *in vitro* DNA cleavage properties and *in vitro* metabolism of **37** were studied in the presence of NADPH:cytochrome P450 reductase under anaerobic conditions. In addition, we also used chemical traps to investigate the DNA damaging reactive species released from activated **37**.

2.3 Synthesis of 37

Compound **37** was obtained by the known synthetic protocols with some minor modifications (Scheme 2.2).[4,5,6] Briefly, TPZ and *tert*-butyl nitrite were dissolved in deoxygenated anhydrous DMF in separate flasks under argon atmosphere. Then TPZ was added slowly to *tert*-butyl nitrite solution at 65 ºC with a gas-tight syringe while maintaining the whole setup under argon. The reaction mixture was stirred at 65 ºC for additional 10 min and then cooled to room temperature. DMF was removed under vaccum at 60 ºC to yield a brownish yellow residue that was then purified by flash column chromatography to yield **37**.

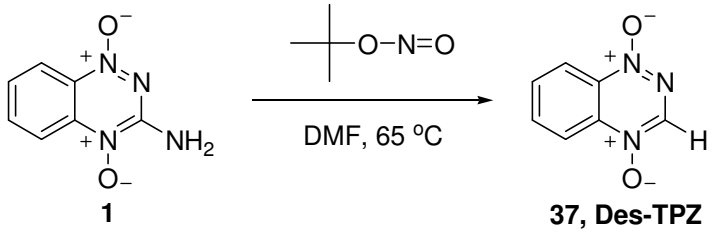

1 **37, Des-TPZ**

Scheme 2.2: Synthesis of 1,2,4-benzotriazine-1,4-di-*N*-oxide (**37**)

The compound 1-*N*-oxide of Des-TPZ (**40**) was also obtained utilizing the same protocol as for **37** except using 1-*N*-oxide of TPZ (**3**) as the starting material. Compound no-*N*-oxide of Des-TPZ (**41**) was obtained by reducing **40** with xanthine:xanthine oxidase under anaerobic conditions. TPZ and **3** were obtained by using the synthetic route reported by Fuchs et al.[7]

2.4 Compound 37 behaves like TPZ and 8 upon bio-reductive activation

TPZ analogue **37** shows similar hypoxic cytotoxicity to TPZ and **8** *in vitro* cell culture.[1,2,3] The hypoxic cytotoxicity of TPZ is known to derive from its ability to cause DNA strand cleavage.[8,9,10,11,12] Accordingly, we set out to examine the DNA strand cleavage properties of **37**. Such studies will be helpful to understand the role of DNA strand cleavage by **37** in its hypoxic cytotoxicity. In addition, preliminary studies on **37** by Tarra Fuchs in our group showed that compound **37** causes DNA strand cleavage upon bioreductive activation. In our current studies, we examined the DNA strand cleavage properties of **37** in detail and compared our results to TPZ and **8**.

2.4.1 Compound 37 is a bio-reductively activated DNA cleaver

In typical DNA cleavage assays, **37** was activated with NADPH:cytochrome P450 reductase under anaerobic conditions in an identical manner to our earlier experiments in Chapter-2 and supercoiled plasmid DNA was used as a substrate. Our data shows that **37** causes concentration-dependent DNA strand cleavage upon reductive activation (Figure 2.1). In control experiments, NADPH:cytochrome P450 reductase (no **37**) and **37** (no NADPH:cytochrome P450 reductase) no DNA strand cleavage was observed.

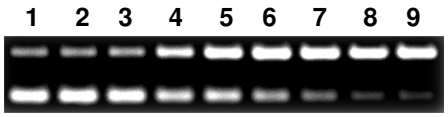

Figure 2.1: Concentration dependent anaerobic DNA-cleavage efficiency by various concentrations of **37** in the presence of NADPH:cytochrome P450 reductase as an activating system. Supercoiled plasmid DNA (33 µg/mL, pGL-2 Basic) was incubated with **37** (25-150 µM), NADPH (500 µM), cytochrome P450 reductase (33 mU/mL), catalase (100 µg/mL), superoxide dismutase (10 µg/mL), sodium phosphate buffer (50 mM, pH 7.0), and desferal (1 mM) under anaerobic conditions at room temperature for 4 h, followed by agarose gel electrophoretic analysis. Lane 1, DNA alone (S = 0.35 ± 0.14); lane 2, NADPH (500 µM) + reductase (1 mU) (S = 0.32 ± 0.11); lane 3, **37** (150 µM) (S = 0.38 ± 0.17); lanes 4-9, NADPH (500 µM) + reductase (1 mU) + **37** (25 µ M, lane 4) (S = 0.49 ± 0.13); (50 µ M, lane 5) (S = 0.76 ± 0.05); (75 µ M, lane 6) (S = 1.07 ± 0.08); (100 µ M, lane 7) (S = 1.30 ± 0.09); (125 µ M, lane 8) (S = 1.42 ± 0.17); (150 µ M, lane 9) (S = 1.62 ± 0.14). The value S represents the mean number of strand breaks per plasmid molecule and is calculated using the equation $S = -\ln f_I$, where f_I is the fraction of plasmid present as form I.[13]

2.4.2 Compound 37 shows comparable DNA cleavage efficiency to TPZ and 8

The data shows that the DNA strand cleavage by **37** is comparable to that of **8** and slightly better than TPZ under the same reaction conditions (Figure 2.2). DNA strand cleavage efficiency of **37** and **8,** despite their inability to undergo a dehydration mechanism, suggests that dehydration of activated benzotriazine dioxides is not necessary for their hypoxic cytotoxicity.

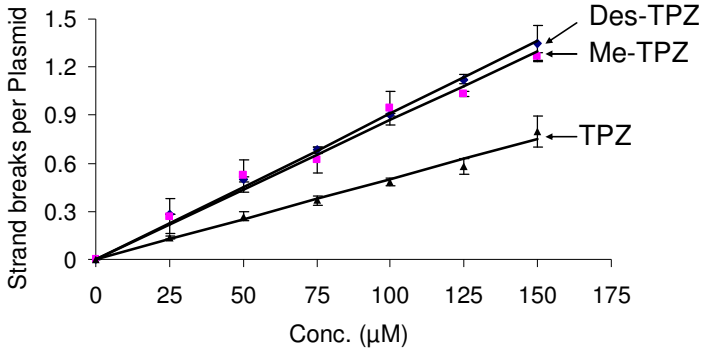

Figure 2.2: Comparision of anaerobic DNA-cleavage efficiency by various concentrations of **37** or **8** or TPZ in the presence of NADPH:cytochrome P450 reductase as an activating system. Supercoiled plasmid DNA (33 µg/mL, pGL-2 Basic) was incubated with **37** or **8** or TPZ (25-150 µM), NADPH (500 µM), cytochrome P450 reductase (33 mU/mL), catalase (100 µg/mL), superoxide dismutase (10 µg/mL), sodium phosphate buffer (50 mM, pH 7.0), and desferal (1 mM) under anaerobic conditions at room temperature for 4 h, followed by agarose gel electrophoretic analysis. The value S represents the mean number of strand breaks per plasmid molecule and is calculated using the equation $S = -\ln f_I$, where f_I is the fraction of plasmid present as form I.[13]

2.4.3 Inhibition of 37 mediated DNA strand cleavage by radical scavengers

As part of our efforts to understand the chemical nature of DNA damaging agent(s) released from activated **37**, we examined the effect of radical scavengers on **37** mediated DNA strand cleavage. The data shows that the radical scavengers methanol, ethanol, *t*-butanol, DMSO, and mannitol (Lanes 4-8 in Figure 2.3) inhibit DNA strand cleavage caused by **37** (Figures 2.3 and 2.4). These results suggest that upon reductive activation, **37** releases radical species, which are responsible for DNA strand cleavage. Under aerobic conditions, **37** did not show any significant DNA cleavage (Lane 9 in Figure 2.3). This data suggests that activated **37** similar to TPZ and **8** produces an oxygen sensitive radical intermediate **38,** which plays a key role in hypoxia selective toxicity. These data together show that compound **37** behaves similar to TPZ and **8** upon enzymatic activation.

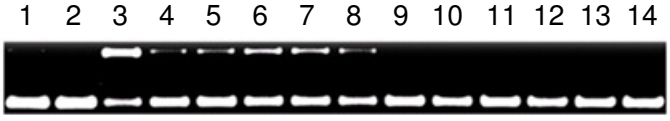

Figure 2.3: Cleavage of supercoiled plasmid DNA by **37** in the presence of NADPH:cytochrome P450 reductase as an activating system. All reactions contained DNA (33 μg/mL, pGL-2 Basic), sodium phosphate buffer (50 mM, pH 7.0), catalase (100 μg/ mL), superoxide dismutase (10 μg/mL), and desferal (1 mM) and were incubated under anaerobic conditions (except lane 9) at 24 °C for 3 h, followed by agarose gel electrophoretic analysis. Lane 1, DNA alone (S = 0.14 ± 0.04); lane 2, NADPH (500 μM) + reductase (1 mU) (S = 0.13 ± 0.02); lane 3, **37** (250 μM) + NADPH (500 μM) + reductase (1 mU) (S = 1.07 ± 0.21); lanes 4-8, **37** (250 μM) + NADPH (500 μM) + reductase (1 mU) + methanol (500 mM, lane 4) (S = 0.29 ± 0.04); ethanol (500 mM, lane 5) (S = 0.30 ± 0.01); *tert*-butyl alcohol (500 mM, lane 6) (S = 0.46 ± 0.06); DMSO (500 mM, lane 7) (S = 0.45 ± 0.07); mannitol (500 mM, lane 8) (S = 0.42 ± 0.08); lane 9, **37** (250 μM) + NADPH (500 μM) + reductase (1 mU) + air (S = 0.17 ± 0.05); lane 10, **40** (250 μM) + NADPH (500 μM) + reductase (1 mU) (S = 0.18 ± 0.09); lane 11, **41** (250 μM) + NADPH (500 μM) + reductase (1 mU) (S = 0.17 ± 0.07); lanes 12-14, **37** alone (250 μM, lane 12) (S = 0.18 ± 0.91); **40** alone (250 μM, lane 13) (S = 0.16 ± 0.05); **41** alone (250 μM, lane 14) (S = 0.17 ± 0.08). The value S represents the mean number of strand breaks per plasmid molecule and is calculated using the equation $S = -\ln f_I$, where f_I is the fraction of plasmid present as form I.[13]

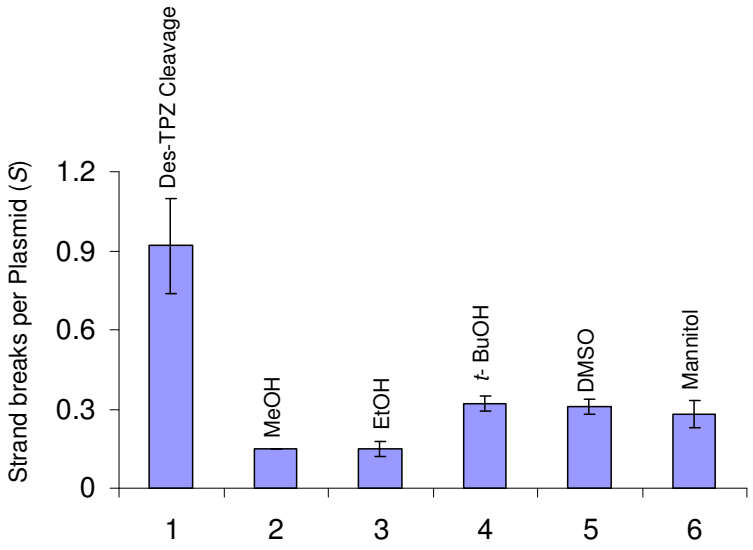

Figure 2.4: Inhibition of **37** mediated DNA damage by radical scavengers. All reactions contained DNA (33 μg/mL, pGL-2 Basic), sodium phosphate buffer (50 mM, pH 7.0), superoxide dismutase (10 μg/mL), catalase (100 μg/mL), and desferal (1 mM) and were incubated under anaerobic conditions at 25 ˚C for 3 h, followed by agarose gel electrophoresis. Lane 1, **37** (250 μM) + NADPH (500 μM) + reductase (33 mU/mL); lanes 2-6, **37** (250 μM) + NADPH (500 μM) + reductase (1 mU) + methanol (500 mM, lane 2); ethanol (500 mM, lane 3); *t*-butyl alcohol (500 mM, lane 4); DMSO (500 mM, lane 5); mannitol (500 mM, lane 6). The value *S* represents the mean number of strand breaks per plasmid molecule and is calculated using the equation $S = -\ln f_I$, where f_I is the fraction of plasmid present as form I.[13]

2.4.4 Compound 37 yields 1-*N*-oxide (40) as a major metabolite upon reductive activation.

In the *in vitro* metabolic studies, **37** was activated with NADPH:cytochrome P450 reductase under anaerobic conditions. Metabolites generated from activated **37** were identified on HPLC. Further, the identity of the metabolites was confirmed by co-injection of authentic compounds with metabolites generated from activated **37** on HPLC. Our results show that **37** generates the 1-*N*-oxide (**40**) as a major metabolite elutes at ~13.3 min and no-*N*-oxide (**41**) as a minor metabolite elutes at ~12.8 min (Figure 2.5). Our data also shows that both the minor and the major metabolites of **37** are incapable of

cleaving DNA under anaerobic conditions (Lanes 11 and 12 in Figure 2.3). All the measured properties of **37** were essentially identical to TPZ and **8**.[11,14]

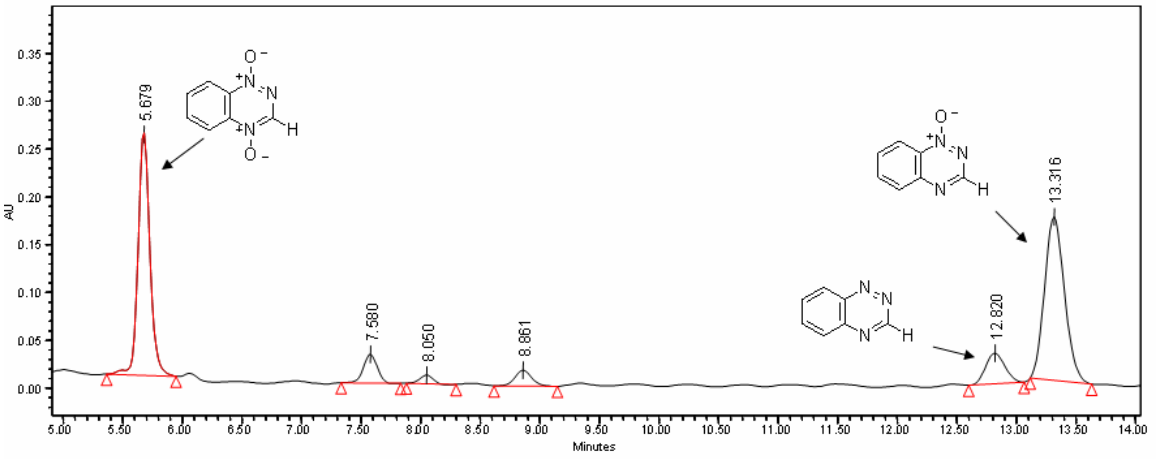

Figure 2.5: HPLC trace of products arising from *in vitro* anaerobic metabolism of 1,2,4-benzotriazine *di*-oxide (**37**). A 300 µL solution containing **37** (500 µM) and sodium phosphate buffer (pH 7.0, 50 mM) was incubated with cytochrome P450 reductase (33 mU/mL) and NADPH (500, µM) under anaerobic conditions for 3 h.

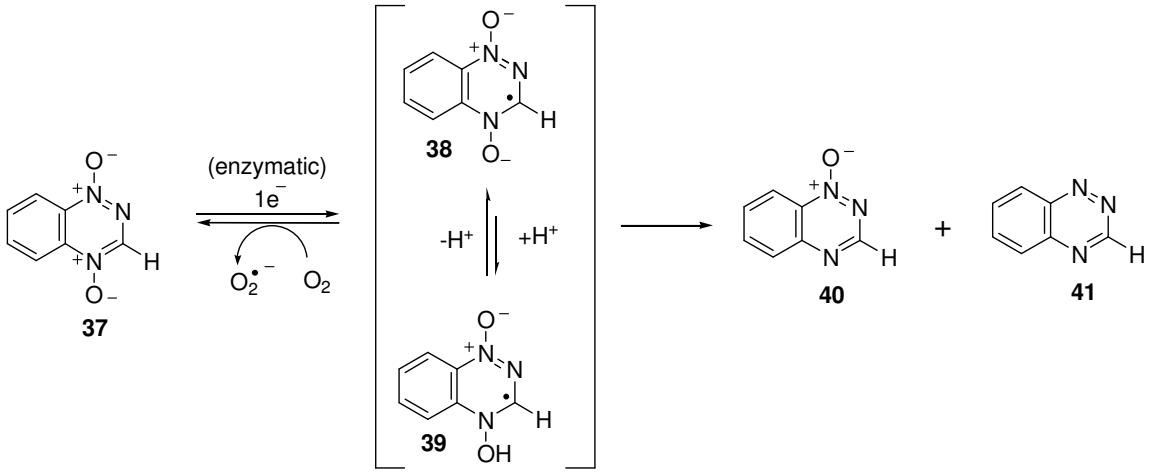

Scheme 2.3: *In vitro* metabolism of 1,2,4 benzotriazine di-*N*-oxide (**37**)

2.4.5 Compound 37 shows sequence independent DNA strand cleavage

Based on the similar DNA cleaving properties of **37** to TPZ and **8,** irrespective of its inability to undergo a dehydration mechanism, we hypothesized that **37** releases hydroxyl radical analogous to TPZ and **8**. If compound **37** releases hydroxyl radical, the DNA strand cleavage by this compound should be sequence independent. To examine this hypothesis, Ujjal Sarkar in our group examined the sequence specificity of DNA strand cleavage of a 30 base pair DNA fragment by **37**, and compared the results to that by the well known hydroxyl radical generating iron-EDTA system.[15] Our data shows that **37** cleaves the DNA at all base pairs with little sequence dependence similar to TPZ and **8**. The reason for moderate preference for cleavage at G-residues by these 1,2,4-benzotriazine class of drugs is not clear. One possible reason is that a portion of the damaged guanine sites may lead to strand breaks under our experimental conditions.[16]

Our *in vitro* DNA strand cleavage assays, radical scavenging experiments and metabolic studies on **37** suggest that TPZ, **8** and **37** derive their medicinal properties by the same chemical mechanism. Further, sequence independent DNA strand cleavage by activated **37** supports the hypothesis that this TPZ analogue **37** releases small and diffusible species like hydroxyl radical. Accordingly, we set to trap hydroxyl radical produced from activated **37** with salicylic acid (**34**).

2.4.6 Activated 37 hydroxylates salicylic acid (34)

Salicylic acid (**34**) is known to trap hydroxyl radical to give 2,3-dihydroxy benzoic acid (**36**) and 2,5-dihydroxy-benzoic acid (**35**).[17,18] Accordingly, Sarmistha Sinha in our group examined the hydroxylation of **34** in the presence of activated **37** under anaerobic conditions. The data shows that activated **37** in the presence of **34** gives hydroxylated products **35** and **36,** which is a qualitative test for hydroxyl radical. This data shows that

similar to TPZ and **8**, compound **37** releases the known DNA damaging agent, hydroxyl radical upon one-electron enzymatic activation.

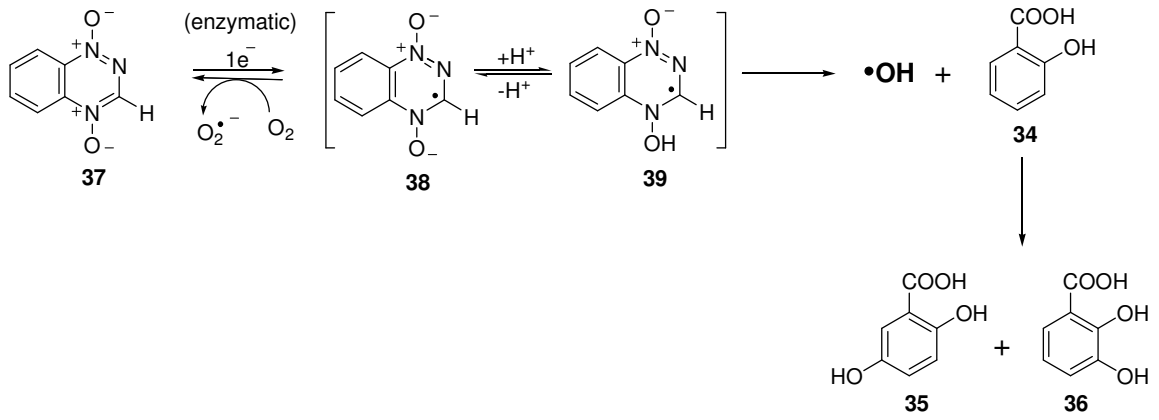

Scheme 2.4: Trapping of hydroxyl radical from activated **37** with salicylic acid (**34**)

2.5 Conclusions

In vitro DNA strand cleavage assays, radical scavenging experiments and metabolic studies on **37** show that TPZ analogue **37** behaves in an identical manner to TPZ and **8** upon reductive activation. Sequence-independent DNA strand cleavage by **37** is consistent with small and diffusible species, like hydroxyl radical. The similar DNA strand cleavage properties of **37** to TPZ and **8,** irrespective of its inability of undergoing

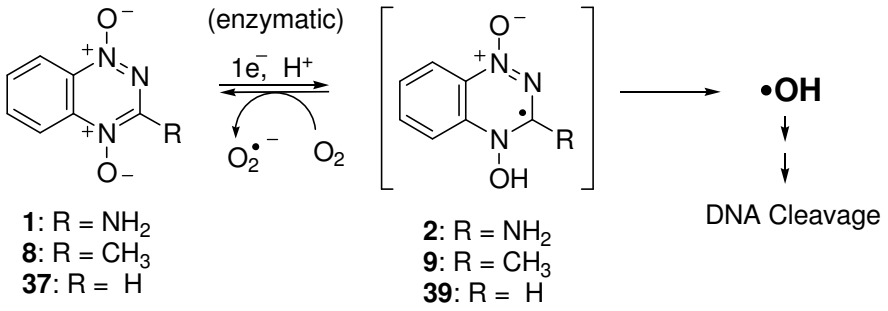

Scheme 2.5: Common mechanism for DNA strand cleavage by benzotriazine di-*N*-oxides

dehydration mechanism, suggests that activated **37** might release hydroxyl radical. Hydroxylation of salicylic acid in the presence of activated **37** is consistent with hydroxyl radical. Overall, the results suggest that 1,2,4-benzotriazine-dioxide (**37**), upon one-electron reductive-activation, releases the well known DNA-damaging agent, hydroxyl radical.

Our mechanistic studies reported in Chapters 1-2 reveal that the 1,2,4-benzotrizine dioxide class of compounds, upon one-electron reductive activation, release the DNA damaging agent, hydroxyl radical. Thus, our overall studies suggest that the benzotriazine dioxide class of compounds upon reductive activation deliver hydroxyl radical, the active agent of radiotherapy, selectively to the hypoxic cells found in solid tumors.

2.6 Experimental

2.6.1 Synthesis of 1,2,4-benzotriazine-1,4-di-*N*-oxide (37). Compound **37** was obtained using known synthetic protocols.[4-6] Tirapazamine (25 mg, 0.14 mmol) was dissolved in deoxygenated anhydrous DMF (2 mL) under argon atmosphere. In a separate flask *tert*-butyl nitrite (0.05 mL, 0.42 mmol) was taken in deoxygenated anhydrous DMF (8 mL) and the mixture was heated to 65 ºC under argon atmosphere. To this mixture tirapazamine solution was added slowly with a gas-tight syringe while maintaining the whole setup under argon atmosphere. The reaction mixture was stirred at 65 ºC for additional 10 min and then cooled to room temperature. DMF was removed under vaccum at 60 ºC to yield a brownish yellow residue that was then purified by a flash column chromatography (5:3 EtOAc/hexane) to yield **37** (12 mg, 53%). R_f of **37** is 0.77 (100% EtOAc): ^{1}H-NMR (250 MHz, $CDCl_3$) δ 8.88 (s, 1H), 8.52 (dd, 1H), 8.51 (dd, 1H), 8.05 (m, 1H), 7.93 (m, 1H); (250 MHz, DMSO- *d6*) 9.31 (s, 1H), 8.35 (m, 2H), 8.13 (m, 1H), 7.99 (m, 1H); ^{13}C-NMR (DMSO- *d6*, 62.9 MHz) 142.54, 140.05, 135.92, 135.61, 133.29 121.54, 119.44; HRMS ESI $[M+H]^+$ calcd for $C_7H_6N_3O_2$ 164.0460, found 164.0469.

2.6.2 Synthesis of 1,2,4-benzotriazine-1-*N*-oxide (40). Compound **40** was obtained by following the same synthetic protocol that we used for **37** except using 1-*N*–oxide of TPZ (**3**) as a starting material. Briefly, **3** (100 mg, 0.602 mmol) in the presence of *tert*-butyl nitrite (0.2 mL, 1.68 mmol) under the above conditions yield a yellow residue, which was then purified by a flash column chromatography (1:19 EtOAc/hexane) to give **40** (22 mg, 28 %). R_f of **40** is 0.6 (1:2 EtOAc/hexane): ^{1}H-NMR (250 MHz, Acetone-*d6*) 9.07 (s, 1H), 8.43 (d, *J* = 8.5 Hz, 1H), 8.12 (m, 2H), 7.94 (m, 1H); (500 MHz, DMSO- *d6*) 9.18

(s, 1H), 8.40 (d, *J* = 8.5 Hz, 1H), 8.11(m, 2H), 7.9 (m, 1H); ^{13}C-NMR (DMSO- *d6*, 125.8 MHz) 154.09, 146.93, 136.21, 135.11, 131.56, 128.89, 119.70; HRMS ESI $[M+H]^+$ calcd for $C_7H_6N_3O$ 148.0511, found 148.0511.

2.6.3 Synthesis of 1,2,4-Benzotriazine (41). Compound **40** (1 mg, 0.007 mmol) was dissolved in sodium phosphate buffer (2 mL, 50 mM at pH 7) containing 20% acetonitrile. The resultanting solution was deoxygenated by passing argon for 2 min and then incubated in the presence of xanthine (1 mg, 0.007 mmol) and xanthine oxidase (100 mU/mL) reductive system under argon atmosphere at 25 ºC for 4 h. The product was then extracted with dichloromethane (5 mL) and the solvent evaporated to afford **41** as a yellow solid (0.2 mg, 0.002 mmol, 20%). R_f of **41** is 0.7 (1:2 EtOAc/hexane): ^{1}H-NMR (250 MHz, acetone-*d6*) 9.99 (s, 1H), 8.53-8.56 (d, *J* = 9 Hz, 1H), 8.05-8.17 (m, 3H).

2.6.4 DNA cleavage assays. Concentration dependent DNA cleavage assays of **37** were carried out in an identical manner to earlier DNA cleavage experiments that we reported for TPZ and **8** in the second chapter. Briefly, solutions of 30 μL containing supercoiled plasmid DNA (33 μg/mL), NADPH (500 μM), cytochrome P450 reductase (33 mU/mL), catalase (100 μg/mL), superoxide dismutase (10 μg/mL), sodium phosphate buffer (pH 7, 50 mM), and desferal (1 mM) were incubated with different concentrations of **37** (25-150 μM) under anaerobic conditions while protecting from light and at 25 ^{o}C for 4 h.

DNA cleavage assays containing radical scavengers were performed as described above with the exception that radical scavengers such as a methanol, ethanol, *tert*-butyl alcohol, DMSO, or mannitol (500 mM) were added to the reactions before addition of

NADPH:cytochrome P450 reductase. To prevent the background DNA cleavage from superoxide radical, superoxide dismutase, catalase and desferal were added to reactions. DNA cleavage assays containing radical scavengers were incubated under anaerobic conditions while protecting from light and at 25 ^{o}C for 3 h.

2.6.4 ***In vitro*** **metabolic studies of 37.** In a metabolic studies assay, a solution of 300 µL of **37** (500 µM) and desferal (1 mM) in sodium phosphate buffer (pH 7, 50 mM) was deoxygenated by three freeze-pump-thaw cycles and then torch-sealed under vacuum. The sealed tube was scored before being transferred to an argon filled glove bag. The tube was then opened and, NADPH (1 mM), and cytochrome P450 reductase (33 mU/mL), were added and samples were incubated in an argon filled glove bag at 25 ºC for 4 h. The proteins were then removed by centrifugation through Amicon Microcon (YM3) filters. The filtrate was analyzed by HPLC employing a C18 reverse phase Rainin Microsorb-MV column (5 µm particle size, 100 A˚ pore size, 25 cm length, 4.6 mm i.d.) eluted with gradient solvent system starting with 80% A (0.5% acetic acid in water) and 20% B (2:1 methanol/acetonitrile) followed by linear increase to 30% B from 0 min to 20 min. Then, 30% B was held until 30 min and in next 10 min 20% B was achieved. The flow rate of 0.9 mL/min was used and the products were monitored by UV-absorbance at 240 nm. In *vitro* metabolism of **37** by NADPH:cytochrome P450 reductase yields two products whose relative yields were estimated on the basis of their relative peak areas in the HPLC chromatogram. The major product was identified as 1-*N*-oxide (**40**) and minor product was identified as no-*N*-oxide (**41**) by co-injection of the reaction mixture with authentic compounds.

Supporting information:

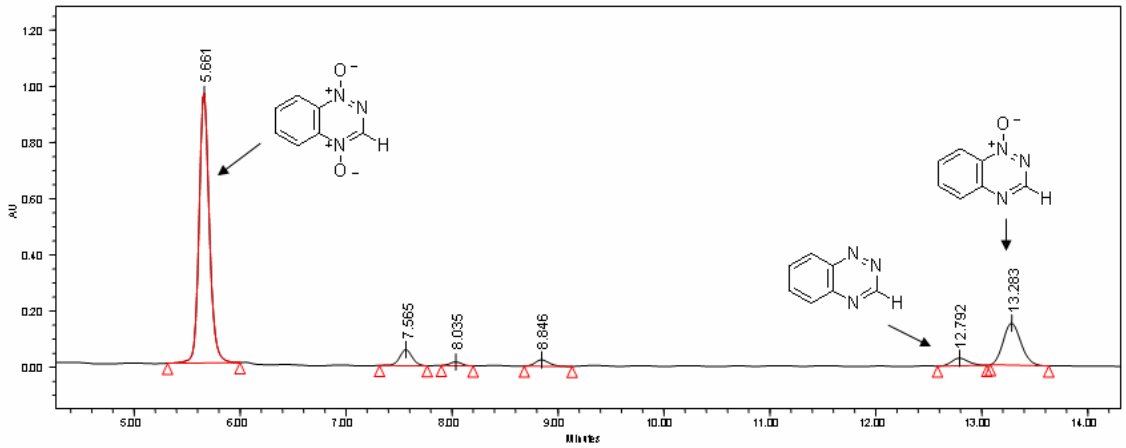

Figure S2.1: HPLC trace of Des-TPZ reaction with co-injection of Des-TPZ

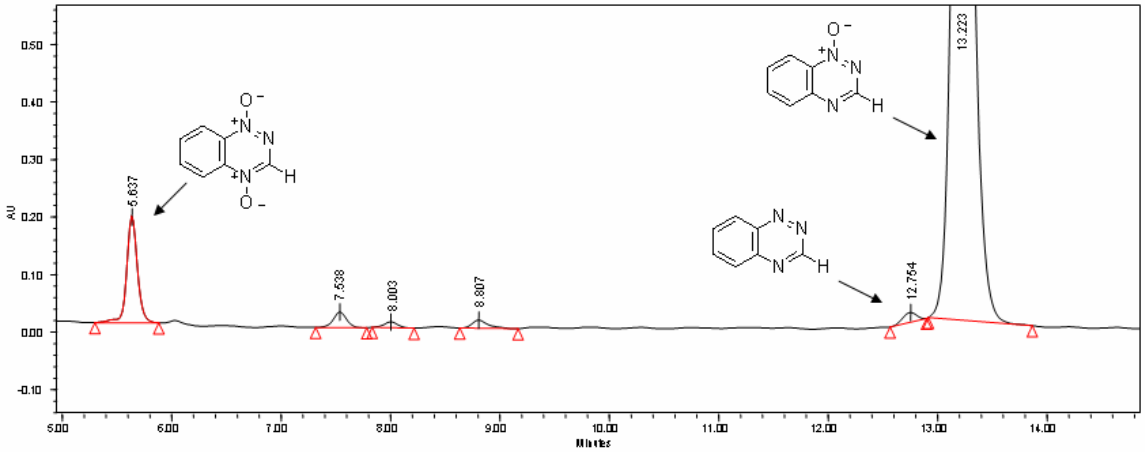

Figure S2.2: HPLC trace of Des-TPZ reaction with co-injection of 1-*N*-oxide of Des-TPZ

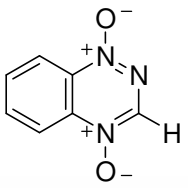

^{1}H-NMR of **37** in $CDCl_3$

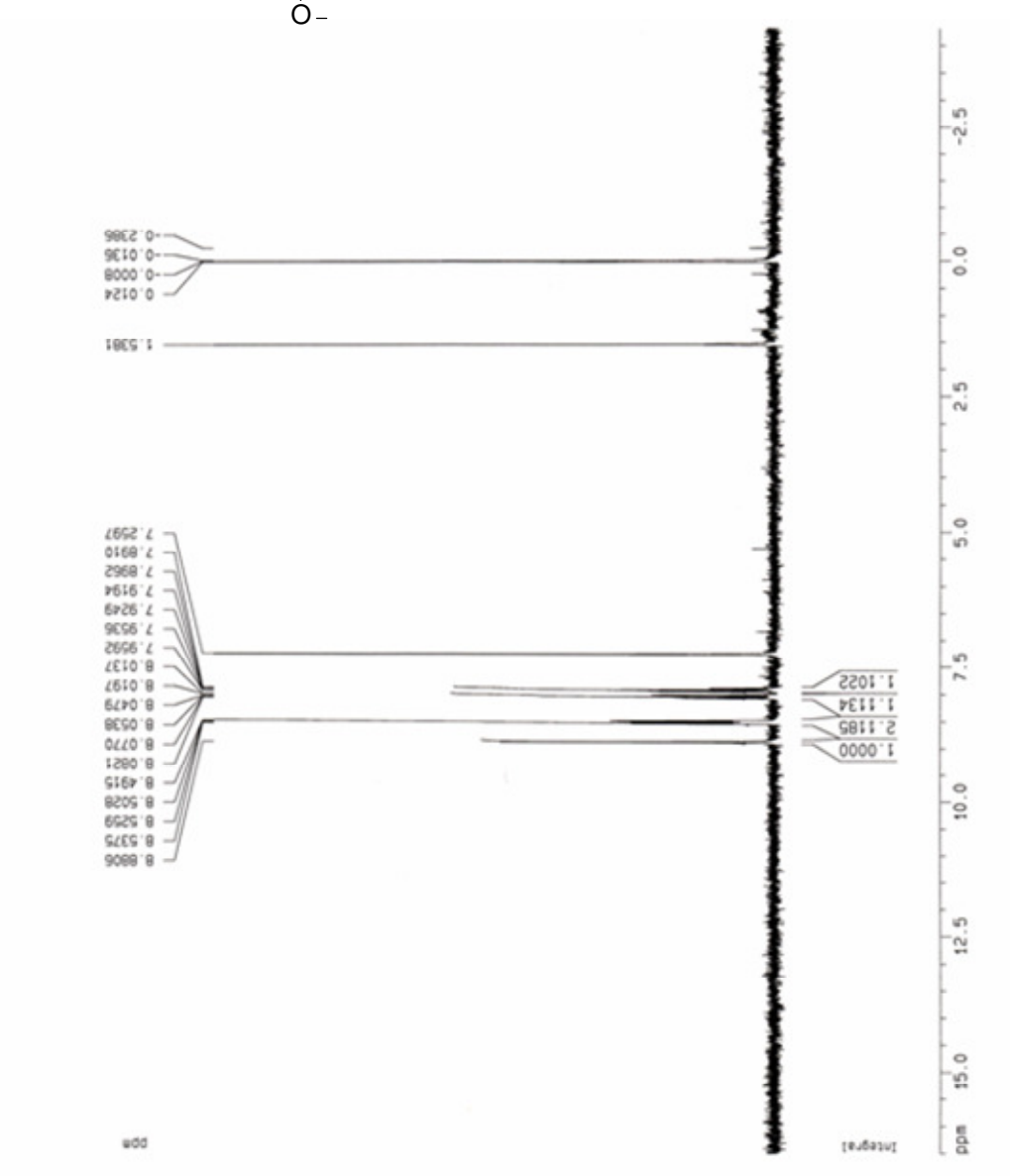

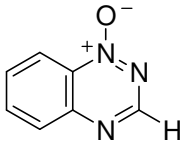

^{1}H-NMR of **40** in Acetone-d_6

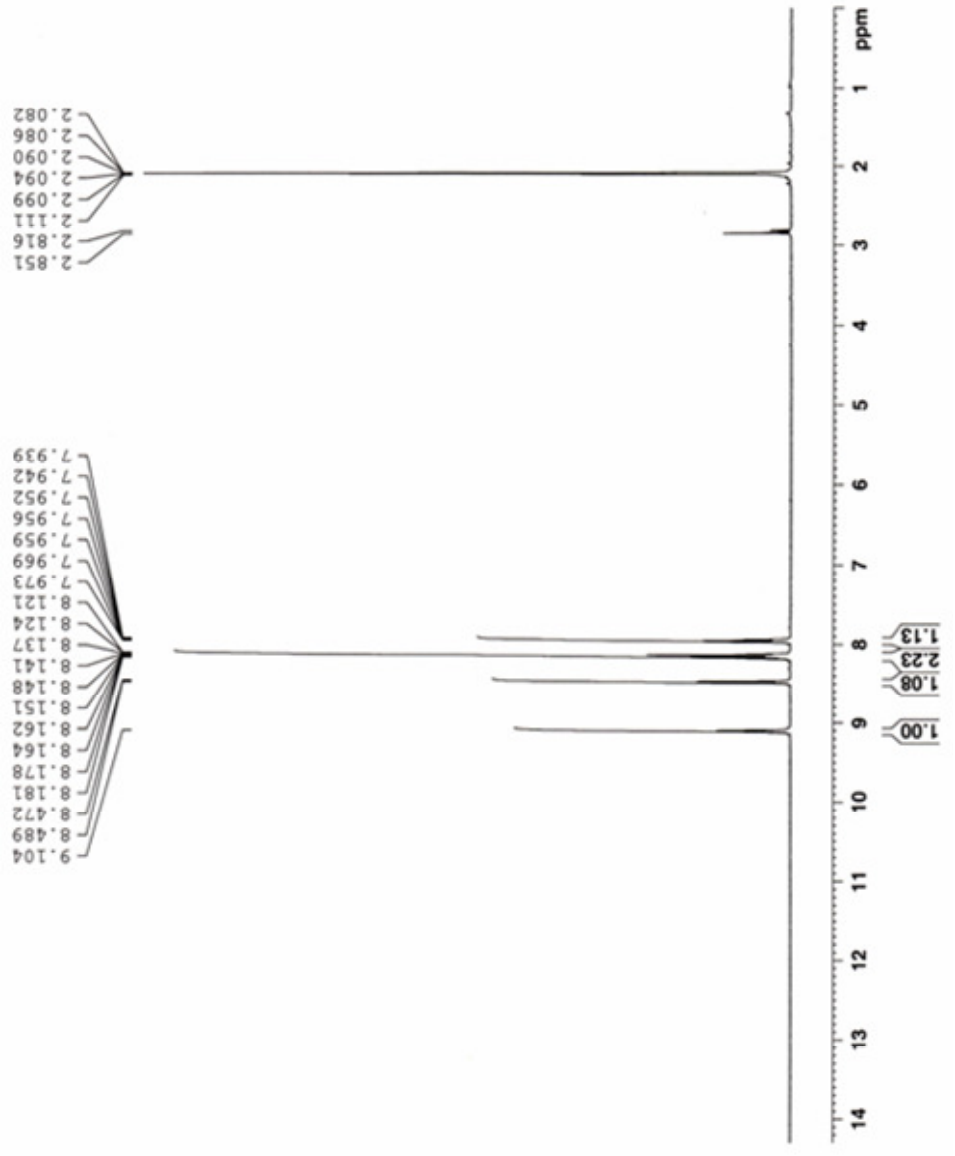

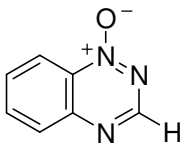

^{1}H-NMR of **40** in DMSO-d_6

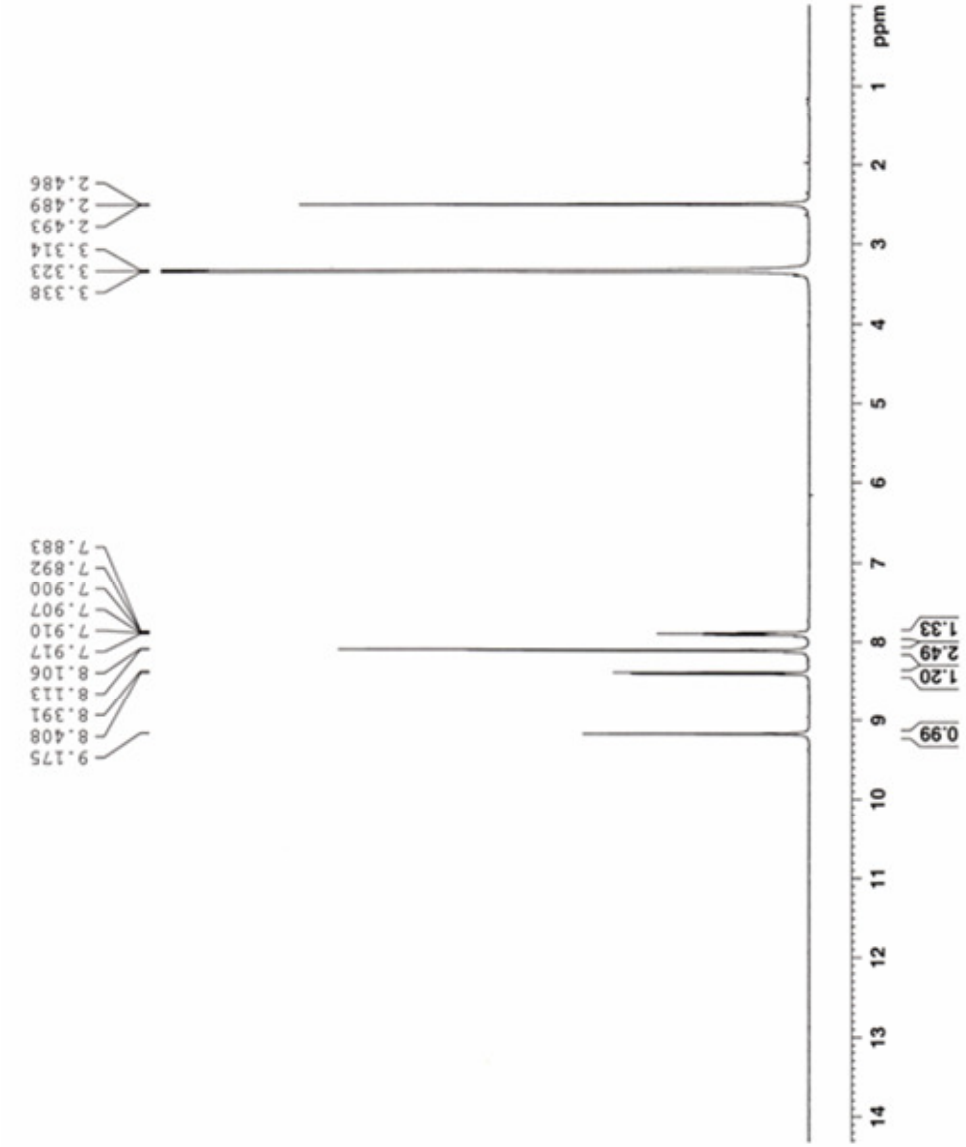

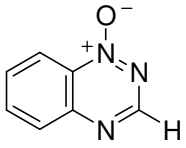

^{13}C-NMR of **40** in DMSO-d_6

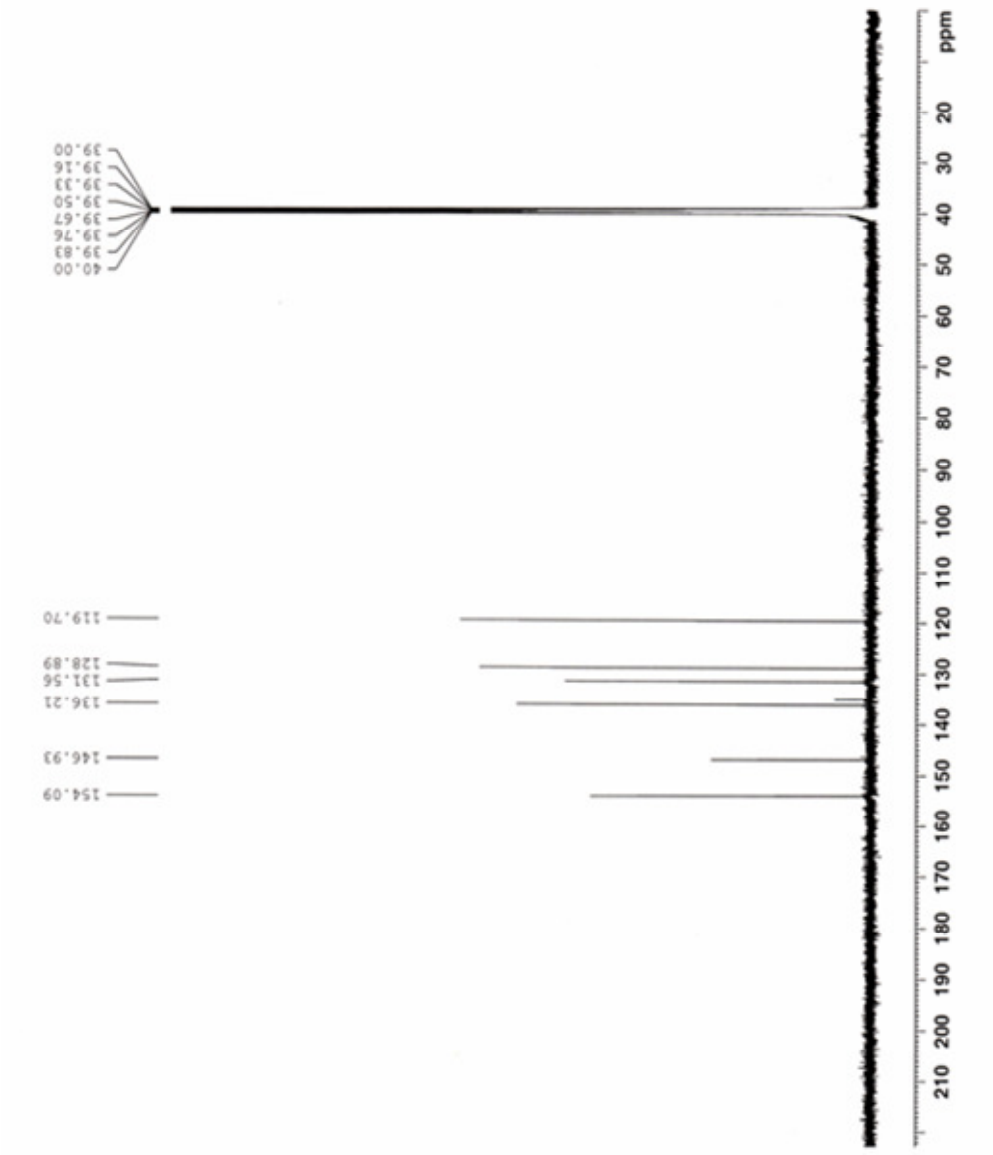

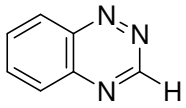

^{1}H-NMR of **41** in $CDCl_3$

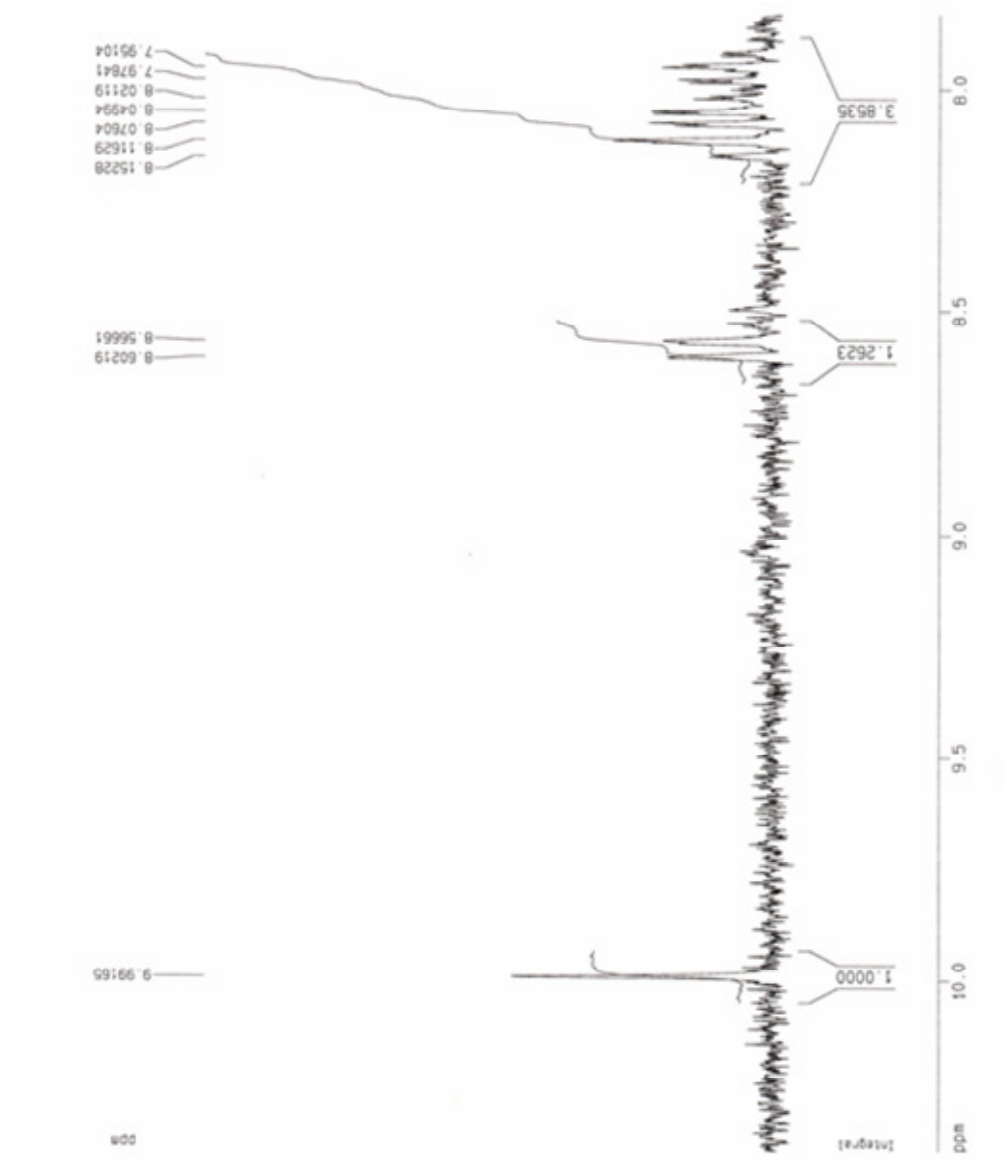

References:

[1] Kelson, A. B.; McNamara, J. P.; Ryan, K. J.; Dorie, M. J.; McAfee, P. A.; Menke, D. R.; Brown, J. M.; Tracy. M. *Anti-Cancer Drug Design*. **1998**, 13, 575-592.

[2] Zeman, E. M.; Baker, M. A.; Lemmon, M. J.; Pearson, C. I.; Adams, J. A.; Brown, J. M.; Lee, W. W.; Tracy, M. *Int. J. Radiat. Oncol. Biol. Phys.* **1989**, 16, 977-981.

[3] Michinton, A. I.; Lemmons, M. J.; Pearson, C. I.; Adams, J. A.; Brown, J. M. *Int. J. Radiat. Oncol. Biol. Phys.* **1992**, 22, 701-705.

[4] Lee, W. W.; Brown, J. M.; Grange, E. W.; Martinez, A. P.; Tracy, M.; Pollart, D. J. In US Patent 5, 624, 925: USA,1997.

[5] Doyle, M. P.; Dellaria, J. F.; Siegfried, B.; Bishop, S. W. *J. Org. Chem.* **1997**, 42, 3494-3498.

[6] Fuchs, T. Ph.D dissertation theisis, Chapter-5.

[7] Fuchs, T.; Chowdhary, G.; Barnes, C. L.; Gates, K. S. *J. Org. Chem.* **2001**, 66, 107-114.

[8] Vaupel, P.; Kelleher, D. K.; Thews, O. (1998) M *Int. J. Radiat. Oncol., Biol., Phys.* **1998,** *42*, 843-848.

[9] Siemann, D. W. Int. J. Radiat. Oncol., Biol., Phys. **1998**, 42, 697-699.

[10] Baker, M. A., Zeman, E. M., Hirst, V. K., and Brown, J. M. *Cancer Res.***1988**, *48*, 5947-5952.

[11] Daniels, J. S.; Gates, K. S. *J. Am. Chem. Soc.* **1996**, 118, 3380-3385.

[12] Chowdhury, C.; Junnotula, V.; Daniels, J. S.; Greenberg, M. M.; Gates, K. S. *J. Am. Chem. Soc.* **2007**, *129*, 12870-12877

[13] Povirk, L. F.; Wubker, W.; Kohnlein, W.; Hutchinson, F. *Nuceic Acid Res.* **1977,** 4, 3573-3580.

[14] Junnotula, V.; Sarkar, U.; Sinha, S.; Gates, K. S. *Manuscript is in a preparation.*

[15] Pogozelski, W. K.; McNeese, T. J.; Tullius, T. D. *J. Am. Chem. Soc.* **1995**, 117, 6428-6433.

[16] Burrows, C. J.; Muller, J. G. *Chem. Rev.* **1998**, *98*, 1109-1152.

[17] Jen, Jen-Fon; Leu, Meei-Fan; Yang, Thomas C. *Journal of Chromatography. A*. **1998**, 796, 283-288.

[18] Yang, Chung-Shi; Tsai, Pi-Ju; Lin, Nai-Nu; Liu, Lin; Kuo, Jon-Son. *Free Radical Biology & Medicine*. **1995**, 19, 453-459.

Chapter 3: Redox-Activated, DNA-Cleavage by 2-Arylcarbonyl-3-Trifluoromethylquinoxaline 1,4-di-*N*-Oxides

3.1 Introduction

Studies reported in Chapters 1-2 on 1,2,4-benzotriazine 1,4-di-*N*-oxides show that these compounds upon bio-reductive activation cause oxidative DNA strand cleavage under hypoxic conditions. In addition, studies also suggest that the release of hydroxyl radical from activated benzotriazine *di*-oxides can explain their ability to cause the DNA strand cleavage. These studies may provide a chemical mechanism underlying the antitumor activity of benzotriazine *di*-oxides. Particularly, because of clinically promising anti-tumor activity of tirapazamine, it is important to examine the structural activity relationships within a new class of drugs. Such studies not only will be helpful to discover drugs with improved anticancer activity but may help define chemical mechanisms by which various heterocyclic *N*-oxides show the anti-cancer activity.

3.1.1 Quinoxaline analogs posses anti-cancer activity

Quinoxaline analogs are known to posses hypoxia selective cytotoxicity against cancer cell lines in culture.[1,2,3,4,5] Due to the fact that quinoxaline dioxide compounds possess potent antitumor activity, various analogs were synthesized and tested on cancer cell lines.[6,7,8,9] Monge and coworkers synthesized 3-trifluoromethyl-2-carbonylquinoxaline di-*N*-oxide derivatives and examined their anticancer activity on human cancer cell lines.[5] Data revealed that the compound 2-benzoyl-6,7-difluoro-3-trifluoromethylquinoxaline 1,4-di-*N*-oxide (**42**) shows potent anticancer activity *in vitro* assays but not *in vivo* hollow

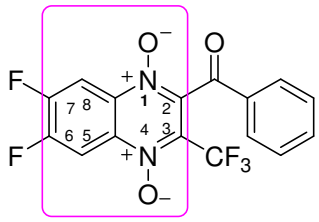

42

Figure 3.1: 2-benzoyl-6,7-difluoro-3-trifluoromethylquinoxaline 1,4-di-*N*-oxide (**42**)

fibers.[5] However, these studies suggested that electron withdrawing groups in the position 6 or/and 7, and aromatic groups attached to carbonyl improve the anticancer activity of 2-carbonylquinoxaline di-*N*-oxide analogs.[5] In the search of quinoxaline analogs with improved anticancer activity, Monge and co-workers synthesized compounds **43-48** and examined their anticancer activity against 60 human tumor cell lines and *in vivo* hollow fibers.[10] The *in vitro* data show that quinoxaline analogs, **43**-**48** show potent anticancer activity in cell lines with the growth inhibition activity (GI_{50}) of 0.74-0.07 μM.[10] The *in vivo* hollow fibers assays on these compounds show that the compound **48** shows potent anti-tumor activity against more than one cancer cell line.[10]

In addition, it is important to note that quinoxaline di-oxides with the loss of one or two oxygens do not show the potent anticancer activity.[10] This data suggests that the presence of di-*N*-oxide is necessary for the anti-cancer activity of quinoxaline compounds.

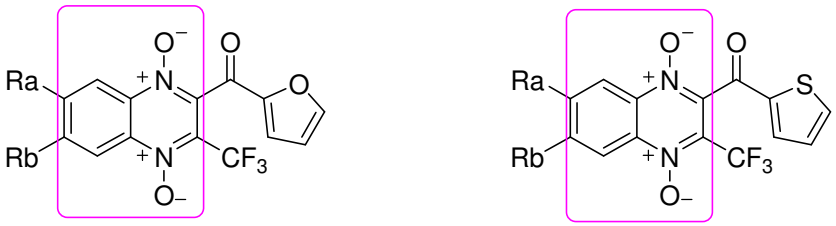

43: Ra=Rb=Cl
44: Ra=Rb=F
45: Ra=Cl; Rb=H

46: Ra=Rb=Cl
47: Ra=Rb=F
48: Ra=Cl; Rb=H

Figure 3.2: Quinoxaline analogs with potent anticancer activity *in vitro* studies

3.2 Goal: Examine the chemistry responsible for the anticancer activity of 2-arylcarbonyl-3-trifluoromethylquinoxaline 1,4-di-*N*-oxides

In our current studies, we aimed to understand the chemistry responsible for the anti-cancer activity of quinoxaline analogs **43-48** in collaboration with Monge and Co-workers. It is known that many heterocyclic *N*-oxides including phenazine dioxides and benzotriazine dioxides derive their anti-cancer activity via their ability to cause the DNA strand cleavage.[11,12,13,14,15,16] Accordingly, we hypothesized that the DNA strand cleavage by compounds **43-48** is responsible for their anticancer activity. As part of our studies, compounds **43-48** were obtained from Monge and Co-workers and *in vitro* redox-activated DNA cleavage by these compounds was examined. More importantly, we performed systematic mechanistic studies on the compound **48** to examine the chemistry responsible for medicinal properties of compounds **43-48**.

3.3 2-Arylcarbonyl-3-trifluoromethylquinoxaline 1,4-di-*N*-oxides cause DNA strand cleavage under anaerobic conditions

As part of our efforts to examine the role of DNA strand cleavage in the anticancer activity of quinoxaline analogs, we performed concentration dependent (25-150 μM) DNA strand cleavage assays with quinoxaline di-oxides **43-48** under anaerobic conditions. Our preliminary data show that upon reductive activation, compounds **43-48** cause the DNA strand cleavage (Figures 3.3-3.10). Studies also show that compounds **44, 47** and **48** show better DNA strand cleavage and compounds **43, 45** and **46** show relatively poor DNA strand cleavage compared to TPZ at 25 μM (Figure 3.11). It is important to note that the compounds **43-48** precipitated out from the reactions at higher concentrations. Hence, clear concentration-dependent DNA strand cleavage by **43-48** was not observed at higher concentrations (Figure 3.10).

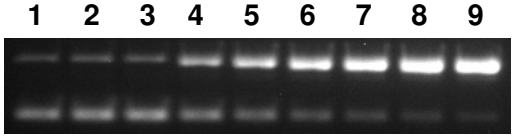

Figure 3.3: DNA cleavage by various concentrations of reductively activated TPZ under anaerobic conditions. Supercoiled plasmid DNA (33 μg/mL, pGL-2 Basic) was incubated with TPZ (25-150 μM), NADPH (500 μM), cytochrome P450 reductase (0.03 units/mL), catalase (100 μg/mL), superoxide dismutase (10 μg/mL), sodium phosphate buffer (50 mM, pH 7.0), and desferal (1 mM) under anaerobic conditions at room temperature for 16 h, followed by agarose gel electrophoretic analysis. Lane 1, DNA alone (S = 0.24); lane 2, NADPH (500 μM) + reductase (1 mU) (S = 0.27); lane 3, TPZ (150 μM) (S = 0.27); lanes 4-9, NADPH (500 μM) + reductase (0.03 units/mL) + TPZ (25 μM, lane 4) (S = 0.84); (50 μM, lane 5) (S = 1.29); (75 μM, lane 6) (S = 1.78); (100 μM, lane 7) (S = 2.20); (125 μM, lane 8) (S = 2.62); (150 μM, lane 9) (S = 3.19);. The value S represents the mean number of strand breaks per plasmid molecule and is calculated using the equation $S = -\ln f_I$, where f_I is the fraction of plasmid present as form I.[17] Acetonitrile (40% by volume in water) was introduced to prepare stock solution of TPZ (400 μM).

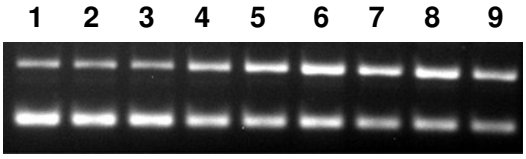

Figure 3.4: DNA cleavage by various concentrations of reductively activated **43** under anaerobic conditions. Supercoiled plasmid DNA (33 μg/mL, pGL-2 Basic) was incubated with **43** (25-150 μM), NADPH (500 μM), cytochrome P450 reductase (0.03 units/mL), catalase (100 μg/mL), superoxide dismutase (10 μg/mL), sodium phosphate buffer (50 mM, pH 7.0), and desferal (1 mM) under anaerobic conditions at room temperature for 16 h, followed by agarose gel electrophoretic analysis. Lane 1, DNA alone (S = 0.27); lane 2, NADPH (500 μM) + reductase (1 mU) (S = 0.29); lane 3, **43** (150 μM) (S = 0.30); lanes 4-9, NADPH (500 μM) + reductase (0.03 units/mL) + **43** (25 μM, lane 4) (S = 0.50); (50 μM, lane 5) (S = 0.62); (75 μM, lane 6) (S = 0.75); (100 μM, lane 7) (S = 0.72); (125 μM, lane 8) (S = 0.83); (150 μM, lane 9) (S = 0.76). The value S represents the mean number of strand breaks per plasmid molecule and is calculated using the equation $S = -\ln f_I$, where f_I is the fraction of plasmid present as form I.[17] Acetonitrile (40% by volume in water) was introduced to prepare stock solution of **43** (400 μM).

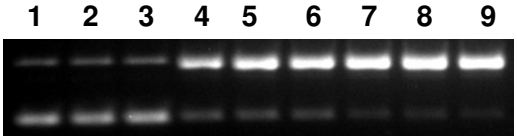

Figure 3.5: DNA cleavage by various concentrations of reductively activated **44** under anaerobic conditions. Supercoiled plasmid DNA (33 μg/mL, pGL-2 Basic) was incubated with **44** (25-150 μM), NADPH (500 μM), cytochrome P450 reductase (0.03 units/mL), catalase (100 μg/mL), superoxide dismutase (10 μg/mL), sodium phosphate buffer (50 mM, pH 7.0), and desferal (1 mM) under anaerobic conditions at room temperature for 16 h, followed by agarose gel electrophoretic analysis. Lane 1, DNA alone (S = 0.25); lane 2, NADPH (500 μM) + reductase (1 mU) (S = 0.28); lane 3, **44** (150 μM) (S = 0.28); lanes 4-9, NADPH (500 μM) + reductase (0.03 units/mL) + **44** (25 μM, lane 4) (S = 1.57); (50 μM, lane 5) (S = 1.90); (75 μM, lane 6) (S = 2.02); (100 μM, lane 7) (S = 2.66); (125 μM, lane 8) (S = 2.76); (150 μM, lane 9) (S = 2.96). The value S represents the mean number of strand breaks per plasmid molecule and is calculated using the equation $S = -\ln f_I$, where f_I is the fraction of plasmid present as form I.[17] Acetonitrile (40% by volume in water) was introduced to prepare stock solution of **44** (400 μM).

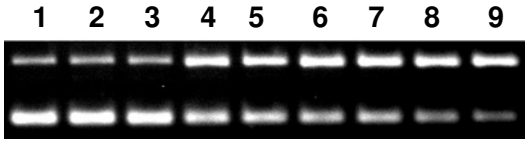

Figure 3.6: DNA cleavage by various concentrations of reductively activated **45** under anaerobic conditions. Supercoiled plasmid DNA (33 μg/mL, pGL-2 Basic) was incubated with **45** (25-150 μM), NADPH (500 μM), cytochrome P450 reductase (0.03 units/mL), catalase (100 μg/mL), superoxide dismutase (10 μg/mL), sodium phosphate buffer (50 mM, pH 7.0), and desferal (1 mM) under anaerobic conditions at room temperature for 16 h, followed by agarose gel electrophoretic analysis. Lane 1, DNA alone (S = 0.27); lane 2, NADPH (500 μM) + reductase (1 mU) (S = 0.29); lane 3, **45** (150 μM) (S = 0.28); lanes 4-9, NADPH (500 μM) + reductase (0.03 units/mL) + **45** (25 μM, lane 4) (S = 0.63); (50 μM, lane 5) (S = 0.62); (75 μM, lane 6) (S = 0.80); (100 μM, lane 7) (S = 0.83); (125 μM, lane 8) (S = 0.91); (150 μM, lane 9) (S = 1.07). The value S represents the mean number of strand breaks per plasmid molecule and is calculated using the equation $S = -\ln f_I$, where f_I is the fraction of plasmid present as form I.[17] Acetonitrile (40% by volume in water) was introduced to prepare stock solution of **45** (400 μM).

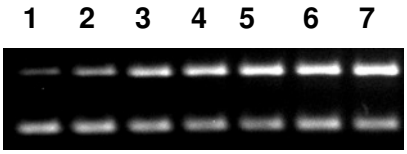

Figure 3.7: DNA cleavage by various concentrations of reductively activated **46** under anaerobic conditions. Supercoiled plasmid DNA (33 μg/mL, pGL-2 Basic) was incubated with **46** (25-150 μM), NADPH (500 μM), cytochrome P450 reductase (0.03 units/mL), catalase (100 μg/mL), superoxide dismutase (10 μg/mL), sodium phosphate buffer (50 mM, pH 7.0), and desferal (1 mM) under anaerobic conditions at room temperature for 16 h, followed by agarose gel electrophoretic analysis. Lane 1, **46** (150 μM) (S = 0.28); lanes 2-7, NADPH (500 μM) + reductase (0.03 units/mL) + **46** (25 μM, lane 2) (S = 0.44); (50 μM, lane 3) (S = 0.65); (75 μM, lane 4) (S = 0.77); (100 μM, lane 5) (S = 0.91); (125 μM, lane 6) (S = 0.80); (150 μM, lane 7) (S = 0.94). The value S represents the mean number of strand breaks per plasmid molecule and is calculated using the equation $S = -\ln f_I$, where f_I is the fraction of plasmid present as form I.[17] Acetonitrile (40% by volume in water) was introduced to prepare stock solution of **46** (400 μM).

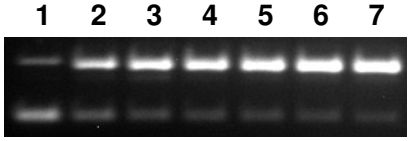

Figure 3.8: DNA cleavage by various concentrations of reductively activated **47** under anaerobic conditions. Supercoiled plasmid DNA (33 μg/mL, pGL-2 Basic) was incubated with **47** (25-150 μM), NADPH (500 μM), cytochrome P450 reductase (0.03 units/mL), catalase (100 μg/mL), superoxide dismutase (10 μg/mL), sodium phosphate buffer (50 mM, pH 7.0), and desferal (1 mM) under anaerobic conditions at room temperature for 16 h, followed by agarose gel electrophoretic analysis. Lane 1, **47** (150 μM) (S = 0.30); lanes 2-7, NADPH (500 μM) + reductase (0.03 units/mL) + **47** (25 μM, lane 2) (S = 1.28); (50 μM, lane 3) (S = 1.80); (75 μM, lane 4) (S = 1.96); (100 μM, lane 5) (S = 2.15); (125 μM, lane 6) (S = 2.41); (150 μM, lane 7) (S = 2.59). The value S represents the mean number of strand breaks per plasmid molecule and is calculated using the equation $S = -\ln f_I$, where f_I is the fraction of plasmid present as form I.[17] Acetonitrile (40% by volume in water) was introduced to prepare stock solution of TPZ (400 μM).

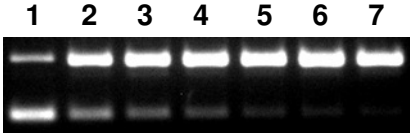

Figure 3.9: DNA cleavage by various concentrations of reductively activated **48** under anaerobic conditions. Supercoiled plasmid DNA (33 μg/mL, pGL-2 Basic) was incubated with **48** (25-150 μM), NADPH (500 μM), cytochrome P450 reductase (0.03 units/mL), catalase (100 μg/mL), superoxide dismutase (10 μg/mL), sodium phosphate buffer (50 mM, pH 7.0), and desferal (1 mM) under anaerobic conditions at room temperature for 16 h, followed by agarose gel electrophoretic analysis. Lane 1, **48** (150 μM) (S = 0.37); lanes 2-7, NADPH (500 μM) + reductase (0.03 units/mL) + **48** (25 μM, lane 2) (S = 1.32); (50 μM, lane 3) (S = 1.85); (75 μM, lane 4) (S = 2.17); (100 μM, lane 5) (S = 2.59); (125 μM, lane 6) (S = 2.86); (150 μM, lane 7) (S = 2.92). The value S represents the mean number of strand breaks per plasmid molecule and is calculated using the equation $S = -\ln f_I$, where f_I is the fraction of plasmid present as form I.[17] Acetonitrile (40% by volume in water) was introduced to prepare stock solution of TPZ (400 μM).

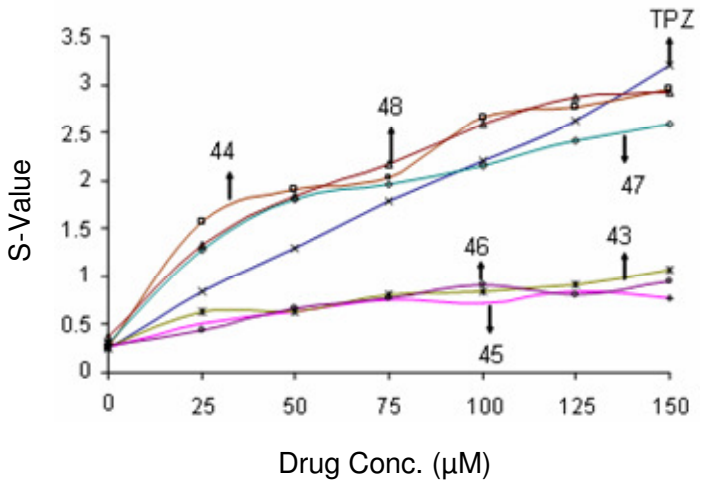

Figure 3.10: DNA cleavage efficiency of quinoxaline analogs **43-48** and TPZ at various concentrations (25 μM-150 μM). The *S*-value is the mean number of strand breaks per plasmid molecule and is calculated using the following equation: $S=-\ln f_I$ where f_I is the fraction of uncut, form I DNA remaining.[17] Acetonitrile (40% by volume) was introduced to prepare stock solutions of TPZ and **43-48** (400 μM).

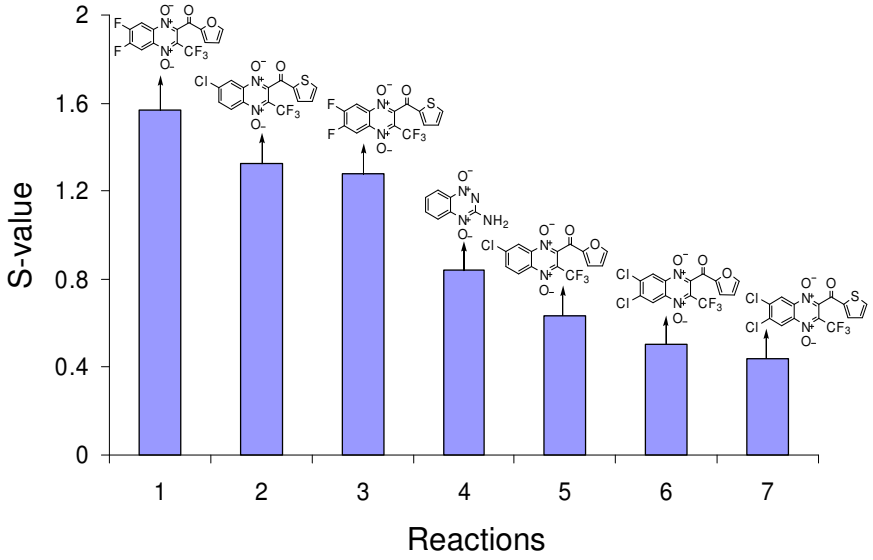

Figure 3.11: Comparison of DNA cleavage ability of quinoxaline analogs **43-48** with TPZ at 25 μM. Acetonitrile (40% by volume) was introduced to prepare stock solutions of TPZ and **43-48** (400 μM).

Our preliminary DNA strand cleavage data on quinoxaline analogs **43-48** suggests that redox-activated DNA cleavage by these compounds might be responsible for their anticancer activity. In analogy with TPZ that is known to derive its biological activity

from the DNA damage. We further explored to study the detailed chemistry responsible for the DNA strand cleavage by these quinoxaline compounds using the compound **48**. The reason for choosing the quinoxaline analog **48** is that this compound showed potent anticancer activity in more than two human tumor cell lines *in vivo* hollow fibers.[10]

3.4 Quinoxaline analog 48 causes redox-activated DNA strand cleavage under anaerobic conditions

As part of our goal to understand the detailed chemistry underlying the anticancer activity of **48** and its analogs**,** we carried out *in vitro* DNA strand cleavage assays on **48** at low concentrations (5-25 μM) under anaerobic conditions. Our data show that the compound **48** shows concentration-dependent DNA strand cleavage at low concentrations (5-25 μM) (Figure 3.12). Further, comparative DNA strand cleavage assays on **48** and TPZ under the same conditions show that the compound **48** causes similar DNA strand cleavage to TPZ (Figures 3.12-3.14). In control experiments with **48** (no NADPH:cytochrome P450 reductase) and with NADPH:cytochrome P450 reductase (no **48**), significant DNA cleavage was not observed.

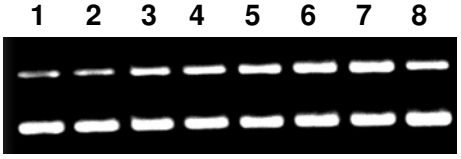

Figure 3.12: DNA cleavage by various concentrations of reductively activated **48** under anaerobic conditions. Supercoiled plasmid DNA (33 μg/mL, pGL-2 Basic) was incubated with **48** (5-25 μM), NADPH (500 μM), cytochrome P450 reductase (0.03 units/mL), catalase (100 μg/mL), superoxide dismutase (10 μg/mL), sodium phosphate buffer (50 mM, pH 7.0), and desferal (1 mM) under anaerobic conditions at room temperature for 16 h, followed by agarose gel electrophoretic analysis. Lane 1, DNA alone (S = 0.25 ± 0.04); lane 2, NADPH (500 μM) + reductase (1 mU) (S = 0.25 ± 0.04); lanes 3-7, NADPH (500 μM) + reductase (0.03 units/mL) + **48** (5 μ M, lane 3) (S = 0.37 ± 0.05); (10 μ M, lane 4) (S = 0.43 ± 0.05); (15 μ M, lane 5) (S = 0.52 ± 0.03); (20 μ M, lane 6) (S = 0.58 ± 0.02); (25 μ M, lane 7) (S = 0.68 ± 0.04); lane 8, **48** (25 μM) (S = 0.26 ± 0.05);. Acetonitrile (40% by volume in water) was introduced to prepare stock solution of **48** (400 μM).

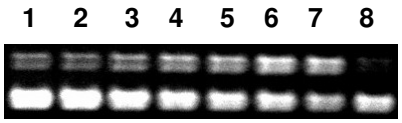

Figure 3.13: DNA cleavage by various concentrations of reductively activated TPZ under anaerobic conditions. Supercoiled plasmid DNA (33 μg/mL, pGL-2 Basic) was incubated with TPZ (5-25 μM), NADPH (500 μM), cytochrome P450 reductase (0.03 units/mL), catalase (100 μg/mL), superoxide dismutase (10 μg/mL), sodium phosphate buffer (50 mM, pH 7.0), and desferal (1 mM) under anaerobic conditions at room temperature for 16 h, followed by agarose gel electrophoretic analysis. Lane 1, DNA alone (S = 0.23 ± 0.06); lane 2, NADPH (500 μM) + reductase (1 mU) (S = 0.24 ± 0.06); lanes 3-7, NADPH (500 μM) + reductase (0.03 units/mL) + TPZ (5 μM, lane 3) (S = 0.30 ± 0.07); (10 μM, lane 4) (S = 0.36 ± 0.07); (15 μM, lane 5) (S = 0.40 ± 0.07); (20 μM, lane 6) (S = 0.46 ± 0.04); (25 μM, lane 7) (S = 0.48 ± 0.08); lane 8, TPZ (25 μM) (S = 0.24 ± 0.02);. The value S represents the mean number of strand breaks per plasmid molecule and is calculated using the equation $S = -\ln f_I$, where f_I is the fraction of plasmid present as form I.[17] Acetonitrile (40% by volume in water) was introduced to prepare stock solution of TPZ (400 μM).

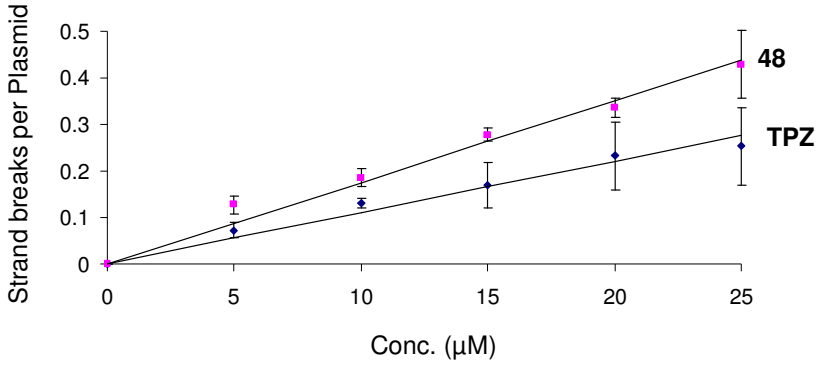

Figure 3.14: A plot comparing DNA cleavage efficiency of reductively activated **48** and TPZ under anaerobic conditions. Supercoiled plasmid DNA (33 μg/mL, pGL-2 Basic) was incubated with **48** or TPZ (5-25 μM), NADPH (500 μM), cytochrome P450 reductase (0.03 units/mL), catalase (100 μg/mL), superoxide dismutase (10 μg/mL), sodium phosphate buffer (50 mM, pH 7.0), and desferal (1 mM) under anaerobic conditions at room temperature for 16 h, followed by agarose gel electrophoretic analysis. The values, S, derived from agarose gel data such as that shown in Figures 4.12 and 4.13 and represent the mean number of strand breaks per plasmid molecule and were calculated using the equation $S = -\ln f_I$, where f_I is the fraction of plasmid present as form I.[17] Background cleavage in the untreated plasmid was substracted to allow direct comparision of DNA cleavage yields between different experiments.

3.5 Compound 48 gives metabolites with the loss of oxygen

The *in vitro* metabolic studies on the compound **48** were carried out in the presence of NADPH:cytochrome P450 reductase under anaerobic conditions. Metabolites generated from activated **48** were analyzed by HPLC and LC/ESI-MS analysis. Our data show that upon metabolic activation the quinoxaline analog **48** generates 1-*N*-oxide (**51**)

as a major metabolite that elutes at ~23 min and 4-*N*-oxide (**52**) as a minor metabolite that elutes at ~25 min (Figure 3.15). The DNA cleavage assays on metabolites **51** and **52** show that these compounds do not cleave the DNA upon reductive activation under anaerobic conditions. This data is consistent with *in vitro* studies on human tumor cell lines, where quinoxaline di-oxides with loss of oxygen do not show potent anticancer activity. In addition, quinoxaline di-oxides do not cause DNA-cleavage without reductive activation. This data suggests that compound **48** generates the DNA-damaging intermediate on metabolic activation similar to other heterocyclic di-*N*-oxides. To understand the exact chemical nature of DNA damaging intermediate, we carried out mechanistic studies similar to those carried out with TPZ. In our mechanistic studies, we hypothesized that reductively-activated **48** generates radical intermediate, which causes the DNA-cleavage like in other di-*N*-oxides. If so, the DNA cleavage by activated **48** should be inhibited in the presence of typical radical scavengers methanol, ethanol, *t*-butanol, DMSO and mannitol.

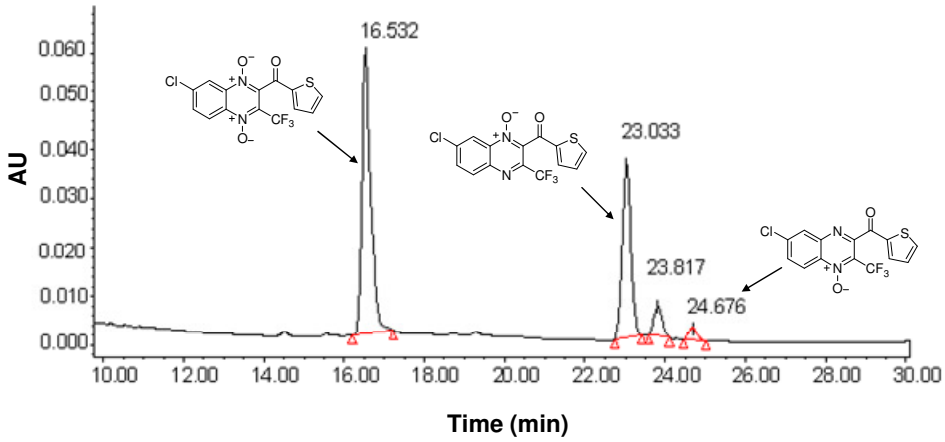

Figure 3.15: HPLC analysis of products arising from *in vitro* metabolism of **48** by NADPH:cytochrome P450 reductase under anaerobic conditions. Compound **48** (200 µM) was incubated with NADPH:cytochrome P450 reductase (0.33 units/mL) and NADPH (500 µM) in sodium phosphate buffer (pH 7.0, 50 mM) containing desferal (1 mM) for 16 h, under anaerobic conditions. The resulting mixture was analyzed by reverse phase HPLC as described in the experimental section.

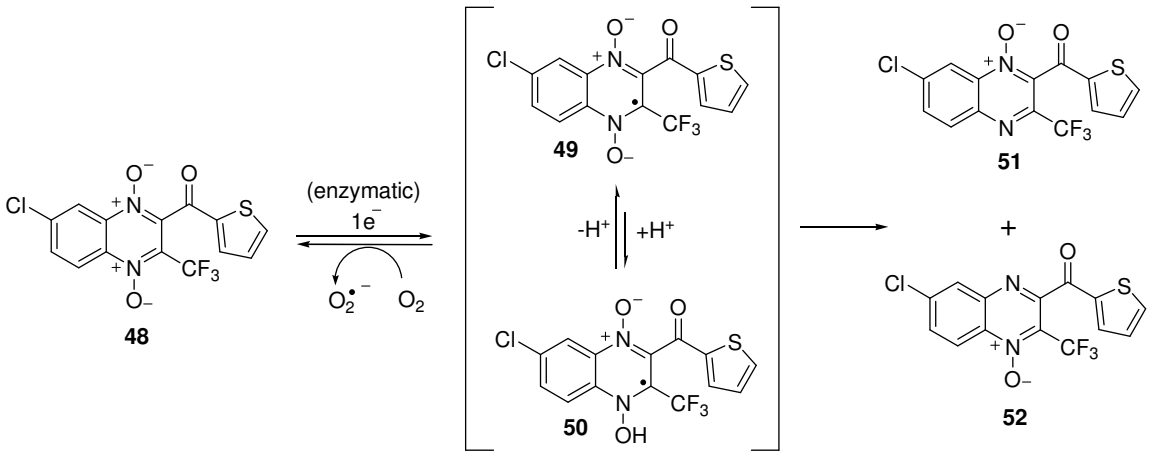

Scheme 3.1: *In vitro* metabolism of quinoxaline di-*N*-oxide (**48**)

3.6 Radical scavengers inhibit the anaerobic DNA cleavage by 48

DNA cleavage assays containing radical scavengers were carried out similar to concentration dependent DNA cleavage assays except adding deoxygenated radical scavengers before addition of NADPH and cytochrome P450 reductase. The extent of inhibition of DNA strand cleavage by activated **48** was analyzed and quantified similar to earlier experiments that we reported in Chapter 2. Data show that the DNA cleavage by activated **48** is inhibited (68%-80%) by the typical radical scavengers (Figures 3.15-3.17). Further, we compared the inhibition of compound **48** mediated DNA-cleavage to that of TPZ in the presence of radical scavengers. Data reveal that radical scavengers show similar inhibition effects on the DNA-cleavage by **48** and TPZ (Figure 3.18). This information shows that the DNA-damaging agent released from activated **48** is radical in nature. Based on this information, we hypothesized that activated **48** releases hydroxyl radical similar to benzotriazine dioxides. To examine our hypothesis, we set out to trap hydroxyl radical with dimethyl sulfoxide similar to our earlier studies that we reported in Chapter 1.

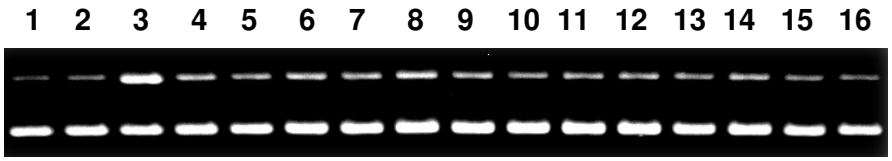

Figure 3.16: Cleavage of supercoiled plasmid DNA by **48** in the presence of NADPH:cytochrome P450 reductase as an activating system. All reactions contained DNA (33 µg/mL, pGL-2 Basic), sodium phosphate buffer (50 mM, pH 7.0), catalase (100 μg/ mL), superoxide dismutase (10 μg/mL), and desferal (1 mM) and were incubated under anaerobic conditions (except lane 16) at 24 °C for 16 h, followed by agarose gel electrophoretic analysis. Lane 1, DNA alone (S = 0.23 ± 0.00); lane 2, NADPH (500 μM) + reductase (33 mU/mL) (S = 0.24 ± 0.02); lane 3, **48** (25 μM) + NADPH (500 μM) + reductase (33 mU/mL) (S = 0.77 ± 0.17); lanes 4-8, **48** (25 μM) + NADPH (500 μM) + reductase (33 mU/mL) + methanol (500 mM, lane 4) (S = 0.42 ± 0.13); ethanol (500 mM, lane 5) (S = 0.40 ± 0.15); *tert*-butyl alcohol (500 mM, lane 6) (S = 0.44 ± 0.15); DMSO (500 mM, lane 7) (S = 0.41 ± 0.15); mannitol (500 mM, lane 8) (S = 0.34 ± 0.00); lane 9, **48** alone (25 µM) (S = 0.26 ± 0.02); lane 10, **51**alone (25 µM) (S = 0.25); lane 11, **52** alone (25 µM) (S = 0.25); lane 12, no-*N*-oxide alone (25 µM) (S = 0.25); lane 13, **51** (25 μM) + NADPH (500 μM) + reductase (33 mU/mL) (S = 0.25); lane 14, **52** (25 μM) + NADPH (500 μM) + reductase (33 mU/mL) (S = 0.31); lane 15, no-N-oxide (25 μM) + NADPH (500 μM) + reductase (33 mU/mL) (S = 0.29); lane 16, **48** (25 µM) + NADPH (500 µM) + reductase (1 mU) + air (S = 0.29). The value S represents the mean number of strand breaks per plasmid molecule and is calculated using the equation $S = -\ln f_I$, where f_I is the fraction of plasmid present as form I.[17] Acetonitrile (40% by volume) was introduced to prepare stock solution of **48** (400 µM).

Figure 3.17: Cleavage of supercoiled plasmid DNA by TPZ in the presence of NADPH:cytochrome P450 reductase as an activating system. All reactions contained DNA (33 µg/mL, pGL-2 Basic), sodium phosphate buffer (50 mM, pH 7.0), catalase (100 μg/ mL), superoxide dismutase (10 μg/mL), and desferal (1 mM) and were incubated under anaerobic conditions at 24 °C for 16 h, followed by agarose gel electrophoretic analysis. Lane 1, DNA alone (S = 0.25 ± 0.01); lane 2, NADPH (500 μM) + reductase (33 mU/mL) (S = 0.26 ± 0.03); lane 3, TPZ (25 μM) + NADPH (500 μM) + reductase (33 mU/mL) (S = 0.52 ± 0.07); lanes 4-8, TPZ (25 μM) + NADPH (500 μM) + reductase (33 mU/mL) + methanol (500 mM, lane 4) (S = 0.28 ± 0.01); ethanol (500 mM, lane 5) (S = 0.29 ± 0.00); *tert*-butyl alcohol (500 mM, lane 6) (S = 0.28 ± 0.02); DMSO (500 mM, lane 7) (S = 0.30 ± 0.04); mannitol (500 mM, lane 8) (S = 0.33 ± 0.01); lane 9, TPZ alone (S = 0.26 ± 0.01); lane 10, TPZ (25 µM) + NADPH (500 µM) + reductase (1 mU) + air (S = 0.28 ± 0.02). The value S represents the mean number of strand breaks per plasmid molecule and is calculated using the equation $S = -\ln f_I$, where f_I is the fraction of plasmid present as form I.[17] Acetonitrile (40% by volume) was introduced to prepare stock solution of TPZ (400 µM).

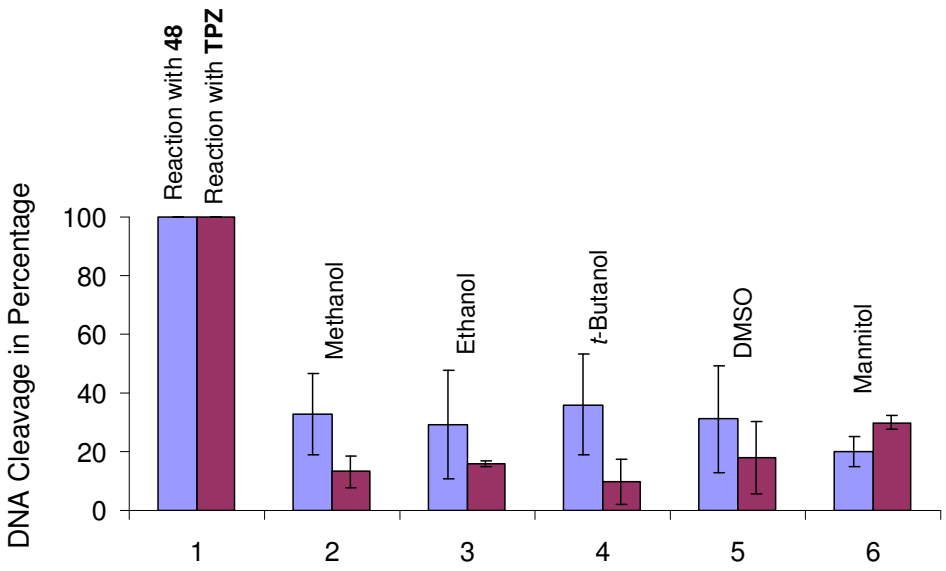

Figure 3.18: Effect of radical scavengers on DNA-cleavage by **48** and TPZ under anaerobic conditions

3.7 Activated 48 hydroxylates DMSO to methane sulfinic acid

In the hydroxyl radical trapping experiments, the compound **48** in DMSO containing solution was activated with NADPH:cytochrome p450 reductase under hypoxic conditions. Then the methanesulfinic acid produced in the presence of activated **48** was derivatized with the diazonium salt **32** to give the diazosulfone **33**. The diazosulfone **33** was detected and quantified using HPLC as we described in Chapter 1. Our HPLC data

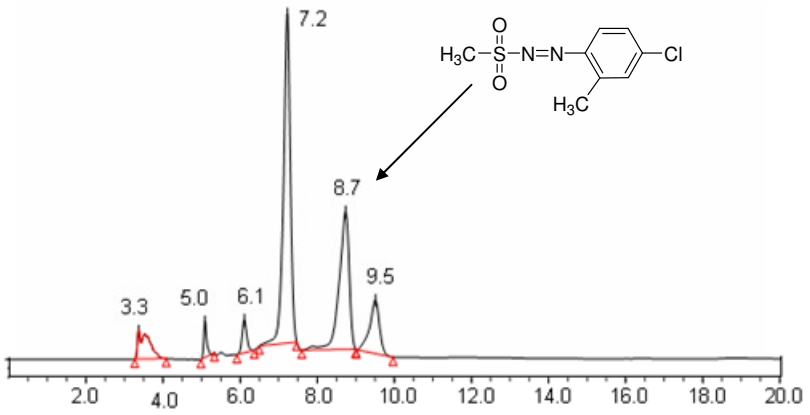

Figure 3.19: HPLC trace of diazosulfone generated in the reaction of reductively activated **48**

Assay	HPLC Peak Area for MSA-Diazosulfone
NADPH+Cytochrome P450 Reductase	317967
NADPH+**48**	227446
NADPH+Cytochrome P450 Reductase+**48**	778198

Figure 3.20: HPLC peak areas of diazosulfone produced in control reactions and in the reaction of **48**.

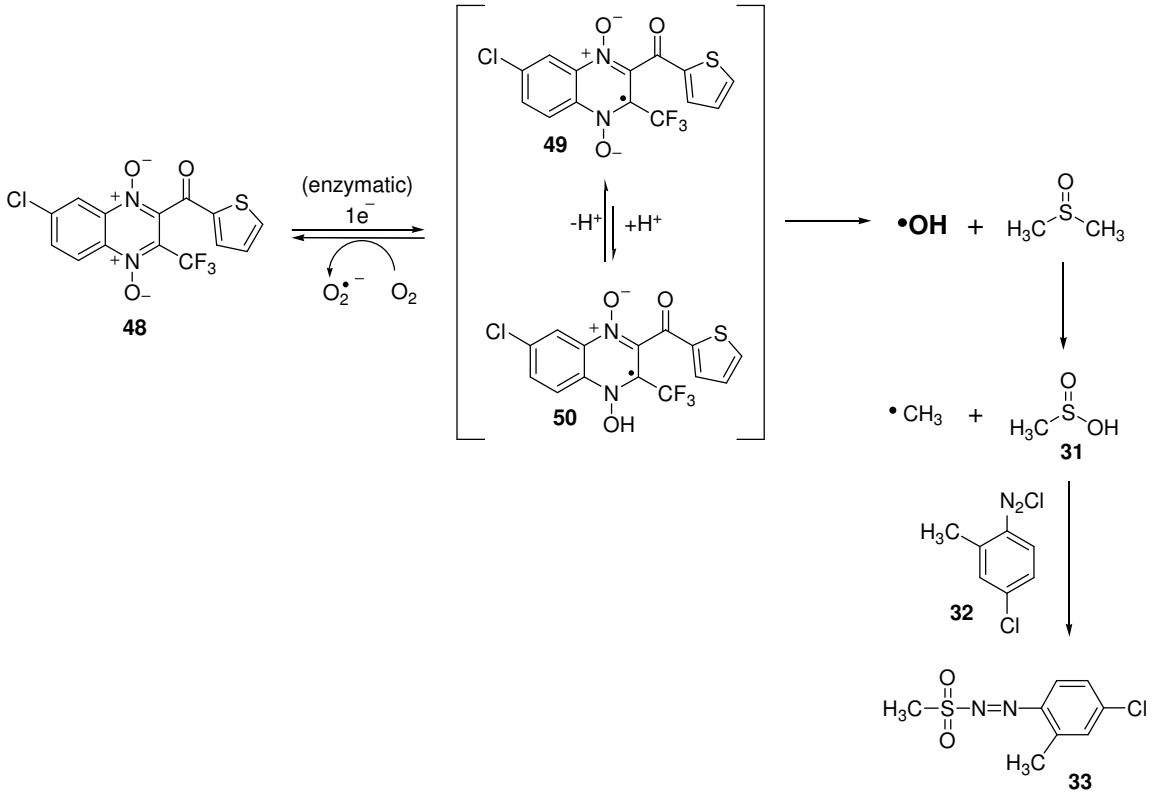

Scheme 3.2: Activated **48** hydroxylates DMSO

show that activated **48** does indeed generate diazosulfone 33, which elutes ~8.7 min under the reaction conditions employed here (Figure 3.19). Further, formation of diazosulfone **33** from activated **48** was confirmed by co-injection of authentic diazosulfone with the diazosulfone produced in **48** reaction. The amount of methane sulfinic acid generated in the presence of activated **48** was determined by constructing

calibration curves with the quantitative detection of known amounts of methane sulfinic acid. The extent of metabolism of **48** was determined by using UV-Vis spectroscopy. Our data reveal that the compound **48** produces methanesulfinic acid in ~50% yield under our reaction conditions.

3.8 Proposed mechanism for anaerobic DNA-cleavage by 48 and its analogs

Studies reported here show that metabolic activation is required for DNA strand cleavage by quinoxaline analogs. *In vitro* metabolic studies on **48** show that quinoxaline analogs lose oxygen upon metabolic activation. Data also show that metabolites of **48** do not cause DNA-cleavage. Inhibition of DNA-cleavage by radical scavengers suggests

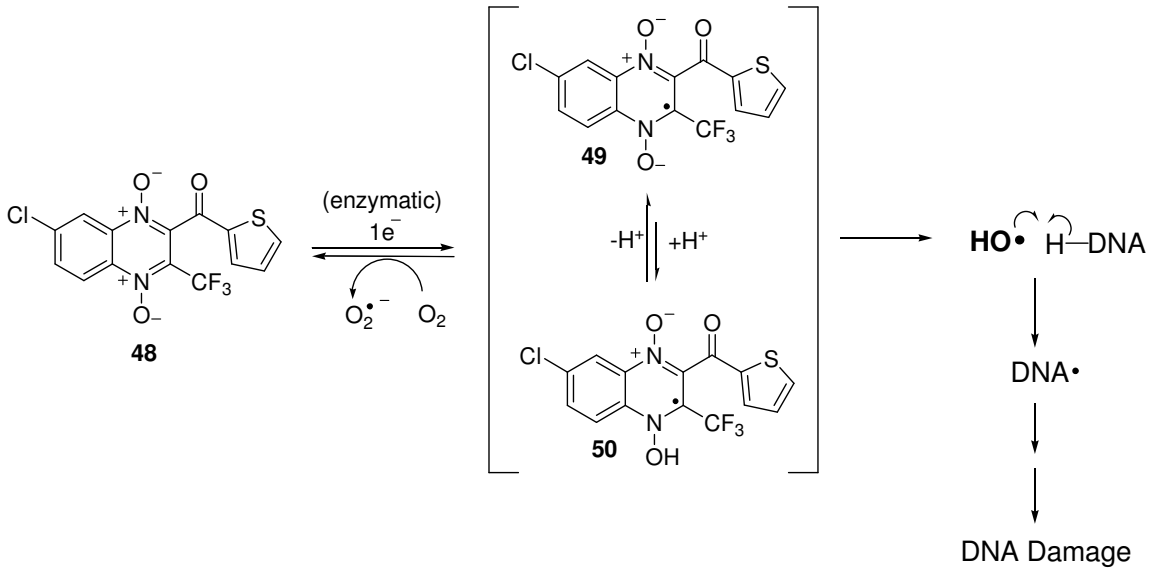

Scheme 3.3: Proposed mechanism for the DNA-cleavage by quinoxaline analogs under anaerobic conditions

that the compound **48** upon metabolic activation generates radical DNA damaging agent. Hydroxylation of DMSO to methane sulfinic acid by activated **48** suggests that quinoxaline analogs release hydroxyl radical upon reductive-activation. Thus, overall

data suggest that quinoxaline di-oxides upon reductive activation produce known DNA damaging agent hydroxyl radical similar to TPZ and its analogs.

3.9 Compound 48 cleaves the DNA upon reductive activation under aerobic conditions

Although hypoxia selective cytotoxicity is an important property for an anticancer activity of quinoxaline analogs, it is important to note that some of the cancer cell lines are more prone to oxidative stress compared to normal cells and some cancer cells exist at near normal oxygen concentrations.[18] This data suggest that oxidative stress caused by quinoxaline analogs via producing superoxide radical might contribute to the anticancer activity of quinoxaline analogs.[19] For example, various heterocyclic *N*-oxides and quinones are known to generate superoxide radical *via* redox cycling under aerobic conditions.[11,12,13,14,15,16,20] Under physiological conditions, superoxide radical is known to produce hydrogen peroxide, which in the presence of metals yields DNA-damaging agent, hydroxyl radical.[21] Hence, generation of superoxide radical *in vivo* causes the oxidative damage to DNA, proteins, and lipids which lead to cytotoxicity.[22,23,24,25]

In our studies, we examined the possible role of superoxide radical mediated chemistry in the antitumor activity of quinoxaline analogs. As part of these studies, the compound **48** was activated with NADPH:cytochrome P450 reductase under aerobic conditions and the DNA-cleavage was analyzed using agarose gel electrophoresis. Our data show that activated **48** causes DNA-damage under aerobic conditions. Further, our comparative DNA cleavage studies with known redox cycling agent menadione (MD) and TPZ show that the compound **48** causes similar DNA-cleavage to that of menadione

and three folds better than that of clinically promising drug TPZ under the same experimental conditions (Figures 3.21-3.23).

Figure 3.21: Effect of various additives on DNA cleavage by QDA in the presence of NADPH:cytochrome P450 reductase under aerobic conditions. Reactions with DNA (33 µg/mL, pGL-2 Basic) and sodium phosphate buffer (50 mM, pH 7.0) containing 2.5 % acetonitrile were incubated under aerobic conditions at 24 °C for 2 h, followed by agarose gel electrophoretic analysis. Lane 1, DNA alone (S = 0.20 ± 0.01); lane 2, NADPH (500 μM) + reductase (33 mU/mL) (S = 0.24 ± 0.03); lane 3, QDA alone (25 µM) (S = 0.22 ± 0.02); lane 4, QDA (25 μM) + NADPH (500 μM) + reductase (33 mU/mL) (S = 0.72 ± 0.09); lanes 5-12, QDA (25 μM) + NADPH (500 μM) + reductase (33 mU/mL) + superoxide dismutase (10 µg/mL, lane 5) (S = 0.40 ± 0.05); catalase (100 µg/mL, lane 6) (S = 0.41 ± 0.09); desferal (1 mM, lane 7) (S = 0.37 ± 0.06); methanol (500 mM, lane 8) (S = 0.29 ± 0.07); ethanol (500 mM, lane 9) (S = 0.25 ± 0.04); *tert*-butyl alcohol (500 mM, lane 10) (S = 0.32 ± 0.02); DMSO (500 mM, lane 11) (S = 0.25 ± 0.07); mannitol (500 mM, lane 12) (S = 0.28 ± 0.08). The value S represents the mean number of strand breaks per plasmid molecule and is calculated using the equation $S = -\ln f_I$, where f_I is the fraction of plasmid present as form I.[17]

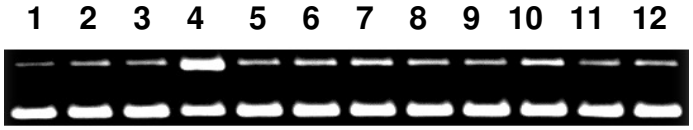

Figure 3.22: Effect of various additives on DNA cleavage by menadione (MD) in the presence of NADPH:cytochrome P450 reductase under aerobic conditions. Reactions with DNA (33 µg/mL, pGL-2 Basic) and sodium phosphate buffer (50 mM, pH 7.0) containing 2.5 % acetonitrile were incubated under aerobic conditions at 24 °C for 2 h, followed by agarose gel electrophoretic analysis. Lane 1, DNA alone (S = 0.18 ± 0.02); lane 2, NADPH (500 μM) + reductase (33 mU/mL) (S = 0.22 ± 0.02); lane 3, MD alone (25 µM) (S = 0.20 ± 0.00); lane 4, MD (25 μM) + NADPH (500 μM) + reductase (33 mU/mL) (S = 0.73 ± 0.12); lanes 5-12, MD (25 μM) + NADPH (500 μM) + reductase (33 mU/mL) + superoxide dismutase (10 µg/mL, lane 5) (S = 0.21 ± 0.00); catalase (100 µg/mL, lane 6) (S = 0.22 ± 0.02); desferal (1 mM, lane 7) (S = 0.23 ± 0.05);methanol (500 mM, lane 8) (S = 0.22 ± 0.00); ethanol (500 mM, lane 9) (S = 0.21 ± 0.00); *tert*-butyl alcohol (500 mM, lane 10) (S = 0.29 ± 0.02); DMSO (500 mM, lane 11) (S = 0.19 ± 0.02); mannitol (500 mM, lane 12) (S = 0.21 ± 0.00). The value S represents the mean number of strand breaks per plasmid molecule and is calculated using the equation $S = -\ln f_I$, where f_I is the fraction of plasmid present as form I[17]

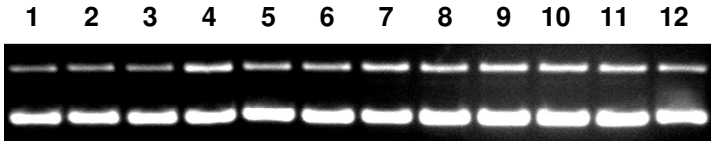

Figure 3.23: Effect of various additives on DNA cleavage by TPZ in the presence of NADPH:cytochrome P450 reductase under aerobic conditions. Reactions with DNA (33 µg/mL, pGL-2 Basic) and sodium phosphate buffer (50 mM, pH 7.0) containing 2.5 % acetonitrile were incubated under aerobic conditions at 24 °C for 2 h, followed by agarose gel electrophoretic analysis. Lane 1, DNA alone (S = 0.18 ± 0.00); lane 2, NADPH (500 μM) + reductase (33 mU/mL) (S = 0.20 ± 0.01); lane 3, TPZ alone (25 µM) (S = 0.21 ± 0.03); lane 4, TPZ (25 μM) + NADPH (500 μM) + reductase (33 mU/mL) (S = 0.31 ± 0.00); lanes 5-12, QDA (25 μM) + NADPH (500 μM) + reductase (33 mU/mL) + superoxide dismutase (10 µg/mL, lane 5) (S = 0.21 ± 0.00); catalase (100 µg/mL, lane 6) (S = 0.21 ± 0.01); desferal (1 mM, lane 7) (S = 0.26 ± 0.01); methanol (500 mM, lane 8) (S = 0.21 ± 0.02); ethanol (500 mM, lane 9) (S = 0.21 ± 0.00); *tert*-butyl alcohol (500 mM, lane 10) (S = 0.22 ± 0.01); DMSO (500 mM, lane 11) (S = 0.21 ± 0.00); mannitol (500 mM, lane 12) (S = 0.20 ± 0.02). The value S represents the mean number of strand breaks per plasmid molecule and is calculated using the equation $S = -\ln f_I$, where f_I is the fraction of plasmid present as form I.[17]

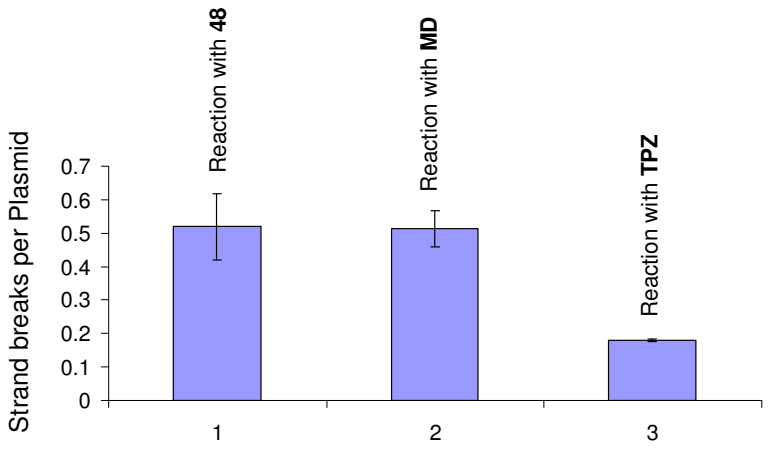

Figure 3.24: Comparative DNA cleavage efficiency of activated **48,** TPZ and menadione (**MD**) under aerobic conditions

We further studied the chemical mechanisms responsible for the DNA strand cleavage by activated **48** under aerobic conditions. As part of these studies, we tested the role of superoxide radical, hydrogen peroxide and metals in the DNA cleavage by **48**. For example, superoxide dismutase (SOD) is known to destroy superoxide radical, catalase is known to destroy hydrogen peroxide, desferal is known to chelate the metals,

and radical scavenging agents are known to quench hydroxyl radicals. Accordingly, we carried out reactions with activated **48** in the presence of SOD, catalase, desferal and radical scavenging agents under aerobic conditions. Our data show that aerobic DNA cleavage by activated **48** was inhibited by SOD (64%), catalase (63%), desferal (70%), and radical scavengers (83%-95%). In addition, we also compared effects of these

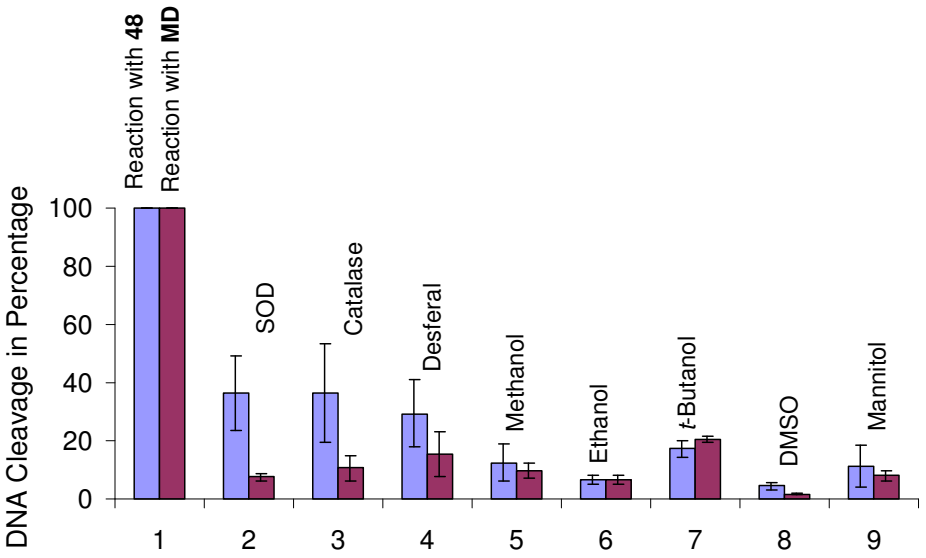

Figure 3.25: Effect of SOD, catalase, desferal and radical scavengers on the DNA-cleavage by activated **48** and MD under aerobic conditions

additives on the DNA-cleavage by **44** to that of DNA cleavage by known biologically active redox-cycling agent menadione (MD) upon reductive activation under the identical conditions. Our studies show that additives show similar inhibition effects on the DNA cleavage by both MD and **48**. It is interesting to note that SOD, catalase and desferal show some what less inhibition effects on DNA cleavage by **48**. This might be due to minor oxygen-independent DNA-cleavage (anaerobic DNA cleavage) occurs in case of **48**. Overall the data indicates that upon metabolic activation and under aerobic conditions compound **48** does redox cycling similar to menadione and produces

superoxide radical, which further produce DNA damaging agent hydroxyl radical (Scheme 3.4).

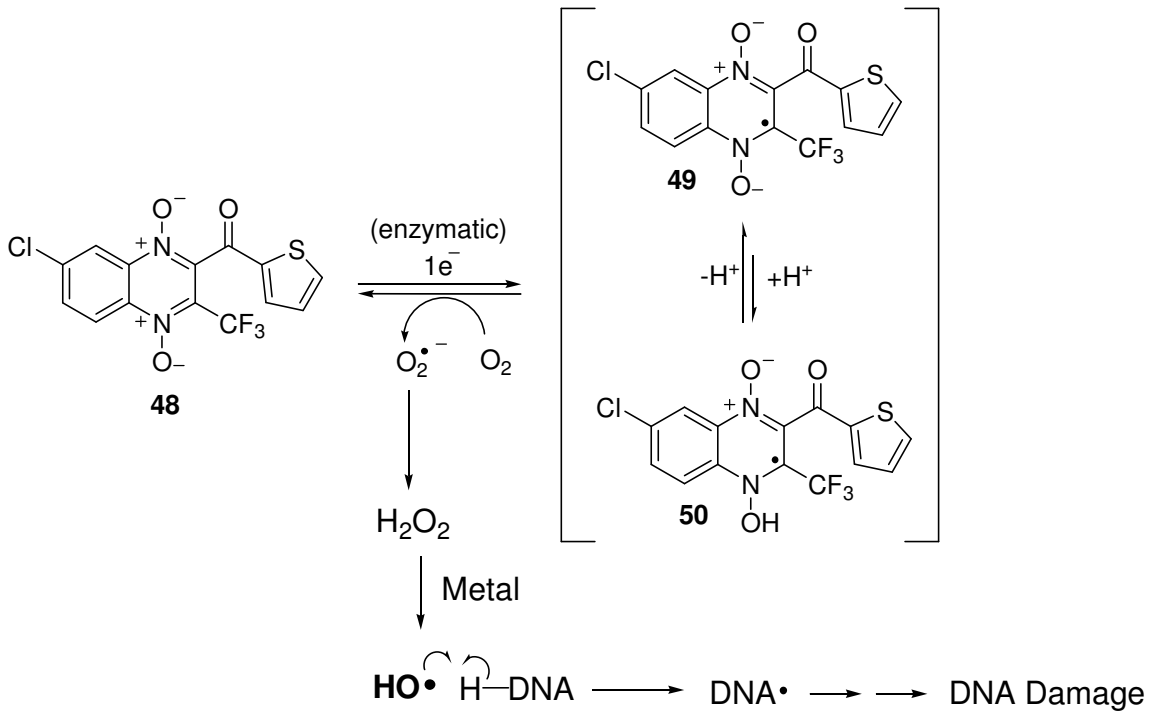

Scheme 3.4: Proposed mechanism for DNA-cleavage by quinoxaline analogs under aerobic conditions

3.10 Conclusions

Our data on quinoxaline analogs reported in this Chapter showed that these compounds cause oxidative DNA-damage upon reductive activation under both aerobic and anaerobic conditions. Studies on quinoxaline analog **48** show that this compound causes DNA-cleavage under anaerobic conditions. Studies also show that DNA-cleavage by activated **48** is comparable to that of clinically promising drug TPZ under anaerobic conditions. The *in vitro* metabolic studies on compound **48** under anaerobic conditions show that it produces metabolites with the loss of oxygen. Metabolites of **48** do not cleave the DNA under anaerobic conditions. Anaerobic DNA-cleavage by **48** was

inhibited by the radical scavenging agents, which suggests that radical intermediate is responsible for the DNA-damage. Further, oxidation of DMSO to methanesulfinic acid in the presence of activated **48** under anaerobic conditions provides evidence for the release of hydroxyl radical. Our DNA cleavage assays with **48** under aerobic conditions show that activated **48** produces superoxide radical, which further decomposes to generate known DNA damaging agent hydroxyl radical. The oxidative DNA damage by **48** under aerobic conditions is comparable to that of known biologically active redox cycling agent menadione. Our overall data suggests that oxidative DNA-cleavage by quinoxaline analogs under both aerobic and anaerobic conditions provides plausible chemical mechanisms for their anticancer activity.

3.11 Experimental

3.11.1 Anaerobic DNA cleavage assays. The *in vitro* anaerobic DNA strand cleavage assays were carried out similar to our earlier experiments that we reported in Chapter-2. Briefly, in a typical assay, supercoiled plasmid DNA (33 μg/mL, pGL-2 Basic) was incubated with TPZ or quinoxaline analogs (5-25 μM or 25-150 μM), NADPH (500 μM), cytochrome P450 reductase (1 mU), catalase (100 μg/mL), superoxide dismutase (10 μg/mL), sodium phosphate buffer (50 mM, pH 7.0), and desferal (1 mM) under anaerobic conditions at 25 ˚C for 16 h. Acetonitrile (40% by volume) was introduced into stock solutions of TPZ or **48** (400 μM). All components of the reactions except enzymes, NADPH, and DNA were deoxygenated by three freeze-pump-thaw cycles. Enzymes, NADPH, and DNA were diluted with deoxygenated water in an argon filled glove bag to prepare stock solutions. Reactions were initiated by adding cytochrome P450 reductase, then wrapped with aluminium to prevent exposure to light. Anaerobic conditions were maintained by incubating reactions in an argon filled glove bag. DNA strand cleavage in reactions was detected by quantified as we reported in Chapter-2.

DNA cleavage assays containing radical scavengers were carried out similar to the above experiments except adding radical scavengers such as methanol, ethanol, *tert*-butyl alcohol, DMSO, or mannitol (500 mM) before intiating reactions with the cytochrome P450 reductase. In air control reaction, the reaction was carried out similar to anaerobic assays except without degassing reaction components and incubating reaction under normal conditions.

3.11.2 *In vitro* metabolic studies. In an anaerobic metabolic assay, a solution containing **48** (200 μM) and desferal (1 mM) in sodium phosphate buffer (pH 7, 50 mM) was

deoxygenated by three cycles of freeze-pump-thaw. Then degassed solution was transferred to an eppendorf tube in an argon filled glove bag. Then NADPH (500 μM), cytochrome P450 reductase (30 mU/mL), catalase (100 μg/mL), and superoxide dismutase (10 μg/mL) were added and the resultant reaction was incubated under argon at 25 ˚C for 16 h. Control reaction with **48** (no NADPH:cytochrome P450 reductase) was carried out under the same conditions. Enzymes and NADPH were diluted with deoxygenated water. Before analyzing *in vitro* metabolites generated from activated **48,** proteins from the reaction were removed by centrifugation through Amicon Microcon (YM3) filters. The filtrate was analyzed by HPLC employing a C18 reverse phase Rainin Microsorb-MV column (5 μm particle size, 100 A˚ pore size, 25 cm length, 4.6 mm i.d.) eluted with gradient solvent system starting with 50% A (0.5% acetic acid in water) and 50% B (acetonitrile) followed by linear increase to 20% B from 0 min to 40 min. Then, 50% B was achieved in next 5 min. The flow rate of 0.6 mL/min was used and the products were monitored by UV-absorbance at 254 nm. In *vitro* metabolism of **48** by NADPH:cytochrome P450 reductase yields two products whose relative yields were estimated on the basis of their relative peak areas in the HPLC chromatogram. The major product was identified as 1-*N*-oxide (**51**) that elutes at 23 min and minor product was identified as 4-*N*-oxide (**52**) that elutes at 25 min. The identity of metabolites confirmed by the co-injection of authentic compounds with the reaction mixture of **48** and LC/MS analysis.

In LC/MS analysis, metabolites were extracted into ethyl acetate and dried, and redissolved in 50:50 acetonitrile:water. Resultant metabolites were analyzed by LC/ESI-MS in positive ion mode.

3.11.3 Trapping of hydroxyl radical with DMSO. Methanesulfinic acid produced by the oxidation of DMSO was detected and quantitated using a modified version of the protocol reported by Fukui et al.[26] In a typical assay, individual components of the reactions were deoxygenated similar to experiments in Chapter-2. To a degassed solution containing **48** (300 μM), desferal (1 mM), DMSO (2.5 M), and sodium phosphate buffer (50 mM, pH 7.0), NADPH (1 mM) and cytochrome P450 reductase (0.146 U/mL) were added. The reaction (1 mL final volume) was capped, mixed, and allowed to incubate under argon atmoshere at 24 °C for 4 h. Control experiments with NADPH:cytochrome P450 reductase (no **48**) and with **48** (no NADPH:cytochrome P450 reductase) were carried out under the same conditions. Then the amount of **48** consumed in the reaction and controls was quantified by using UV-Vis spectroscopy. Then sodium phosphate (0.5 mL, 500 mM, pH 4.0) was added to the reaction and controls, followed by Fast Red TR diazonium salt (0.5 mL of 10 mg/mL) and the mixture allowed to stand at room temperature for 10 min. During 10 min orange color was developed and the resulting orange color solution was extracted with ethyl acetate (2 X 1 mL) and exactly 1.2 mL of the upper ethyl acetate layer recovered by pipet. A portion of this ethyl acetate solution (20 μL) containing the methane diazosulfone was then analyzed by HPLC. The diazosulfone conjugate monitored at 310 nm has a retention time of approximately 9 min on a Rainin Microsorb-MV propylamine column eluted with hexane-2-propanol (100:3) and flow rate of 1 mL/min.

3.11.4 Aerobic DNA cleavage studies. In a typical aerobic DNA cleavage assay, supercoiled plasmid DNA (33 μg/mL, pGL-2 Basic), compound **48** or menadione (MD) (25 μM), NADPH (500 μM) and cytochrome P450 reductase were incubated in sodium

phosphate buffer (50 mM, pH 7.0) containing 2.5% acetonitrile under aerobic conditions at 24 ˚C for 2 h. The compound **48** and MD were introduced as stock solutions in acetonitrile. Following incubation, the reactions were stopped by adding 5 µL of 50% glycerol loading buffer, and the resulting mixture was loaded onto a 0.9% agarose gel. The DNA mixture was separated by agarose gel electrophoresis at 85 V in 1xTAE buffer and then stained in a solution of aqueous ethidium bromide (0.3µg/mL) for 2 h. DNA in the gel was visualized by UV-transillumination, and the amount of DNA in each band was quantified using an Alpha Innotech IS-1000 digital imaging system. DNA cleavage assays containing SOD, catalase, desferal and radical scavengers were carried out in a manner identical to standard reaction exception that corresponding components were added prior to the addition of NADPH and cytochrome P450.

References:

[1] Monge, A.; Palop, J. A.; Lopez de Cerain, A. L.; Senador, V.; Martinez-Crespo, F. J.; Sainz, Y.; Narro, S.; Garcia, E.; de Miguel, C.; Gonzalez, M.; Hamilton, E.; Barker, A. J.; Clarke, E. D.; Greenhow, D. T. *J. Med. Chem.* **1995**, *38*, 1786-1792.

[2] Azqueta, A.; Pachon, G.; Cascante, M.; Creppy, E. E.; Monge, A.; de Cerain, A. L. *Arzneim.-Forsch.* **2005**, *55*, 177-182.

[3] Ortega, M. A.; Morancho, M. J.; Martinez-Crespo, F. J.; Sainz, Y.; Montoya, M. E.; de Cerain, A. L.; Monge, A. *Eur. J. Med. Chem.* **2000**, *35*, 21-30.

[4] Monge, A.; Palop, J. A.; Gonzalez, M.; Martinez-Crespo, F. J.; Lopez, de Cerain, A. L.; Sainz, Y.; Narro, S.; Barker, A. J.; Hamilton, E. *J. Heterocycl. Chem.* **1995**, *32*, 1213-1217.

[5] Zarranz, B.; Jaso, A.; Aldana, I.; Monge, A. *Bioorg. Med. Chem.* **2004**, *12*, 3711-3721.

[6] Aguirre, G.; Cerecetto, H.; Di Maio, R.; Gonzalez, M.; Alfaro, M. E. M.; Jaso, A.; Zarranz, B.; Ortega, M. A.; Aldana, I.; Monge, A. *Bioorg. Med. Chem. Lett.* **2004**, *14*, 3835-3839.

[7] Jaso, A.; Zarranz, B.; Aldana, I.; Monge, A. *J. Med. Chem.* **2005**, *48*, 2019-2025.

[8] Lima, L. M.; Zarranz, B.; Marin, A.; Solano, B.; Vicente, E.; Silanes, S. P.; Aldana, I.; Monge, A. *J. Heterocycl. Chem.* **2005**, *42*, 1381-1385.

[9] Zarranz, B.; Jaso, A.; Aldana, I.; Monge, A.; Maurel, S.; Deharo, E.; Jullian, V.; Sauvain, M. *Arzneim.-Forsch.* **2005**, *55*, 754-761.

[10] Solano, B.; Junnotula, V.; Marin, A.; Villar, R.; Burguete, A.; Vicente, E. ; Perez-Silanes, S.; Monge, A.; Dutta, S.; Sarkar, U.; Gates, K. S. *J. Med. Chem.* **2007**, 50, 5485-5492.

[11] Wardman, P. *Curr. Med. Chem.* **2001**, *8*, 739-761.

[12] Cerecetto, H.; Gonzalez, M.; Lavaggi, M. L.; Azqueta, A.; Lopez, de Cerain, A.; Monge, A. *J. Med. Chem.* **2005**, *48*, 21-23.

[13] Daniels, J. S.; Gates, K. S. *J. Am. Chem. Soc.* **1996**, *118*, 3380-3385.

[14] Ganley, B.; Chowdhury, G.; Bhansali, J.; Daniels, J. S.; Gates, K. S. *Bioorg. Med. Chem.* **2001**, *9*, 2395-2041.

[15] Chowdhury, G.; Kotandeniva, D.; Daniels, J. S.; Barnes, C. L.; Gates, K. S. *Chem. Res. Toxicol.* **2004**, *17*, 1399-1405.

[16] Monge, A.; Martinez-Crespo, F. J.; Lopez de Cerain, A.; Palop, J. A.; Narro, S.; Senador, V.; Marin, A.; Sainz, Y.; Gonzalez, M.; Hamilton, E.; Barker, A. J.; Clarke, E. D.; Greenhow, D. T. *J. Med. Chem.* **1995**, *38*, 4488-4494.

[17] Povirk, L. F.; Wubker, W.; Kohnlein, W.; Hutchinson, F. *Nuceic Acid Res.* **1977,** 4, 3573-3580.

[18] Shumacker, P. T. *Cancer Cells.* **2006**, *10*, 175-176.

[19] Pelicano, H.; Feng, L.; Zhou, Y.; Carew, J. S.; Hileman, E. O.; Plunkett, W.; Keating, M. J.; Huang, P. *J. Biol. Chem.* **2003**, 278, 37832-37839.

[20] Nutter, Louise M.; Ngo, Emily O.; Fisher, Geoffrey R.; Gutierrez, Peter L. *J. Biol. Chem.* **1992**, 267(4), 2474-2479.

[21] Halliwell, B.; Gutteridge, J. M. C. *Methods Enzymol.* **1990**, *186*, 1-85.

[22] Bagley, A. C.; Krall, J.; Lynch, R. E. *Proc. Natl. Acad. Sci. U.S.A.* **1986**, *83*, 9189-9193.

[23] Hassan, H. M.; Fridovich, I. *Arch. Biochem. Biophys.* **1979**, *196*, 385-395.

[24] Finkel, T.; Holbrook, N. J. *Nature* **2000**, *408*, 239-247.

[25] Davis, W. J.; Ronai, Z.; Tew, K. D. *J. Pharmacol. Exp. Ther.* **2001**, *296*, 1-6.

[26] Fukui, S.; Hanasaki, Y.; Ogawa, S. *J. Chromatogr.* 1993, *630*, 187-193.

Chapter 4: Mechanisms of Strand Cleavage by Tirapazamine

4.1 Introduction

Studies reported in Chapters 1-3 show that benzotriazine-di-*N*-oxides and quinoxaline di-*N*-oxides upon reductive-activation cause oxidative DNA strand cleavage. In our current studies, we examined chemical mechanisms responsible for the DNA strand cleavage by heterocyclic di-*N*-oxides using the clinically promising anti-cancer agent, tirapazamine. The data on TPZ shows that the abstraction of hydrogen atoms from the deoxyribose backbone is responsible for the DNA strand cleavge.[1,2] However, the exact hydrogen atoms abstraction responsible for the DNA strand cleavage is not well understood. In our group studies, we examined the abstraction of exact hydrogens involved in TPZ mediated DNA strand cleavage by characterizing the end products. It is important to note that the abstraction of each hydrogen atom from the deoxyribose backbone yields diagnostic end products based on conditions via cascade of reactions.[3] For example, the abstraction of C1$^{'}$-hydrogen under both aerobic and anaerobic conditions leads to the formation of 5-methylene-furanone (**54**) as an end

product and where as abstraction of C4'-hydrogen under aerobic conditions leads to the formation of phosphoglycolate (**55**) and base propenals (**56**) or malondialdehyde (**57**), and under anaerobic conditions leads to the formation of compounds **58**-**61** (Scheme 4.1).[3,4,5,6,7] Data also show that abstraction of C5'-hydrogen under aerobic conditions yields 1,4-butene-dial (**62**) as an end product and under anaerobic conditions furfural (**63**) as an end product (Scheme 4.1).[3,8]

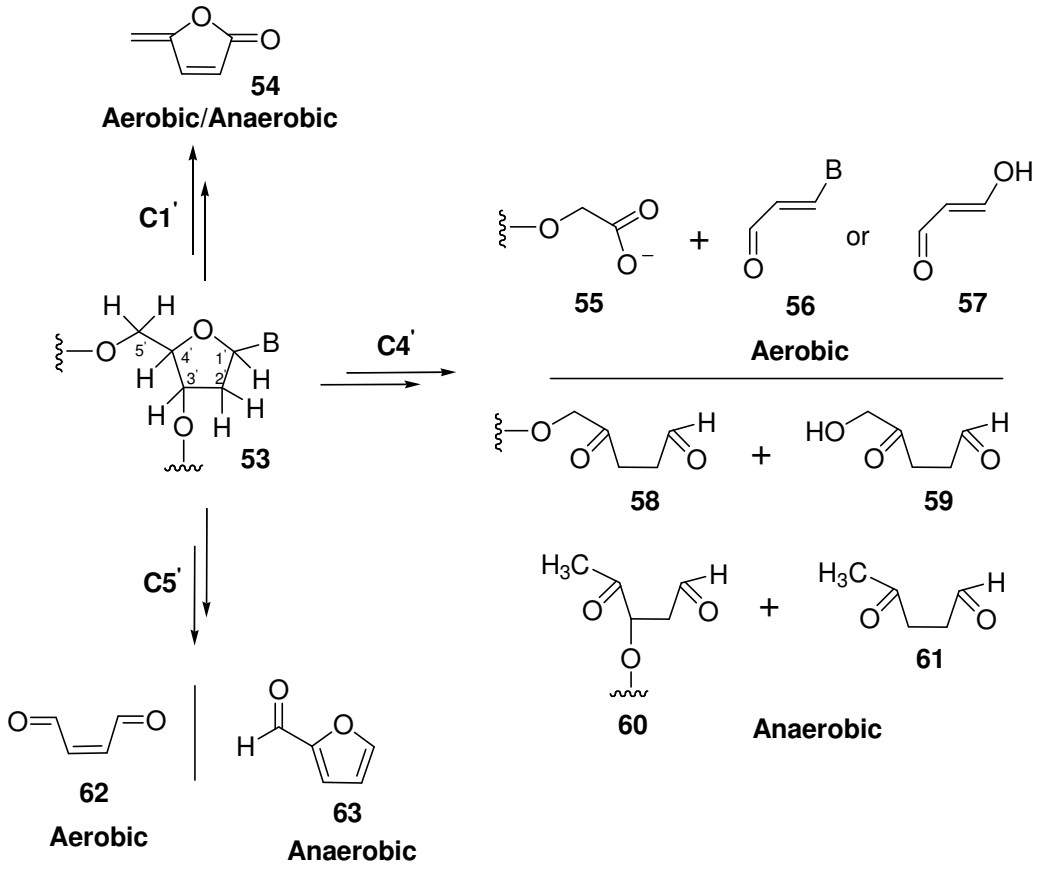

Scheme 4.1: End products generated from C1', C4' and C5'-hydrogen atoms abstraction under both aerobic and anaerobic conditions

So, careful analysis of end products generated from TPZ mediated DNA damage not only reveal the information about the exact hydrogen abstraction involved in DNA strand

cleavage but also will be helpful to understand the size of the DNA damaging agent and the interaction of TPZ and its mono-*N*-oxide metabolites with the DNA radicals generated from hydrogen atoms abstraction. For example, the small and diffusible species like hydroxyl radical abstracts not only the least hindered C4$^{'}$ and C5$^{'}$-hydrogens and but also the most hindered C1$^{'}$-hydrogen of duplex DNA.[3,9,10,11,12] On the other hand, larger DNA damaging agents can not access sterically hindered hydrogen atoms. In addition, earlier group studies show that TPZ and its mono-*N*-oxide substitute molecular oxygen in converting DNA radicals into strand breaks.[13,14,15]

Based on low sequence dependent DNA strand cleavage by TPZ and its ability to hydroxylate DMSO and salicylic acid, we proposed that activated TPZ releases hydroxyl radical, which leads to abstraction of not only least hindered C4$^{'}$- and C5$^{'}$-hydrogens and but also most hindered C1$^{'}$ under anaerobic conditions.[1,16] In addition, based on our understanding of TPZ and 1-*N*-oxide of TPZ ability to convert DNA radicals into strand breaks, we also proposed that under anaerobic conditions TPZ yields characteristic end products, which normally produced via hydrogen atoms abstraction under aerobic conditions.[13,14,15]

As part of our studies, we treated Calf-thymus DNA with enzymatically activated TPZ under anaerobic conditions. Then, we analyzed end products generated from TPZ mediated DNA damage. Our data show that the activated TPZ generates end products, which were produced *via* abstraction of hydrogen's from both least and most hindered sites in duplex DNA.

4.2 Detection of C1'-hydrogen abstraction derived product

The C1'-hydrogen of deoxyribose is the most sterically hindered hydrogen atom in the duplex DNA. We hypothesized that if activated TPZ releases small and diffusible species like hydroxyl radical, it might lead to the abstraction of C1'-hydrogen, which yields 5-methylene-2-furanone as an end product (Scheme 4.2). Accordingly, Goutam in our group examined the possible formation of 5-methylene-2-furanone (**54**) in TPZ mediated DNA damage. As part of these studies, Calf-thymus DNA was treated with the activated TPZ under anaerobic conditions and end products produced in TPZ mediated DNA damage was analyzed by HPLC analysis. The HPLC data shows that TPZ treated

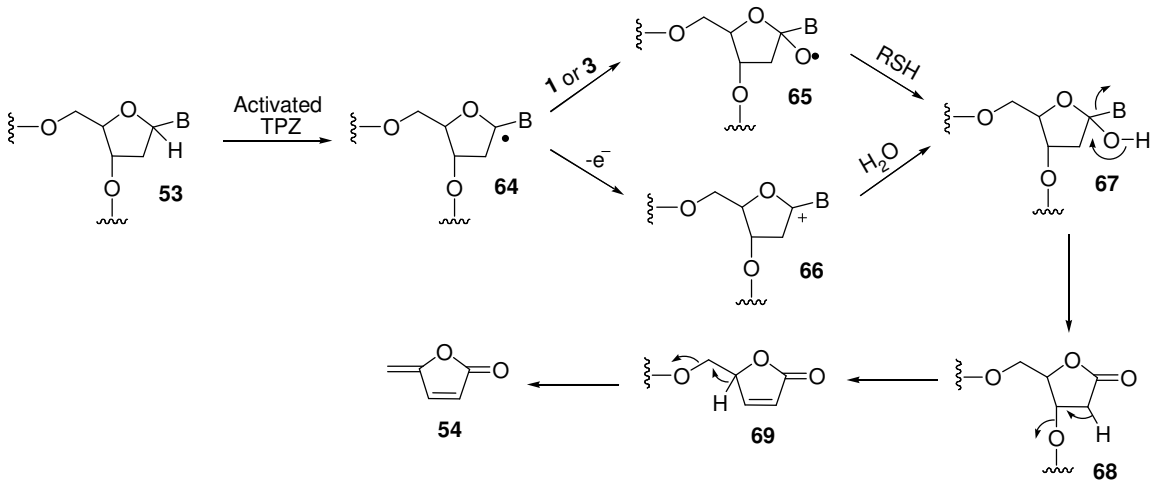

DNA yields 5-methylene-2-furanone (**54**).

Scheme 4.2: Proposed mechanism for the formation of 5-methylene-2-furanone in TPZ mediated DNA damage

4.3 Detection of C4'-hydrogen abstraction derived products

Data shows that hydrogen atom abstraction from the C4'-position under aerobic conditions yields the formation of phosphoglycolate (**55**) and malondialdehyde equivalents (**56** or **57**) or base propenals). Accordingly, we hypothesized that

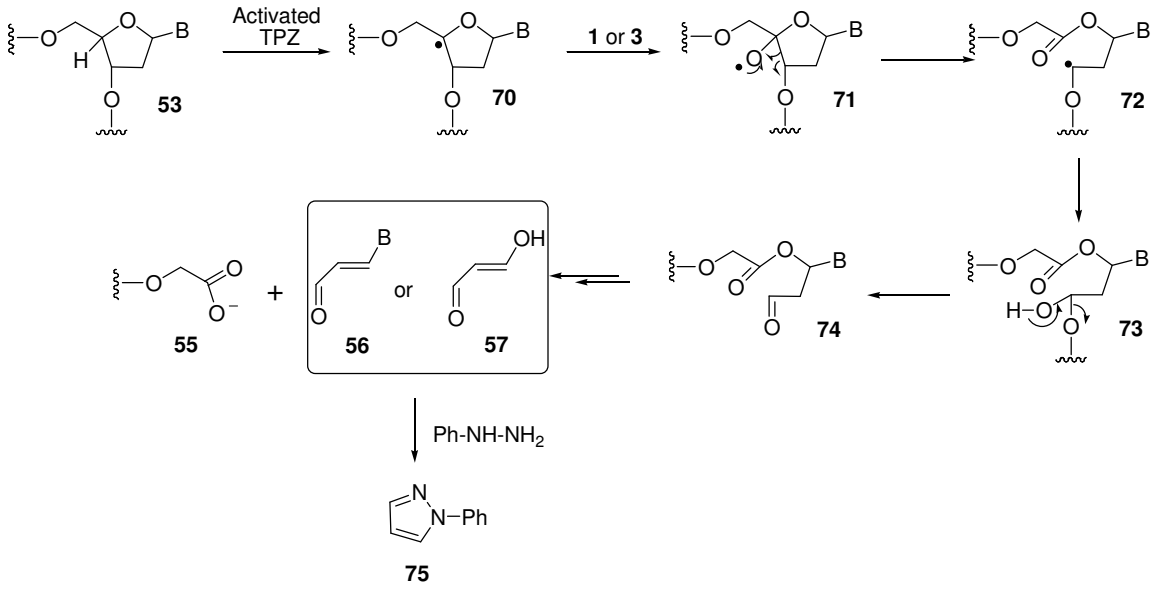

Scheme 4.3: Proposed mechanism for the formation of phosphoglycolate and malondialdehyde equivalents in TPZ mediated DNA damage

C4'-radical (**70**) produced in TPZ mediated DNA damage from hydrogen atom abstraction reacts with TPZ or 1-*N*-oxide metabolite (**3**) under anaerobic conditions and produces phosphoglycolate (**55**) and malondialdehyde equivalents (**56** or **57**) (Scheme 4.3). As part of our studies to examine the possible formation of malondialdehyde equivalents (**56** or **57**) in TPZ mediated DNA damage, we set out to derivatize these compounds with phenylhydrazine to yield phenylpyrazole (**75**) (Scheme 4.3). The DNA damage by activated TPZ was carried out under anaerobic conditions and TPZ-damaged

duplex DNA was incubated with phenylhydrazine (20 mM) for 15h. Then the phenyhydrazine derivatized products

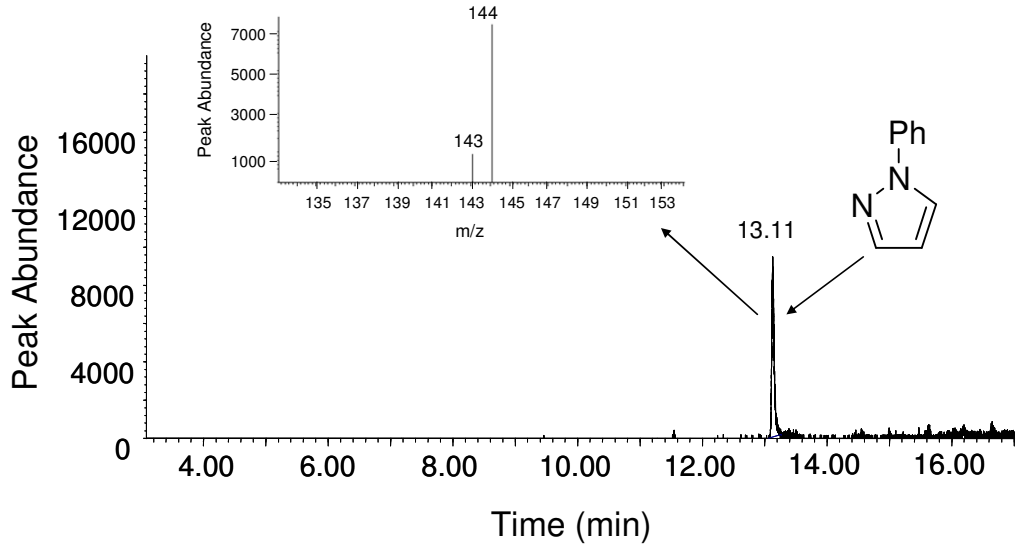

Figure 4.1: GC/MS trace of phenyl pyrazole formed in TPZ mediated deoxyribose damage in duplex DNA

were extracted into hexane and the resultant sample was analyzed by GC-MS-SIM analysis. The GC-MS-SIM data shows that the peak with *m*/*z* of 144 eluting at 13 min, which correspond to the compound **75** (Figure 4.1). The significant amount of **75** was not observed in control reactions of untreated DNA, DNA treated with TPZ alone (no enzyme), or DNA treated with the NADPH:cytochrome P450 reductase enzyme system (no TPZ). As expected, a positive control reaction involving treatment of DNA with the Fe(II)/ETDA/H_2O_2/ascorbate system, followed by derivatization as described above, generates **75**. The formation of **75** in TPZ mediated DNA damage assays show that formation of malondialdehyde equivalents (**56** or **57**).

In our studies, we further attempted to identity the exact malondialdehyde equivalents (**56** or **57**) formed in TPZ mediated DNA damage. For example, studies reported by Grollman and coworkers showed that base propenals and malondialdehyde

can be separated and visualized on TLC after staining with 0.6 % 2-thiobarbituric acid (TBA).[7] Accordingly, in our studies, we utilized TBA assay to identify the exact malondialdehyde equivalent formed in TPZ mediated DNA damage. As part of these studies, Calf-thymus DNA was treated with activated TPZ and C4'-hydrogen abstraction derived products were attempted to identify using TLC analysis. However, under our experimental conditions, we were unable to detect either base propenals (**56**) or malondialdehyde (**57)** using TLC method. It may be due to low yields of these products to detect with TLC method in our reaction conditions.

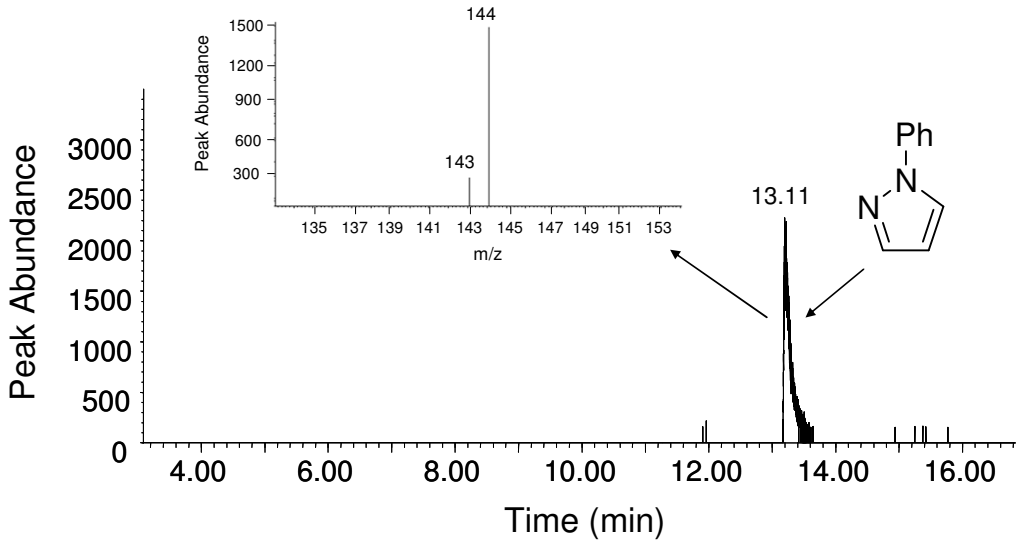

Figure 4.5: GC/MS trace of phenyl pyrazole formed in Fe(II)/EDTA/H_2O_2/ascorbate mediated deoxyribose damage in duplex DNA

In addition to our data on detection of malondialdehyde equivalents (**56** or **57**) upon derivatization with phenyl hydrazine, it is important to note that studies by Scott Daniels in our group revealed that the DNA damage by enzymatically activated TPZ also yields 3'-phospoglycolate (**55**) as an end product. This data is consistent with the observation

that activation of TPZ under anaerobic conditions leads to the abstraction of C4'-hydrogen from duplex DNA.

4.4 Detection of C5'-hydrogen abstraction derived products

In our studies, we also examined the possibility of abstraction of C5'-hydrogen atom in TPZ mediated DNA strand cleavage. Data show that C5'-hydrogen atom abstraction under aerobic conditions yields the formation of 1,4-*di*-oxo-butene (**62**) (Scheme 4.1), which can be readily derivatized by hydrazine to give pyridazine (**83**).[8] Accordingly, we hypothesized that oxygen transfer from TPZ and its 1-*N*-oxide metabolite to C5' radical would lead to the formation of **62**. If so, the compound **62** can be derivatized with hydrazine to give **83**, which can be detected by GC/MS/SIM analysis (Scheme 4.4). Accordingly, we carried out Calf-thymus DNA damage assay with enzymatically activated TPZ under anaerobic conditions. Then we set out to derivatize the possible 1,4-*di*-oxo-butene equivalents produced in TPZ mediated DNA damage with hydrazine. We examined the identity of derivatized product pyridazine (**83**) using GC/MS/SIM analysis at m/z 80. Our GC/MS/SIM analysis data shows that the formation of 1,4-*di*-oxo-butene lesions were not detected in our reaction conditions.

On the other hand, HPLC analysis of Goutam in our group showed that TPZ mediated DNA strand cleavage yields furfural as an end product, which is the characteristic end product that normally formed via C5'-hydrogen atom abstraction under anaerobic conditions (Scheme 4.4).

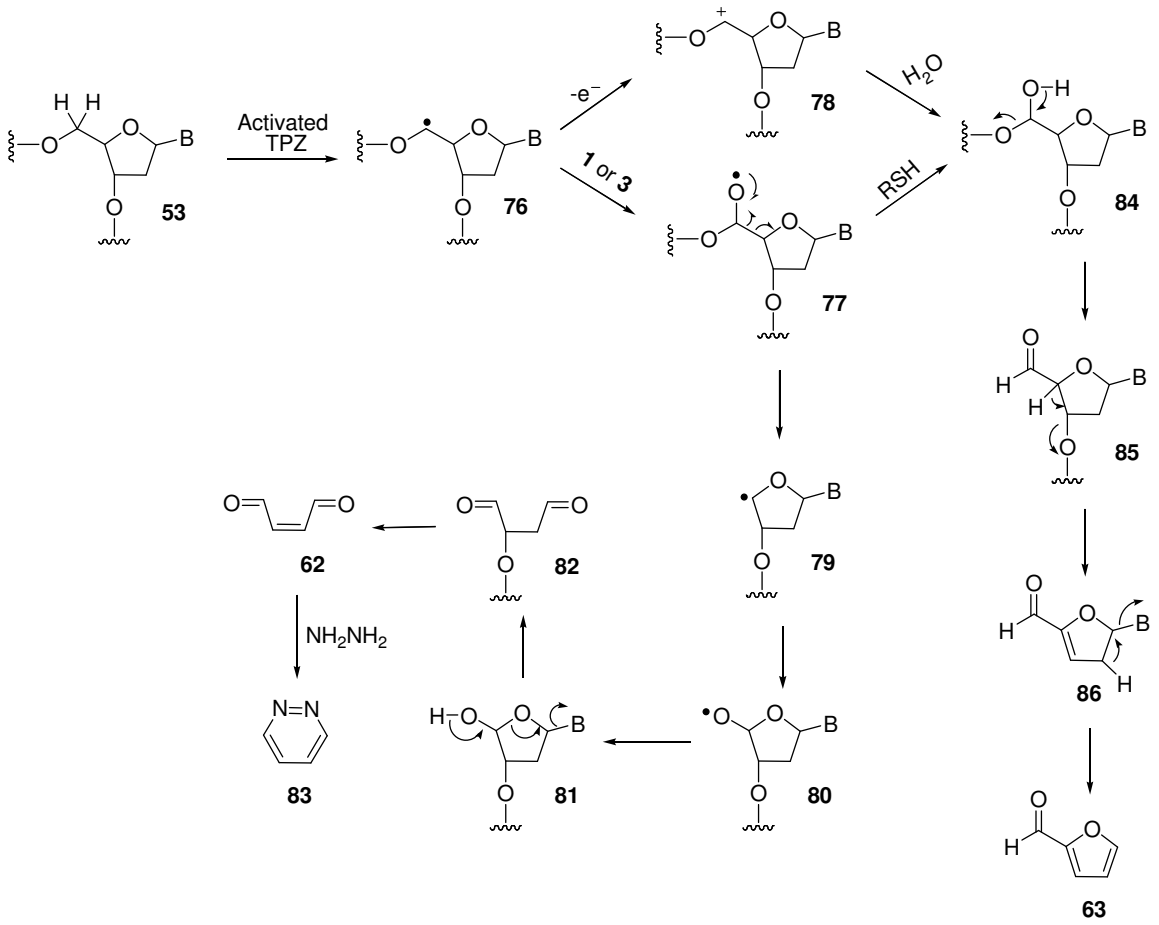

Scheme 4.4: Proposed mechanism for the formation of 1,4-*di*-oxo-butene and furfural in TPZ mediated DNA damage

4.5 Conclusions

Our data shows that activated TPZ mediated DNA strand cleavage proceeds *via* abstraction of not only least hindered C4'- and C5'-hydrogen atoms abstraction but also from most hindered C1'-hydrogen atom abstraction. This information suggests that activated TPZ generate small and diffusible species like hydroxyl radical. Further, our data shows that activated TPZ under anaerobic conditions produces phosphoglycolate (**55**) and malondialdehyde equivalents (**56** or **57**) as C4'-hydrogen abstraction derived end products, which normally formed in hydroxyl radical-mediated DNA-cleavage under aerobic conditions. However, under our reaction conditions, the formation of 1,4-*di*-oxo-

butene (**62**), which is the typical C5'-hydrogen abstraction derived product under aerobic conditions was not observed. Rather, we observed the formation of furfural (**63**) as a C5'-hydrogen atom abstraction derived end product. Hence, overall data shows that the oxygenation of DNA radicals by TPZ is a complex process that proceeds *via* multiple mechanistic pathways.

4.6 Experimental

4.6.1 DNA damage reactions. Typical assays were conducted under hypoxic conditions and contained DNA (125 μg/mL of highly polymerized calf thymus DNA), TPZ (500 μM), desferal (1 mM), NADPH (500 μM), cytochrome P450 reductase (50 mU), catalase (100 μg/mL), SOD (10 μg/mL) and sodium phosphate buffer (50 mM, pH 7.0). The solutions of TPZ, desferal, and buffer were degassed by using three cycles of freezepump-thaw in Pyrex tubes. The tubes were torched sealed under high vacuum, scored and transferred to an argon-filled glove bag. The tubes were then opened and DNA, NADPH and enzymes were added. Desferal, SOD, and catalase were added to abrogate reactive oxgyen species ($O_2^{\bullet-}$, H_2O_2, and HO•) that could potentially be generated by the reaction of **2a** with traces of molecular oxygen in the assay mixtures. The reactions were incubated inside the glove bag protected from light for 240 min for the detection of malondialdehyde equivalents (**56** or **57**) and 1,4-*di*-oxo-butene (**62**). Positive controls involving of Fe-EDTA/H_2O_2/ascorbate damaged DNA were prepared by incubation of calf thymus DNA (125 μg/mL) $FeCl_3$ (10 μM), EDTA (20 μM), ascorbate (1 mM), and H_2O_2 (0.03%) in sodium phosphate buffer (pH 7.0, 50 mM) at room temperature under aerobic conditions for 45 min. The DNA was then isolated by ethanol precipitation, washed with 70% cold ethanol and air dried before further analysis.

4.6.2 Derivatization of C4' hydrogen abstraction derived products with phenyl hydrazine and GC/MS analysis. DNA-damage reactions were carried out in silylated vials as described above. Following DNA damage, 50 μL of acetonitrile and 10 μL of 10% phenylhydrazine (in 10% aqueous acetonitrile) were added to 400 μL of reaction mixture, followed by the addition of 40 μL of water. The final concentration of

phenylhydrazine was 20 mM. The reaction mixture was incubated for 15 h at 24 °C and then extracted with hexane (2 x 300 μL). Two such samples were pooled and the hexane layers dried under a gentle stream of nitrogen gas. The residue was then dissolved in 50 μL of hexane and a 4 μL aliquot analyzed by GC-MS using the following instrument settings: positive ion electron ionization (EI 70 eV); 250 °C inlet in the splitless mode; capillary column DB 624 (28.4m, 0.25mm, 1.4 μM); helium carrier flow 1 mL/min; oven temperature 70 °C, linear gradient to 220 °C at 10 °C/min, hold at 220 °C for 2 min; data was acquired in the SIM mode with a mass range of m/z 143–145 after a 3 min solvent delay.

4.6.3 Derivatization of C5' hydrogen abstraction derived products with hydrazine and GC/MS analysis. TPZ mediated DNA damage was carried out similar to the above experiments. TPZ (500 μM) damaged DNA (125 μg/mL) was dissolved in 400 μL of sodium phosphate buffer (pH 7, 50 mM) and transferred into silylated glass vial. To this solution 4 μL of hydrazine was added. The sample was then heated for 20 min at 90 °C, cooled for 5 min at 4 °C or 30 min at 20 °C and then extracted with ethyl acetate (3 x 200 μL).. The organic layer was concentrated to a final volume of 50 μL. Portion of the resulting solution (3 μL) was analyzed by GC/MS using the following instrument settings: positive ion electron ionization (EI 70 eV); 250 °C inlet in the splitless mode; capillary column DB 624 (28.4 m, 0.25 mm, 1.4 μL); helium carrier flow 1 mL/min; oven temperature hold at 70 °C for 4 min; linear gradient to 240 °C at 25 °C /min and hold at 240 °C for 10 min; data was acquired in the SIM mode at m/z 79-81 after 3 min solvent delay.

4.7. References

[1] Daniels, J. S.; Gates, K. S. *J. Am. Chem. Soc.* **1996**, *118*, 3380-3385.

[2] Siim, B. G.; van Zijl, P. L.; Brown, J. M. *Br. J. Cancer* **1996**, *73*, 952-960.

[3] Pogozelski, W. K.; Tullius, T. D. *Chem. Re*V. **1998**, *98*, 1089-1107.

[4] Dizdaroglu, M.; Von, Sonntag, C.; Schulte-Frohlinde, D. *J. Am. Chem. Soc.* **1975**, *97*, 2277-2278.

[5] Rashid, R.; Langfinger, D.; Wagner, R.; Schuchmann, H.-P.; Von, Sonntag, C. *Int. J. Radiat. Biol.* **1999**, *75*, 101-109.

[6] Zhou, X.; Taghizadeh, K.; Dedon, P. C. *J. Biol. Chem.* **2005**, *280*, 25377-25382.

[7] Giloni, L.; Takashita, M.; Johnson, F.; Iden, C.; Grollman, A. P. *J. Biol. Chem.* **1981**, *256*, 8608-8615.

[8] Chen, B.; Bohnert, T.; Zhou, X.; Dedon, P. C. *Chem. Res. Toxicol.* **2004**, 17, 1406-1413.

[9] Balasubramanian, B.; Pogozelski, W. K.; Tullius, T. D. *Proc. Natl. Acad. Sci. U.S.A.* **1998**, *95*, 9738-9743.

[10] Sy, D.; Savoye, C.; Begusova, M.; Michalik, V.; Charlier, M.; Spotheim-Maurizot, M. *Int. J. Radiat. Biol.* **1997**, *72*, 147-155.

[11] Hong, I. S.; Carter, K. N.; Sato, K.; Greenberg, M. M. *J. Am. Chem. Soc.* **2007**, *129*, 4089-4098.

[12] Tallman, K. A.; Greenberg, M. M. *J. Am. Chem. Soc.* **2001**, *123*, 5181-5187.

[13] Daniels, J. S.; Gates, K. S.; Tronche, C.; Greenberg, M. M. *Chem. Res. Toxicol.* **1998**, *11*, 1254-1257.

[14] Hwang, J.-T.; Greenberg, M. M.; Fuchs, T.; Gates, K. S. *Biochemistry* **1999**, *38*, 14248-14255.

[15] Jones, G. D. D.; Weinfeld, M. *Cancer Res.* **1996**, *56*, 1584-1590.

[16] Junnotula, V.; Sarkar, U.; Sinha, S.; Gates, K. S. *Manuscript in preparation.*

Chapter 5: Activation of the Anti-tumor Agent Tirapazamine by Thiols and Dithiols

5.1 Introduction

Studies reported in Chapters 1-4 revealed that benzotriazine di-*N*-oxides and quinoxaline di-*N*-oxides cause the oxidative DNA strand cleavage upon one-electron reductive activation. DNA strand cleavage by these di-*N*-oxide compounds provided the plausible mechanism for their anti-cancer activity. Further, these studies also provided the evidence that heterocyclic di-*N*-oxide compounds deliver the well known radiotherapeutic DNA damaging agent, hydroxyl radical in oxygen poor environment found in solid tumors.

5.2 Goal: To examine the interaction of thiols with TPZ

In our current studies, we set out to examine the interaction of thiols and dithiols with the anti-tumor agents, heterocyclic di-*N*-oxides. We used clinically promising drug TPZ to examine the interaction of thiols. Such studies are very important and have biological significance. For example, in the cellular conditions, the high concentrations

of thiols are present in the form of glutathione (1-10 mM). Such high concentrations of thiols in cellular conditions can reduce TPZ *via* multiple pathways. For example, studies by Relyea and coworkers reported that thiols deoxygenate pyridine *N*-oxide (**87**).[1] They proposed that deoxygenation involves the protonation of **87** followed by displacement of the pyridine (Scheme 1).[1] This information suggests that de-oxygenation of **87** involves the two electron reduction process (Scheme 5.1).[1]

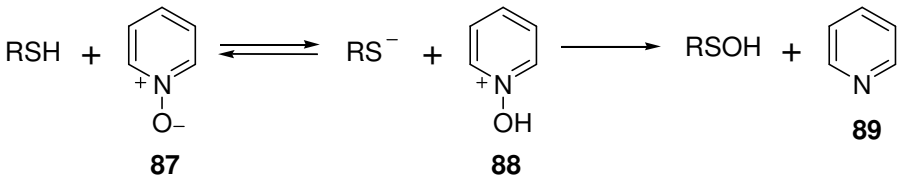

Scheme 5.1: Proposed mechanism for deoxygenation of pyridine *N*-oxide by thiols

On the other hand, studies by Hecht and coworkers showed that dithiothreitol (DTT, **91**) activates phenazine di-*N*-oxide (**90**) by one-electron reduction.[2] Further, authors demonstrated that activation of the compound **90** by DTT leads to the DNA strand cleavage under both aerobic and anaerobic conditions.[2] This data suggests that thiols activate phenezine di-*N*-oxides by one-electron reduction and yields oxygen sensitive radical intermediate, which in the presence of oxygen produces superoxide radical (Scheme 5.2).[2] On the other hand, in the absence of oxygen that oxygen sensitive radical intermediate undergoes homolytic fragmentation to release DNA damaging hydroxyl radical (Scheme 5.2). [2]

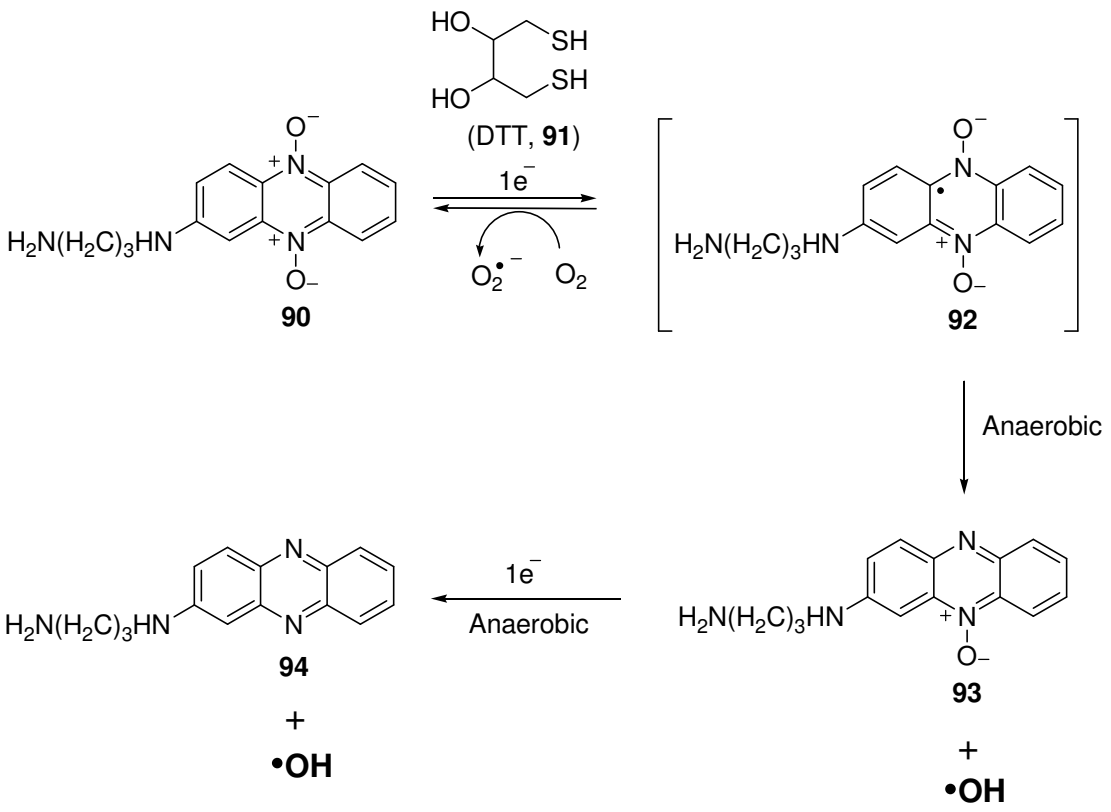

Scheme 5.2: Proposed mechanism for the one-electron reductive-activation of phenazine di-*N*-oxide (**90**) by DTT (**91**)

Based on the above literature data, we hypothesized that thiols and dithiols reduce TPZ by both one-electron and two-electron reduction processes (Schemes 5.3 and 5.4). We designed experiments to distinguish between the one-electron and two-electron reduction processes. For example, if thiols reduce TPZ (**1**) by one-electron reduction, that process leads to the generation of oxygen sensitive radical intermediate (**2a**), which will be back oxidized by the molecular oxygen to give **1** (Scheme 5.3). On the other hand, two-electron reduction of TPZ by thiols does not lead to the formation of oxygen sensitive radical intermediate (Scheme 5.4). Thus, oxygen independent metabolism of TPZ will be observed.

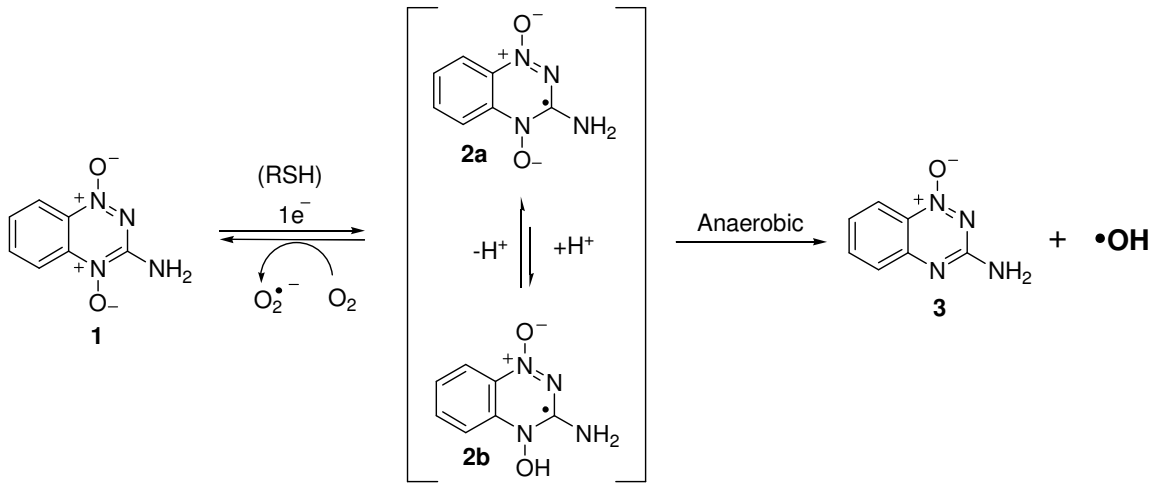

Scheme 5.3: Possible mechanism for the one-electron reductive-activation of TPZ by thiols and dithiols

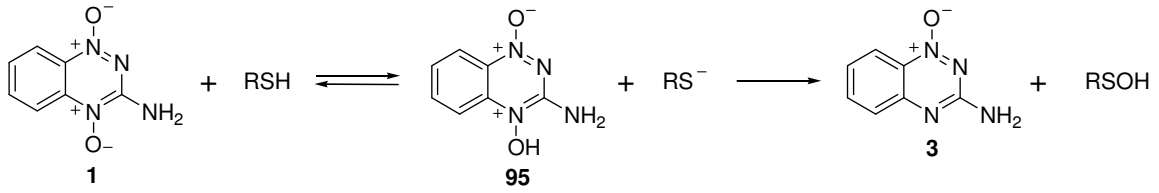

Scheme 5.4: Possible mechanism for two-electron reduction of TPZ by thiols and dithiols

To examine our hypothesis for one-electron and two-electron reduction of TPZ by thiols and dithiols, we used UV-Vis spectroscopy as a tool. UV-Vis spectroscopy provides a useful tool to monitor the rate of metabolism of TPZ since this drug has unique absorbance at 474 nm compared to its possible metabolites. Further, to distinguish in between one-electron and two-electron reduction processes, we monitored the loss of TPZ under both aerobic and anaerobic conditions. If one-electron reductive activation of TPZ occurs in the presence of thiols, oxygen sensitive radical intermediate will be observed. Hence, the metabolism of TPZ will not be observed in the presence of oxygen. On the other hand, if thiols reduce TPZ by two-electron then oxygen

independent metabolism of TPZ occurs. Accordingly, we set out to examine the role of biological thiol, GSH in activating TPZ.

5.3 Cellular thiol, glutathione activates TPZ

As part of our goal to examine the role of glutathione in activating TPZ, we incubated reactions containing TPZ (100 µM), GSH (20 mM) and the sodium phosphate buffer (pH 7, 200 mM) under both aerobic and anaerobic conditions. Rate of metabolism or loss of TPZ was monitored by using UV-Vis spectroscopy at 474 nm. In anaerobic assays, individual components of these reactions except GSH were deoxygenated by using three cycles of freez-pump-thaw. Degassed solutions were used to prepare anaerobic reaction in an argon filled glove bag. GSH was diluted with deoxygenated solutions in an argon filled glove bag. Once the reaction solution prepared immediately

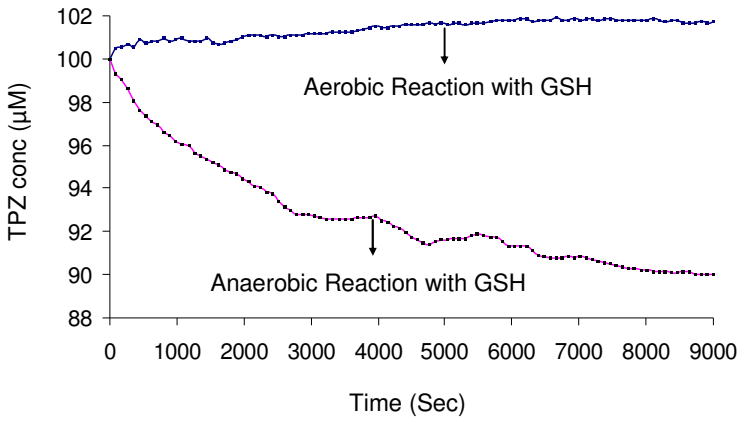

Figure 5.1: Metabolism of TPZ (100 µM) in the presence of GSH (20 mM) and sodium phosphate buffer of (pH 7, 200 mM) under both aerobic and anaerobic conditions. In case of anaerobic reaction, all the components were deoxygenated by three cycles of freez-pump-thaw. Metabolism of TPZ was monitored by using UV-Vis spectroscopy at 474 nm.

reaction solution was transferred into an argon purged cuvette and the resultant cuvette was capped with the septa to avoid oxygenation of the reaction solution. Then the

resultant reaction was monitored by using UV-Vis spectroscopy at 474 nm. Aerobic reaction was performed in an identical manner to anaerobic reactions except with out degassing the reaction components.

Our data shows that GSH metabolizes TPZ under anaerobic conditions but not under aerobic conditions (Figure 5.1). This data shows that GSH activates TPZ and generate oxygen sensitive radical intermediate. This information supports the hypothesis that thiols activate TPZ by the one-electron reduction (Scheme 5.4). This data also argues against the hypothesis that thiols reduce TPZ by the two-electron reduction (Scheme 5.3).

Data reported here on the activation of TPZ by GSH is very important and carries biological significance. The experimental conditions that we used here are relevant to physiological conditions. Particularly, the generation of oxygen sensitive radical intermediate upon reductive-activation of TPZ in the presence of GSH suggests that this process can cause significant amount of oxidative stress *via* producing superoxide radical and hydroxyl radical under aerobic and hypoxic conditions respectively. We further examined whether organic thiol 2-mercaptoethanol activates TPZ similar to GSH or not. Such studies will be helpful to bring the generality in activation of TPZ by thiols.

5.4 2-Mercapto ethanol activates TPZ

As part of our goal to examine the activation of TPZ by 2-mercapto ethanol, we monitored the metabolism of TPZ in the presence of 2-mercaptoethanol under both aerobic and anaerobic conditions by using UV-Vis spectroscopy in an identical manner to our earlier experiments. Our UV-Vis data shows that TPZ was metabolized in the presence 2-mercapto ethanol under anaerobic conditions but not in aerobic conditions

(Figure 5.2). This data is consistent with our earlier observation that GSH causes one-electron reductive-activation of TPZ and generate oxygen sensitive radical intermediate.

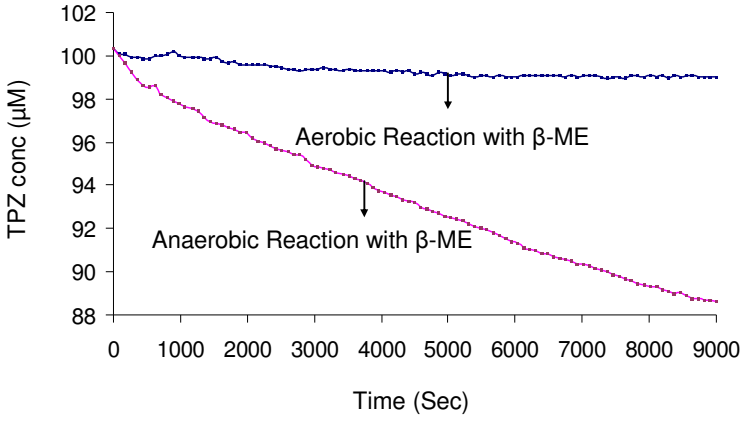

Figure 5.2: Metabolism of TPZ (100 μM) in the presence of 2-mercaptoethanol (β-ME) (20 mM) and sodium phosphate buffer (pH 7, 200 mM) under both aerobic and anaerobic conditions. In case of anaerobic reaction, all the components were deoxygenated by three cycles of freez-pump-thaw. Metabolism of TPZ was monitored by using UV-Vis spectroscopy at 474 nm.

Our data reported here show that biological thiol, GSH and organic thiol, 2-mercapto ethanol activate TPZ by one-electron reduction and generate oxygen sensitive radical intermediate. This data suggests that activation of TPZ by thiols seems to common chemistry that can occur *in vivo* and generate superoxide radical and hydroxyl radical under aerobic and hypoxic conditions respectively. The production of superoxide radical and hydroxyl radical lead to several consequences including oxidative damage to biological macromolecules DNA, proteins and lipids.[3, 4,5,6,7]

In addition, it is important to note that studies on TPZ show that number of cellular enzymes including cytochrome P450 reductase, cytochrome P450, xanthine oxidase, DT diaphorase and nitric oxide synthase II metabolize TPZ.[8,9,10,11,12] Although all these enzymes metabolize TPZ, only those that carry out one-electron reductive activation leads to DNA damage.[13,14] *In vitro* metabolic studies show that one-electron reducing

systems like NADPH:cytochrome P450 reductase and xanthine:xanthine oxidase activate TPZ in a hypoxic environment and cause cytotoxicity.[13,14] However, the cellular enzyme(s) responsible for initiating DNA damage by TPZ *in vivo* is still a matter of debate. For example, studies on breast cancer cell lines suggest that NADPH:cytochrome P450 reductase reducing system present in cytosol activates TPZ.[12,15] However, the metabolic studies on A549 lung cancer cells reveal that, DNA damaging radicals produced in cytosol are not stable enough in reaching the nucleus.[12,15] These studies show that although 20% of TPZ is metabolized inside the nucleus, the extent of DNA damage in isolated nuclei and in a cell is similar.[12] This data suggest that 80% of TPZ metabolism that occurs in cytosol is irrevelant to DNA damage.[15]

As part of our goal to identify the nuclear reductases that responsible for metabolism of TPZ, we hypothesized that nuclear dithiol proteins may activate TPZ *in vivo*. There are several reasons to examine the possibility of activation of TPZ by dithiol proteins. The first, data that we reported here show that thiols activate TPZ by one-electron reduction. The second, dithiol proteins thioreoxin and APE are known to be expressed in high levels in various cancers.[16,17] The third, although thioredoxin expressed in cytosol, it translocates into the nucleus as part of its role in redox regulation of transcription factors.[18,19,20] The fourth, data shows that some cancer cells have higher levels of APE in their nuclei.[21,22] This information together motivated us to examine the possible role of nuclear dithiol proteins in activating TPZ. As part of our efforts to understand the possible role of nuclear dithiol proteins, we used dithiothreitol (DTT) as a chemical model for dithiol proteins in activating TPZ. We used UV-Vis spectroscopy and HPLC

analysis to study the activation of TPZ by DTT under both aerobic and anaerobic conditions.

5.5 DTT activates TPZ

As part of our goal to examine the activation of TPZ by DTT, reactions containing TPZ (100 µM), DTT (20 mM) and the sodium phosphate buffer (pH 7, 200 mM) were incubated under both aerobic and anaerobic conditions similar to our earlier experiments. In anaerobic reaction, oxygen free conditions were achieved exactly in an identical manner to our earlier experiments. The metabolism of TPZ under both aerobic and anaerobic reactions was monitored by using UV-Vis spectroscopy at 474 nm. Our UV-Vis data shows that DTT metabolizes TPZ under anaerobic conditions but not under aerobic conditions (Figure 5.3). This data is consistent with our observation that thiols and dithiols activate TPZ by the one-electron reduction (Scheme 5.4).

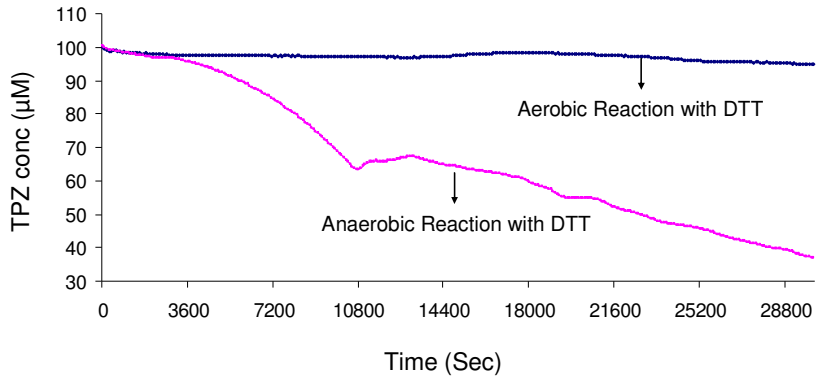

Figure 5.3: Metabolism of TPZ (100 µM) in the presence of DTT (20 mM) and sodium phosphate buffer (pH 7, 200 mM) under both aerobic and anaerobic conditions. In case of anaerobic reaction, all the components were deoxygenated by three cycles of freez-pump-thaw. Metabolism of TPZ was monitored by using UV-Vis spectroscopy at 474 nm.

We further analyzed metabolites generated from *in vitro* metabolism of TPZ in the presence of DTT under anaerobic and aerobic conditions using HPLC. Our HPLC

analysis of anaerobic reaction shows that TPZ produces 1-*N*-oxide as a major metabolite, which elutes at ~31 min (Figure 5.4). The identity of the 1-*N*-oxide metabolite was confirmed by the co-injection of authentic compound with the reaction. Metabolism of

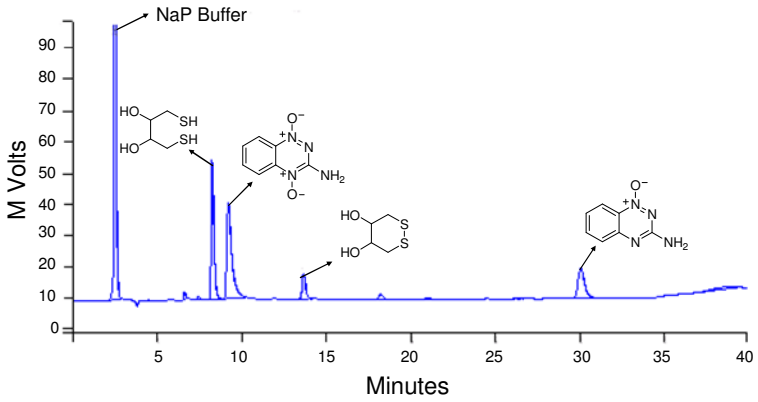

Figure 5.4: HPLC trace of metabolites generated in metabolism of TPZ in the presence of DTT (20 mM), and sodium phosphate buffer (pH 7, 200 mM) under anaerobic conditions. Reaction containing TPZ (100 µM), DTT (20 mM) and sodium phosphate buffer (pH 7, 200 mM) was incubated under argon filled glove bag while protecting from light at 25 ^{o}C for 7h. All the components of anaerobic reaction were deoxygenated by three cycles of freez-pump-thaw.

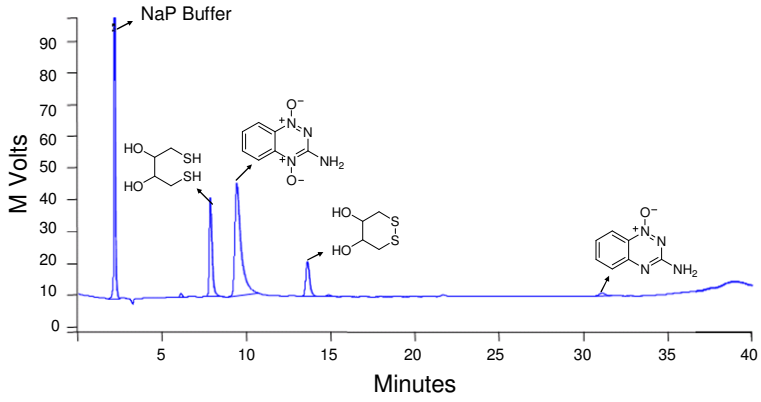

Figure 5.5: HPLC trace of metabolites generated in metabolism of TPZ in the presence of DTT (20 mM), and sodium phosphate buffer (pH 7, 200 mM) under aerobic conditions. Reaction containing TPZ (100 µM), DTT (20 mM) and sodium phosphate buffer (pH 7, 200 mM) was incubated under aerobic conditions while protecting from light at 25 ^{o}C for 7h.

TPZ in the presence of DTT under aerobic conditions yields only small amount of 1-*N*-oxide metabolite (Figure 5.5). These HPLC studies show that the yield of 1-*N*-oxide

metabolite depends on oxygen concentration in reactions. Thus, HPLC data confirms the observations from the UV-Vis data, which suggests that DTT activates TPZ by one-electron reduction.

The data reported here show that thiols and dithiols activate TPZ by one-electron reduction and generate oxygen sensitive radical intermediate. However, the mechanism for activation of TPZ by thiols and dithiols is not completely known. In our current studies, we carried out systematic studies to understand the mechanism for activation of TPZ by thiols and dithiols.

5.6 Mechanistic studies on activation of TPZ by thiols and dithiols

Thiols are known to activate quinone compounds *via* one-electron reduction and generate superoxide radical.[23,24,25] Thiol mediated activation of quinones requires metals and thiolate form of thiols.[23,24,25] Accordingly, we hypothesized that metals and thiolate form of thiols and dithiols play a key role in activation of TPZ. As part of our goal to examine the role metals and thiolate form, we monitored the metabolism of TPZ in the presence and absence of metal chelating agents and at different pH conditions.

5.6.1 pH effect on metabolism of TPZ by DTT

As part our studies to examine the effect of pH on the metabolism of TPZ, reactions containing TPZ (100 μM), DTT (20 mM) and sodium phosphate buffers of pH 6-8 (200 mM) were incubated under anaerobic conditions. The metabolism of TPZ was monitored by using UV-Vis spectroscopy at 474 nm. Data show that pH has an effect on metabolism of TPZ by thiols. For example, in 8 h of incubation time, the amount of TPZ consumed at pH 6, pH 7 and pH 8 is 38%, 61% and 77% respectively (Figure 5.6). This

data show that with the increase in pH the rate of metabolism of TPZ increases. This data suggest that thiolate form of DTT plays a key role in activation of TPZ.

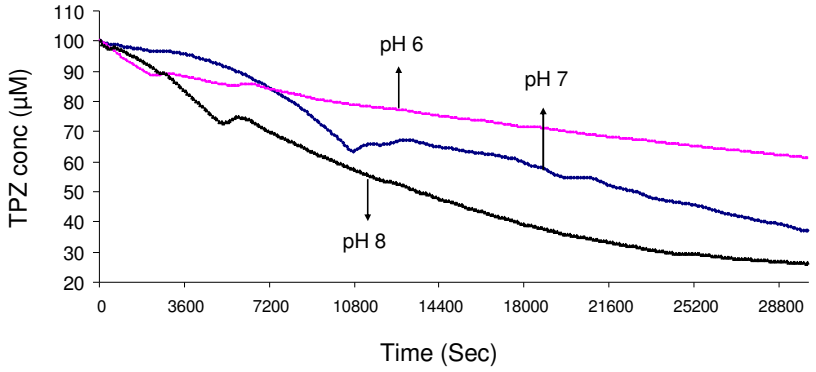

Figure 5.6: Effect of pH on the metabolism of TPZ in the presence of DTT. Reactions containing TPZ (100 µM), DTT (20 mM) and sodium phosphate buffer of pH 6-8 (200 mM) were incubated under anaerobic conditions and metabolism of TPZ was monitored by using UV-Vis spectroscopy at 474 nm.

5.7 Role of metals in the metabolism of TPZ by DTT

As part of our goal to understand the role of metals in the metabolism of TPZ, reactions w/wo metal chelating agents were incubated under anaerobic conditions and the metabolism of TPZ was measured by using UV-Vis spectroscopy. The data show that addition of metal chelating agents, DETAPAC and desferal decrease the rate of metabolism of TPZ. The amount of TPZ consumed in a standard reaction in 8 h was 61%, where as the amount of TPZ consumed in the presence of DETAPAC (3 mM) and desferal (5 mM) was 24% and 2% respectively (Figure 5.7). Further, we confirmed the role of metals on metabolism of TPZ in the presence of thiols by adding Fe (III) salt. Our data shows that addition of Fe (III) salt (1 µM) increases the rate of metabolism of TPZ. When the Fe (III) was added the rate of metabolism increased and 68% of TPZ was consumed in 8 h of incubation (Figure 5.7). This data confirm that metals play a key role in activation of TPZ by thiols.

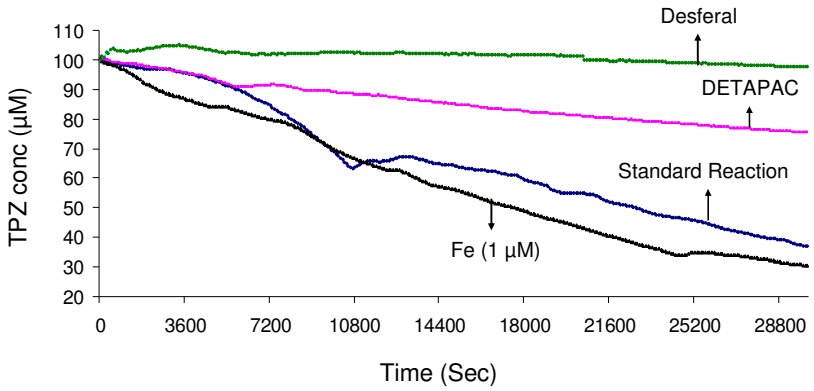

Figure 5.7: Role of metals in the metabolism of TPZ in the presence of DTT. Standard reaction containing TPZ (100 µM), DTT (20 mM) and sodium phosphate buffer (pH 7, 200 mM) were incubated under anaerobic conditions. Reactions containing DETAPAC (3 mM), desferal (5 mM) and Fe-III (1 µM) were carried out exactly the same as a standard reaction except adding DETAPAC, desferal and Fe-III prior to the addition of DTT.

Reaction Conditions	**The Amount of TPZ consumed in 8 h**
Standard Reaction (pH 7)	61%
pH 6	38%
pH 8	77%
DETAPAC (3 mM)	24%
Desferal (5 mM)	02%
Fe-III (1 µM)	68%

Table 5.1: Effect of additives on the rate of metabolism of TPZ in the presence of DTT.

5.8 Proposed mechanism for activation of TPZ by thiols and dithiols

Our data on metabolism of TPZ in the presence of GSH, 2-mercapto ethanol and DTT show that thiol and dithiols cause one-electron reductive activation of TPZ. The pH effect on metabolism of TPZ suggests that thiolate form of thiols and dithiols plays a key role in reductive activation of TPZ. The decrease in metabolism of TPZ in the presence metal chelating agents argues for the involvement of metals in activation of TPZ by thiols and dithiols. Based on these observations, we proposed the mechanism for activation of TPZ by thiols and dithiols (Scheme 5.5). In our mechanism, we proposed that in the first step, the thiolate form of thiols and dithiols reduces metals (presumably Fe III and Cu II)

present in our reaction conditions and generate thiol radicals and reduced metals (Fe II or Cu I). In the second step, reduced metals (Fe II or Cu I) transfer one-electron to TPZ to generate TPZ radical anion (**2a**). The radical anion **2a** is known to back oxidized to TPZ in the presence of oxygen. On the other hand, in the absence of oxygen it generates hydroxyl radical *via* protonated form (**2b**) of activated TPZ. The mechanism we favor here is similar to auto oxidation of thiols in the presence of metals and oxygen.[26] It is also possible that *N*-oxide of TPZ and thiolate form of thiols and dithiols can co-ordinate the metals, which can facilitate the electron transfer in the single step.

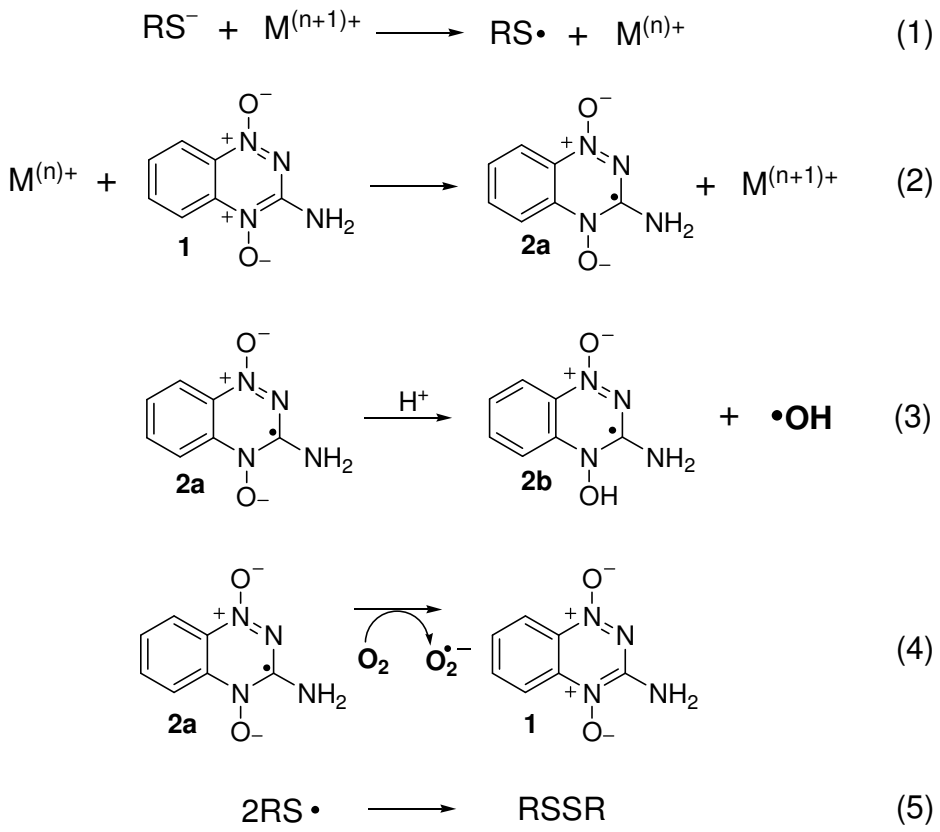

Scheme 5.5: Proposed mechanism for activation of TPZ by thiols and dithiols.

The overall data that we reported here shows that thiols and dithiols cause one-electron reductive activation of TPZ and generates oxygen sensitive radical intermediate.

This data suggests that thiols and dithiols present *in vivo* can reduce heterocyclic compounds by one-electron reduction and in the presence of oxygen produce superoxide radical, which leads to the DNA damage. In our studies, we examined whether activation of heterocyclic *N*-oxides by thiols and dithiols under aerobic conditions leads to the DNA damage or not. In DNA cleavage studies, we used heterocyclic compound 1,2,4-benzotriazine (**41**) as a substrate and GSH or DTT (**57**) as reducing agents.

5.9 GSH and DTT activate 1,2,4-benzotriazine (41) and cause DNA-cleavage under aerobic conditions

As part of our goal to examine the role of thiols and dithols in activating **41** and causing the DNA cleavage, we carried out DNA strand cleavage assays on **41** in the presence of cellular thiol GSH and DTT (**91**) under aerobic conditions. In a typical assay, solution containing DNA (33 μg/mL), GSH (200 μM) or DTT (100 μM), sodium phosphate buffer (pH 7, 50 mM) and **41** (0.1 μM-40 μM) was incubated under aerobic conditions while protecting from light at 25 ^{o}C for 15 h. Then the DNA-cleavage was analyzed and quantified similar to our earlier experiments that we reported in Chapters 1-4. Our data show that both GSH and DTT activate **41** and cause the DNA strand cleavage under aerobic conditions (Figures 5.8 and 5.9 and Tables 5.2 and 5.3). Concentration dependent DNA cleavage assays on **41** in the presence of GSH and DTT further confirm these observations (Figures 5.8 and 5.9 and Tables 5.2 and 5.3). Our data shows that the compound **41** causes better DNA cleavage in the presence of DTT compared to GSH (Figures 5.8 and 5.9 and Tables 5.2 and 5.3).

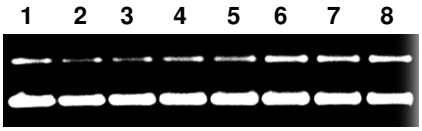

Figure 5.8: DNA cleavage by various concentrations of **41** in the presence of GSH. Reactions containing sodium phosphate buffer (pH 7.0, 50 mM), plasmid DNA (PGL2, 33 μg/mL), and GSH (200 μM) were incubated under aerobic conditions while protecting from light at 25 ^{o}C for 15 h. Lane 1, DNA alone; Lane 2, **41**alone (40 μM); Lane 3, GSH alone (200 μM); Lane 4, GSH (200 μM) + **41** (0.1 μM); Lane 5, GSH (200 μM) + **41** (1 μM); Lane 6, GSH (200 μM) + **41** (10 μM); Lane 7, GSH (200 μM) + **41** (20 μM); Lane 8, GSH (200 μM) + **41** (40 μM).

Reaction	**% Nicked DNA (Form II)**	**S-value**
Untreated DNA	18	0.20
DNA + **41** (40 μM)	18	0.20
DNA + GSH (200 μM)	18	0.20
DNA + GSH (200 μM) + **41** (0.1 μM)	18	0.20
DNA + GSH (200 μM) + **41** (1 μM)	19	0.20
DNA + GSH (200 μM) + **41** (10 μM)	23	0.26
DNA + GSH (200 μM) + **41** (20 μM)	24	0.28
DNA + GSH (200 μM)+ **41** (40 μM)	26	0.31

Table 5.2: DNA damage by various concentrations of **41** in the presence of GSH

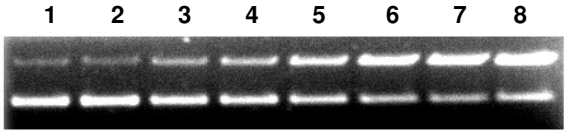

Figure 5.9: DNA cleavage by various concentrations of **41** in the presence of DTT. Reactions containing sodium phosphate buffer (pH 7.0, 50 mM), plasmid DNA (PGL2, 33 μg/mL), and DTT (100 μM) were incubated under aerobic conditions while protecting from light at 25 ^{o}C for 15 h. Lane 1, DNA alone; Lane 2, **41**alone (40 μM); Lane 3, DTT alone (100 μM); Lane 4, DTT (100 μM) + **41** (100 nM); Lane 5, DTT (100 μM) + **41** (1 μM); Lane 6, DTT (100 μM) + **41** (10 μM); Lane 7, DTT (100 μM) + **41** (20 μM); Lane 8, DTT (100 μM) + **41** (40 μM).

Reaction	**% Nicked DNA (Form II)**	**S-value**
Untreated DNA	14	0.15
DNA + **41** (40 μM)	13	0.14
DNA + DTT (100 μM)	28	0.33
DNA + DTT (100 μM) + **41** (0.1 μM)	37	0.46
DNA + DTT (100 μM) + **41** (1 μM)	48	0.65
DNA + DTT (100 μM) + **41** (10 μM)	64	1.02
DNA + DTT (100 μM) + **41** (20 μM)	70	1.20
DNA + DTT (100 μM)+ **41** (40 μM) (Standard Reaction)	74	1.35

Table 5.3: DNA damage by various concentrations of **41** in the presence of DTT

5.9.1 Mechanistic studies for the DNA strand cleavage by 41

In our mechanistic studies, we hypothesized that activated **41** in the presence of DTT produces superoxide radical similar to quinones and phenazine compounds.[2,23,24,25] Superoxide radical is known to produce hydrogen peroxide, which in the presence of metals generates the well known DNA damaging agent hydroxyl radical.[27,28,29,30] To examine our hypothesis, we carried out diagnostic experiments to examine the involvement of superoxide radical, hydrogen peroxide, metals and hydroxyl radical in DNA-cleavage by **41** in the presence of DTT under aerobic conditions. For example, addition of superoxide dismutase is known to enhance the superoxide radical mediated DNA cleavage in the presence of thiols, catalase is known to decrease the DNA cleavage by destroying the hydrogen peroxide, desferal also known to decrease the DNA cleavage by chelating the metals, and radical scavenger's methanol, ethanol and mannitol are known to inhibit the DNA cleavage by quenching the hydroxyl radicals.[28,29,30,] Accordingly, we carried out DNA strand cleavage assays with activated **41** in the presence of Cu,Zn-superoxide dismutase (Cu,Zn-SOD), catalase, desferal and radical scavengers. Our data shows that aerobic DNA cleavage by activated **41** was inhibited by Cu,Zn-SOD (43%), catalase (96%), desferal (89%), and radical scavengers (76%-89%) (Figure 5.10 and Table 5.4). The decrease in DNA-cleavage in the presence of catalase, desferal and radical scavengers is consistent with the involvement of hydrogen peroxide, metals and hydroxyl radical respectively. However, the decrease of DNA cleavage in the presence of Cu,Zn-SOD is not expected under our reaction conditions.

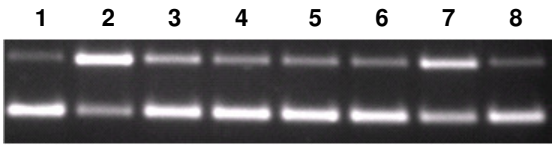

Figure 5.10: Effect of additives on DNA cleavage by the compound **41** in the presence of DTT. Reactions containing sodium phosphate buffer (50 mM, pH 7.0), plasmid DNA (PGL2, 33 μg/mL), and DTT (100 μM) were incubated under aerobic conditions while protecting from light at 25 °C for 15 h. Lane 1, DNA alone; Lane 2, DNA + DTT (100 μM) + **41** (40 μM) (standard reaction); Lanes 3-8, standard reaction with additives: Lane 3, methanol (100 mM); Lane 4, ethanol (100 mM); Lane 5, mannitol (100 mM); Lane 6, desferal (1 mM); Lane 7, Cu,Zn-SOD (100 μg/mL); Lane 8, catalase (100 μg/mL).

Reaction/Additive	% Nicked DNA (Form II)	S-value
Untreated DNA	14	0.15
41 (40 μM) (Standard Reaction)	69	1.17
Std Rxn + methanol (100 mM)	32	0.39
Std Rxn + ethanol (100 mM)	23	0.26
Std Rxn + mannitol (100 mM)	23	0.26
Std Rxn + desferal (1 mM)	23	0.26
Std Rxn +Cu,Zn-SOD (100 μg/mL)	52	0.73
Std Rxn + catalase (100 μg/mL)	17	0.19

Table 5.4: DNA damage by compound **41** in the presence of DTT and the effect of various additives.

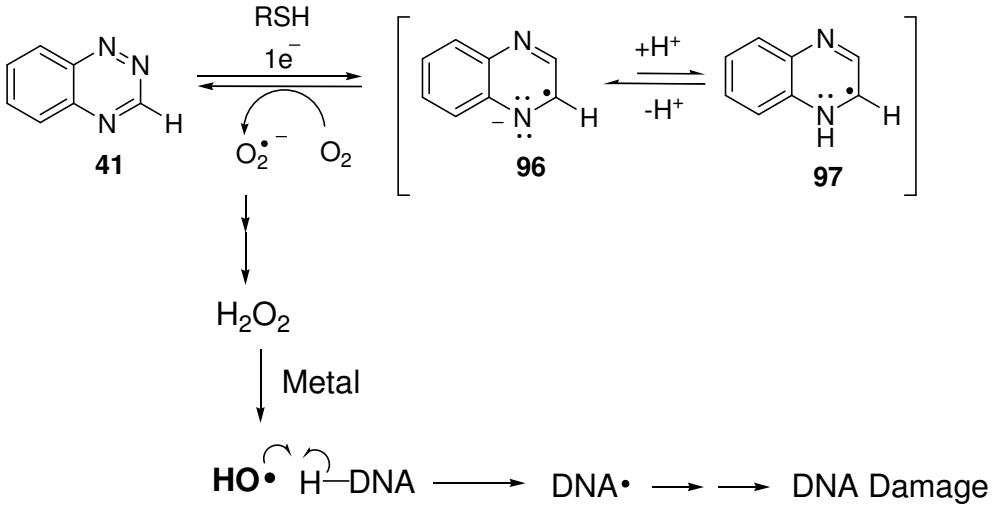

Scheme 5.6: Proposed mechanism for aerobic DNA cleavage by **41** in the presence of thiols and dithiols.

5.10 Cu,Zn-SOD inhibits the activation of TPZ by DTT in the absence of metal chelating agents

To understand the unusual effect of Cu,Zn-SOD on aerobic DNA cleavage by **41**, we hypothesized that superoxide dismutase may interfere with trace metals required for the metabolism of compound **41.** For example, studies by Winterbourn and coworkers showed that thiol oxidase activity of Cu, Zn-SOD was decreased by the trace metals present in reactions.[31] Those studies also showed that the effect of trace metals on Cu, Zn-SOD thiol oxidase activity was diminished in the presence of metal chelating agent desferal.[31] Based on this data, we designed an experiment to examine the effect of Cu,Zn-SOD on the rate of metabolism of TPZ in the presence of DTT under anaerobic conditions. We monitored the rate of metabolism of TPZ w/wo Cu,Zn-SOD using UV-Vis spectroscopy under anaerobic conditions as we described in our earlier experiments. Our data show that with the addition of Cu,Zn-SOD, the rate of metabolism of TPZ decreased and only 34% of TPZ was metabolized where as in the absence of Cu,Zn-SOD, 61% of TPZ was metabolized in 8 h (Figure 5.11). This data is consistent with our DNA cleavage assays, where Cu,Zn-SOD inhibits the aerobic DNA cleavage by **41** in the presence of DTT. Our current observation is consistent with the literature data where trace metals interfere with the thiol oxidase activity of Cu,Zn-SOD. Overall, the literature data and our observation of unusual effect of Cu,Zn-SOD on aerobic DNA cleavage by **41** and on the metabolism of TPZ under anaerobic conditions suggest that superoxide dismutase some how decreases the availability of free metals, which are necessary for the DNA cleavage by **41** and the metabolism of TPZ under our reaction conditions.

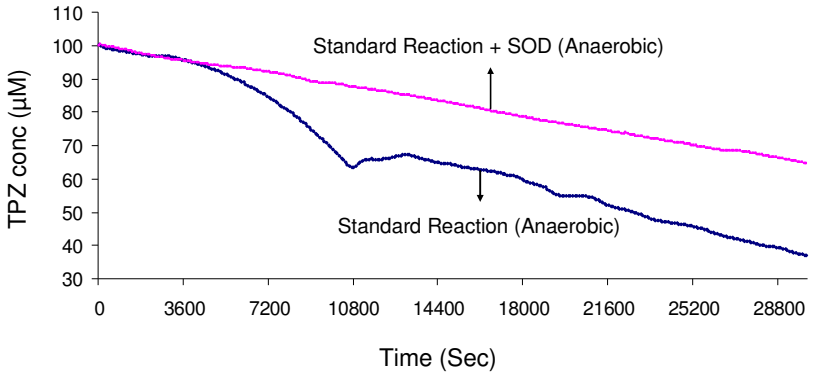

Figure 5.11: Effect Cu,Zn-SOD on the metabolism of TPZ in the presence of DTT and in the absence of metal chelating agent. Reactions containing TPZ (100 µM), DTT (20 mM) and sodium phosphate buffer (pH 7, 200 mM) w/wo Cu,Zn-SOD (1 mg/mL) were incubated under anaerobic conditions and metabolism of TPZ was monitored by using UV-Vis spectroscopy at 474 nm.

5.11 Cu,Zn-SOD catalyzes the activation of TPZ by DTT in the presence of metal chelating agents

The thiol oxidase activity of Cu,Zn-SOD was motivated us to examine the role of Cu,Zn-SOD in catalyzing the activation of TPZ by thiols in the absence of metals. As part of these studies, we examined the effect of superoxide dismutase on the rate of metabolism of TPZ in the presence of metal chelating agent desferal. Our data shows that TPZ (100 µM) was not metabolized in the presence of DTT (20 mM) and desferal (5 mM) under anaerobic conditions in 8 h. However, when the Cu,Zn-SOD (100 µg/mL) was added to the same reaction, 55% of TPZ was metabolized in 8 h (Figure 5.12). This data suggests that Cu,Zn-SOD catalyzes the metabolism of TPZ in the presence of thiols and dithiols. Further, we also examined whether the Cu,Zn-SOD catalyzed metabolism of TPZ is oxygen sensitive or not. As part of these studies, we carried out metabolic assay of TPZ in the presence of Cu,Zn-SOD, DTT and desferal under aerobic conditions. Our UV-Vis data shows that there is no significant amount of metabolism of TPZ occurs

under aerobic conditions (Figure 5.13). This data shows that Cu,Zn-SOD catalyzes the one-electron reductive activation of TPZ in the presence of thiols and dithiols.

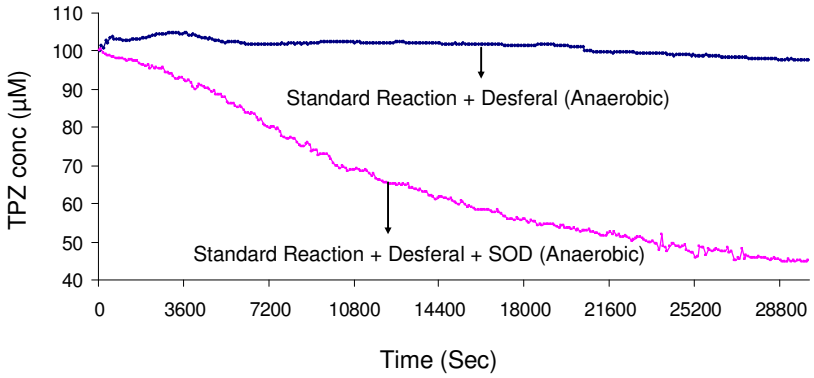

Figure 5.12: Effect Cu,Zn-SOD on the metabolism of TPZ in the presence of DTT and the metal chelating agent desferal. Reactions containing TPZ (100 µM), DTT (20 mM), desferal (5 mM) and sodium phosphate buffer (pH 7, 200 mM) and w/wo Cu,Zn-SOD (100 µg/mL) were incubated under anaerobic conditions and metabolism of TPZ was monitored by using UV-Vis spectroscopy at 474 nm.

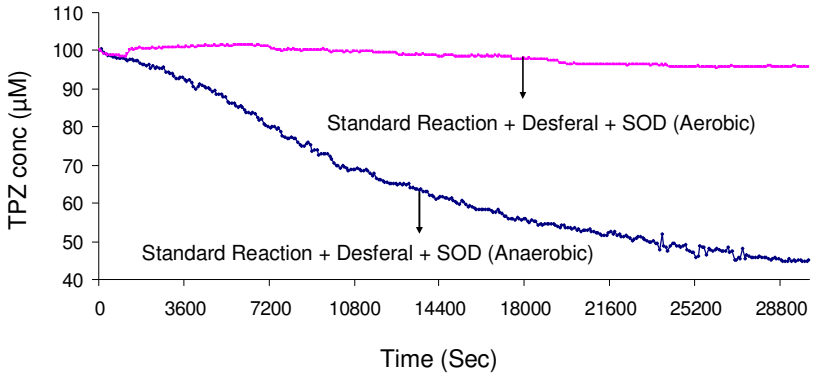

Figure 5.13: Metabolism of TPZ in the presence of DTT (20 mM), desferal (5 mM), Cu,Zn-SOD (100 µg/mL) and sodium phosphate buffer (pH 7, 200 mM) under both aerobic and anaerobic conditions and metabolism of TPZ was monitored by using UV-Vis spectroscopy at 474 nm.

The data that we reported here suggests that activation of TPZ in the presence of Cu, Zn-SOD and thiols leads to generation of oxygen radical species under both aerobic and anaerobic conditions and causes the DNA damage. The catalytic activity of Cu, Zn-SOD that we reported here is similar to its thiol oxidase activity.

5.12 Conclusions

Our studies reported here show that thiols and dithiols cause one-electron reductive activation of TPZ. Mechanistic studies show that metals and thiolate form of thiols and dithiols are involved in the activation of TPZ. Further, data show that thiol mediated activation of **41** under aerobic conditions causes the DNA cleavage. Our mechanistic studies on aerobic DNA cleavage by **41** suggest that the involvement of hydrogen peroxide, metals and hydroxyl radical. This information suggests activated **41** in the presence of thiols generates superoxide radical and causes the DNA strand cleavage. Addition of superoxide dismutase is known to enhance the superoxide radical mediated DNA strand cleavage in the presence of thiols. Accordingly, in our experimental conditions, we expected to see the increase in DNA strand cleavage by **41** in the presence of Cu, Zn-SOD. But in our studies, Cu,Zn-SOD inhibited the aerobic DNA cleavage by **41**. This unusual effect of Cu, Zn-SOD can be explained with the literature data, where trace metals inhibit the thiol oxidase activity of Cu, Zn-SOD. Inhibition of thiol oxidase activity of Cu,Zn-SOD suggests that trace metals some how interact with Cu,Zn-SOD. We also examined the role of Cu, Zn-SOD in catalyzing the activation of TPZ in the presence of thiols. Our data shows that Cu, Zn-SOD catalyzes the one-electron reductive activation of TPZ in the absence of metals.

The data that we reported here is relevant to physiological conditions. This data suggests that cellular thiols including glutathione and cysteine and cellular dithiol proteins including thioredoxin and APE can cause one-electron reductive activation of heterocyclic *N*-oxides and produce DNA damaging oxygen radical species. It is important to note that activation of heterocyclic compounds by thiols require metals. The

availability of free metals *in vivo* is a matter of debate.[32] However, data suggest that weakly bound metals are available *in vivo*.[32] For example, fluorimetric studies by Konijn and coworkers showed that cells contain 0.2-0.5 μM concentrations of weakly bound Fe (II).[33] These observations suggest that weakly bound metals *in vivo*, can facilitate the one-electron reductive activation of TPZ in the presence of thiols and dithiols.

5.13 Experimental

5.13.1 Metabolism of TPZ in the presence of thiols under both aerobic and anaerobic conditions. As part of our goal to examine the role of thiols in activating TPZ, reactions containing TPZ (100 μM), GSH or DTT or β-ME (20 mM) and the sodium phosphate buffer (pH 7, 200 mM) was incubated under both aerobic and anaerobic conditions. Rate of metabolism or loss of TPZ was monitored by using UV-Vis spectroscopy at 474 nm. In anaerobic assays, individual components of these reactions except GSH or DTT or β-ME were deoxygenated by using three cycles of freez-pump-thaw. Degassed solutions were used to prepare anaerobic reaction in an argon filled glove bag. GSH or DTT or β-ME was diluted with deoxygenated solutions in an argon filled glove bag. Once the reaction solution prepared immediately transferred into an argon purged cuvette and the resultant cuvette was capped with the septa to avoid oxygenation of the reaction solution. Then the resultant reaction was monitored by using UV-Vis spectroscopy at 474 nm. Aerobic reaction was performed in an identical manner to anaerobic reactions except with out degassing the reaction components and incubating the reaction under aerobic conditions.

5.13.2 Mechanistic studies for metabolism of TPZ in the presence of DTT. Experiments for mechanistic studies were carried out similar to the above experiments. Briefly, in experiments to examine the effect of pH on the metabolism of TPZ, reactions containing TPZ (100 μM), DTT (20 mM) and sodium phosphate buffers of pH 6-8 (200 mM) were incubated under anaerobic conditions. The metabolism of TPZ was monitored by using UV-Vis spectroscopy at 474 nm. In experiments to examine the role of metals in the metabolism of TPZ, reactions with and without metal chelating agents were

incubated under anaerobic conditions and the metabolism of TPZ was measured by using UV-Vis spectroscopy at 474 nm.

5.13.3 TPZ produces 1-*N*-oxide as a major metabolite upon reductive activation with DTT. *In vitro* metabolic analysis of TPZ, reactions containing TPZ (100 µM), DTT (20 mM), and NaP buffer of pH 7 (200 mM) were incubated under both aerobic and anaerobic conditions at 25 ^{o}C for 7 h. In an anaerobic reaction, oxygen free environment was achieved similar to earlier experiments. Then *in vitro* metabolites that produced were analyzed by HPLC employing a C18 reverse phase Rainin Microsorb-MV column (5 µm particle size, 100 A$^{\circ}$ pore size, 25 cm length, 4.6 mm i.d.) eluted with gradient solvent system starting with 85% A (0.2% acetic acid in water) and 15% B (methanol) followed by linear increase to 25% B from 0 min to 30 min. After that another linear increase to 50% B from 30 min to 35 min. Then 15% B was achieved in next 5 min. The flow rate of 1 mL/min was used and the products were monitored by UV-absorbance at 250 nm. Our HPLC analysis of anaerobic reaction shows that TPZ produces 1-*N*-oxide as a major metabolite, which elutes at ~31 min (Figure 5.4). The identity of the 1-*N*-oxide metabolite was confirmed by the co-injection of authentic compound with the reaction. *In vitro* metabolic experiments of TPZ in the presence of DTT under aerobic conditions were carried out similar anaerobic experiments except with out degassing the reaction components and incubating the reaction under aerobic conditions. Metabolism of TPZ under aerobic conditions yields only small amount of 1-*N*-oxide metabolite (Figure 5.5). These HPLC studies show that the yield of 1-*N*-oxide metabolite depends on oxygen concentration in reactions. Thus, HPLC data confirms the observations from the UV-Vis data, which suggests that DTT activates TPZ by one-electron reduction.

5.13.4 Aerobic DNA cleavage by 41 in the presence of DTT. In a typical concentration dependent aerobic DNA cleavage assays, solutions containing DNA (33 μg/mL), GSH (200 μM) or DTT (100 μM), sodium phosphate buffer (pH 7, 50 mM) and **41** (0.1 μM-40 μM) were incubated under aerobic conditions while protecting from light at 25 ^{o}C for 15 h. DNA cleavage assays for mechanistic studies were carried out in an identical manner to concentration dependent DNA cleavage assays except adding additives, SOD (100 μg/mL), catalase (100 μg/mL), desferal (1 mM) and radical scavengers methanol (100 mM), ethanol (100 mM) and mannitol (100 mM) prior to the addition of GSH or DTT. Control experiments with GSH (200 μM) or DTT (100 μM) (no **41**) and with **41 (**40 μM) (no GSH or DTT) were carried out similar to standard reactions. The DNA-cleavage was analyzed and quantified similar to our earlier experiments that we reported in Chapters 1-4.

5.13.5 Cu, Zn-SOD catalyzed activation of TPZ in the presence of DTT.

Cu, Zn-SOD containing reactions were carried out similar to earlier experiments except adding metal chelating agent desferal prior to the addition of DTT. Briefly, reactions containing TPZ (100 μM), DTT (20 mM), sodium phosphate buffer of pH 7 (200 mM), desferal (1 mM) and Cu, Zn-SOD (100 μg/mL) were incubated under both aerobic and anaerobic conditions. The metabolism of TPZ was monitored similar to earlier experiments.

Supporting information:

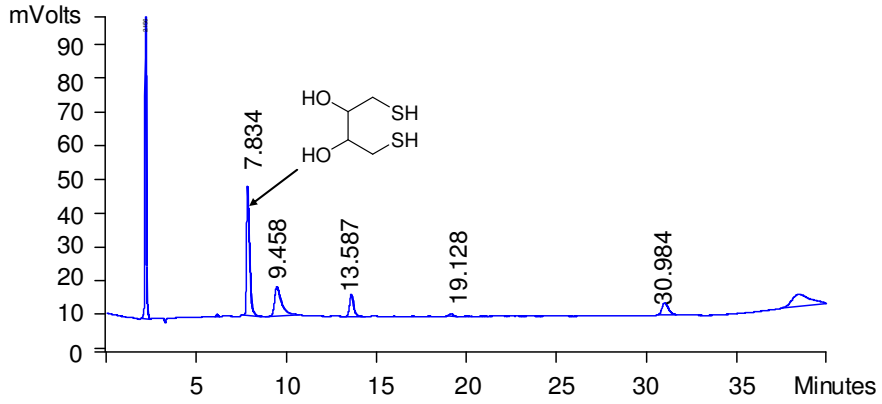

Figure S5.1: HPLC trace of TPZ-DTT reaction with co-injection of DTT

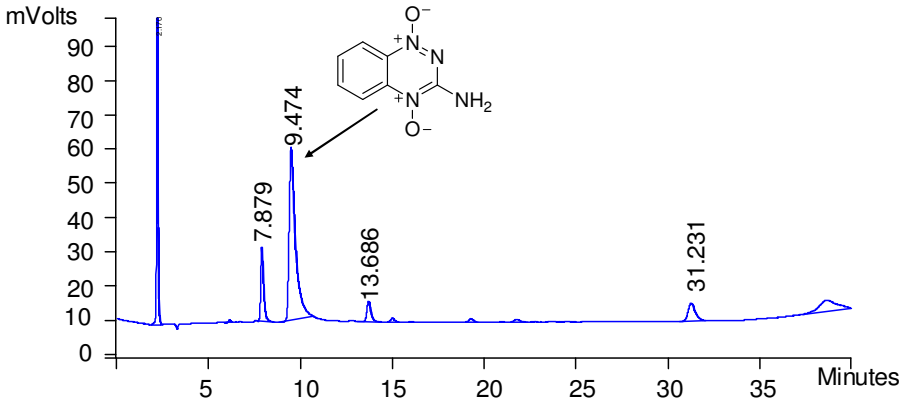

Figure S5.2: HPLC trace of TPZ-DTT reaction with co-injection of TPZ

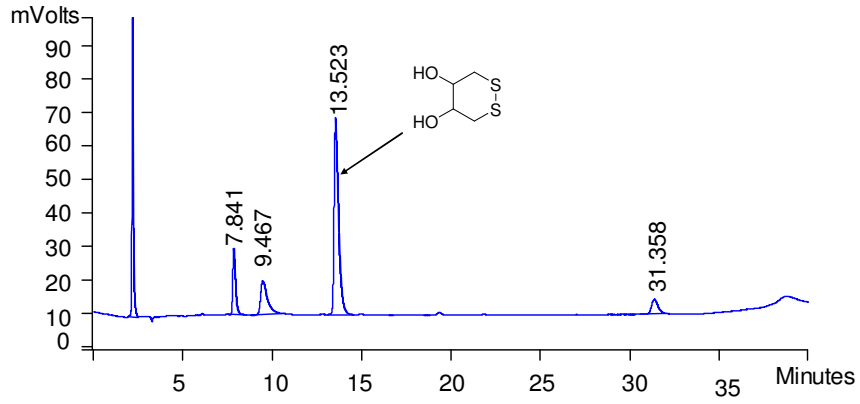

Figure S5.3: HPLC trace of TPZ-DTT reaction with co-injection of oxidized DTT

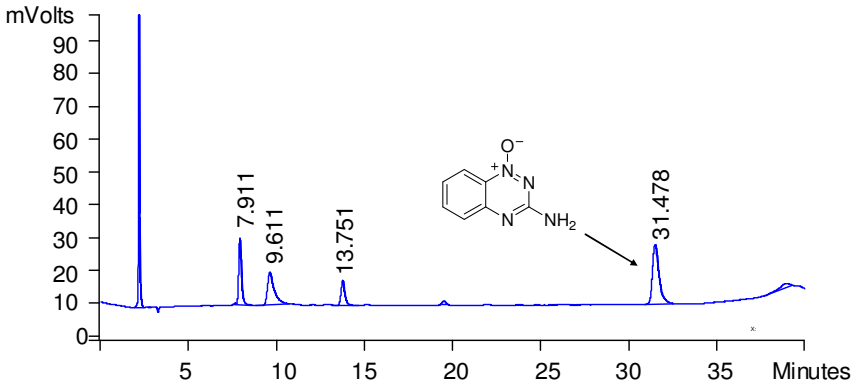

Figure S5.4: HPLC trace of TPZ-DTT reaction with co-injection of 1-*N*-oxide of TPZ

References:

[1] Relyea, D. I.; Tawney, P. O.; Williams, A. R. *J. Org. Chem.* **1962**, 27, 477-481.

[2] Nagai, K.; Carter, B. J.; Xu, J.; Hecht, S. M. *J. Am. Chem. Soc.* **1991**, 113, 5099-5100.

[3] Halliwell, B.; Gutteridge, J. M. C. *Methods Enzymol.* **1990**, *186*, 1-85.

[4] Bagley, A. C.; Krall, J.; Lynch, R. E. *Proc. Natl. Acad. Sci. U.S.A.* **1986**, *83*, 9189-9193.

[5] Hassan, H. M.; Fridovich, I. *Arch. Biochem. Biophys.* **1979**, *196*, 385-395.

[6] Finkel, T.; Holbrook, N. J. *Nature* **2000**, *408*, 239-247.

[7] Davis, W. J.; Ronai, Z.; Tew, K. D. *J. Pharmacol. Exp. Ther.* **2001**, *296*, 1-6.

[8] Laderoute, K.; Wardman, P.; Rauth, A. M. *Biochem. Pharmacol.* **1988**, 37(8), 1487-1495.

[9] Walton, M. I.; Workman, P. *Biochem. Pharmacol.* **1990**, 39, 1735-1742.

[10] Chinje, E. C.; Cowen, R. L.; Feng, J.; Sharma, S. P.; Wind, N. S.; Harris, A. L.; Stratford, I. J. *Mol. Pharmacol.* **2003**, 63, 1248-1255.

[11] Patterson, A. V.; Robertson, N.; Houlbrook, S.; Stephens, M. A.; Adams, G. E.; Harris, A. L.; Stratford, I. J.; Carmichael, J. *Int. J. Radiat. Oncol. Biol. Phys.* **1994**, 29, 369-372.

[12] Patterson, A. V.; Saunders, M. P.; Chinje, E. C.; Patterson, L. H.; Stratford, I. J.; Carmichael, J. *Anti-Cancer Drug Design* **1998**, 13, 541-573.

[13] Daniels, J. S.; Gates, K. S. *J. Am. Chem. Soc.* **1996**, 118, 3380-3385.

[14] Fuchs, T.; Chowdhary, G.; Barnes, C. L.; Gates, K. S. *J. Org. Chem.* **2001**, 66, 107-114.

[15] Evans, J. A.; Yudoh, K.; Delahoussaye, Y. M.; Brown, J. M. *Cancer Res.* **1998**, 58, 2098-2101.

[16] Evans, A. R.; Limp-Foster, M. K.; *Mutat. Res.* **2000**, 461, 83-108.

[17] Voehringer, D. W.; McConkey, D. J.; McDonnell, T. J.; Brisbay, S. M.; *Proc. Natl. Acad. Soc.* **1998**, 95, 2956-2960.

[18] Malik, G.; Gorbounov, N.; Das, S.t; Gurusamy, N.; Otani, H.; Maulik, N.; Goswami, S.; Das, D. K. *Antioxidants & Redox Signaling*. **2006**, 8, 2101-2109.

[19] Nishinaka, Y.; Masutani, H.; Oka, S.; Matsuo, Y.; Yamaguchi, Y.; Nishio, K.; Ishii, Y.; Yodoi, J. *J. Biol. Chem.* **2004**, 279, 37559-37565.

[20] Tanaka, T.; Nishiyama, Y.; Okada, K.; Hirota, K.; Matsui, M.; Yodoi, J.; Hiai, H.; Toyokuni, S. *Laboratory Investigation*. **1997**, 77(2), 145-155.

[21] Gao, Y.; Li, Z.; Gao, J.; Tu, Z.; Gong, Y.; Wang, Y. *Yixianbingxue.* **2006**, 6(2), 74-77.

[22] Tanner, B.; Grimme, S.; Schiffer, I.; Heimerdinger, C.; Schmidt, M.; Dutkowski, P.; Neubert, S.; Oesch, F.; Franzen, A.; Kolbl, H.; Fritz, Gerhard; Kaina, Bernd; Hengstler, Jan Georg. *Gynecologic Oncology.* **2004**, 92(2), 568-577.

[23] Kumagai, Y.; Shimojo, N. *Environmental Health and Preventive Medicine.* **2002**, 7, 141–150.

[24] O'Hara, K. A.; Wu, X.; Patel, D.; Liang, H.; Yalowich, J. C.; Chen, N.; Goodfellow, V.; Adedayo, O.; Dmitrienko, G. I.; Hasinoff, B.B. *Free Radical Biology & Medicine.* 2007, 43, 1132–1144.

[25] Folkes, L. K.; Christlieb, M.; Madej, E.; Stratford, M. R. L.; Wardman, P. *Chem. Res. Toxicol.* **2007,** 20, 1885–1894.

[26] Misra, H. P.; *J. Biol. Chem.* **1974**, 249, 2151-2155.

[27] Solano, B.; Junnotula, V.; Marin, A.; Villar, R.; Burguete, A.; Vicente, E. ; Perez-Silanes, S.; Monge, A.; Dutta, S.; Sarkar, U.; Gates, K. S. *J. Med. Chem.* **2007**, 50, 5485-5492.

[28] Chatterji, T.; Keerthi, K.; Gates, K. S. *Bioorganic Med. Chem. Lett.* **2005**, *46*, 3921-3924.

[29] Chatterji, T.; Gates, K. S. *Bioorg. Med. Chem. Lett.* **2003**, *13*, 1349-1352

[30] Mitra, K.; Kim, W.; Gates, K. S.*Journal of the American Chemical Society* **1997**, *119*, 11691-11692.

[31] Winterbourn, C. C.; Peskin, A. V.; Parsons-Mair, H. N. *J. Biol. Chem.* **2002**, 277, 1906–1911,

[32] Valko, M.; Morris, H.; Cronin, M. T. D. *Current Medicinal Chemistry*. **2005**, 12*,* 1161-1208.

[33] Konijn, A. M.; Glickstein, H.; Vaisman, B.; Meyron-Holtz, E. G.; Slotki, I. N.; Cabantchik, Z. I. *Blood*. **1999**, 94, 2128–2134.